unesp

UNIVERSIDADE ESTADUAL PAULISTA

PROGRAMA DE PÓS-GRADUAÇÃO EM GEOGRAFIA

JEFFERSON FERREIRA-FERREIRA

INFLUENCE OF FLOOD DYNAMICS ON FOREST CARBON STOCKS, LITTERFALL SEASONALITY AND NET PRIMARY PRODUCTIVITY IN AMAZONIAN VÁRZEA FORESTS

INSTITUTO DE GEOCIÊNCIAS E CIÊNCIAS EXATAS

RIO CLARO / SP
DEZEMBRO - 2018

UNIVERSIDADE ESTADUAL PAULISTA
"Júlio de Mesquita Filho"
Instituto de Geociências e Ciências Exatas
Campus de Rio Claro

JEFFERSON FERREIRA-FERREIRA

Influence of flood dynamics on forest carbon stocks, litterfall seasonality and net primary productivity in amazonian várzea forests

Tese de Doutorado apresentada ao Instituto de Geociências e Ciências Exatas do Câmpus de Rio Claro, da Unversidade Estadual Paulista "Júlio de Mesquita Filho", como parte dos requisitos para obtenção do título de Doutor em Geografia.

Orientador: Prof. Dr. Thiago Sanna Freire Silva

Rio Claro - SP
2018

F383i

Ferreira-Ferreira, Jefferson
INFLUENCE OF FLOOD DYNAMICS ON FOREST CARBON STOCKS, LITTERFALL SEASONALITY AND NET PRIMARY PRODUCTIVITY / Jefferson Ferreira-Ferreira. -- Rio Claro, 2018
111 p. : il., tabs., fotos, mapas

Tese (doutorado) - Universidade Estadual Paulista (Unesp), Faculdade de Ciências Farmacêuticas, Araraquara, Rio Claro
Orientador: Thiago Sanna Freire Silva

1. Várzeas amazônicas. 2. Sensoriamento remoto por radar. 3. Estoques de carbono. 4. Produtividade primária líquida. 5. Serrapilheira. I. Título.

Sistema de geração automática de fichas catalográficas da Unesp. Biblioteca da Faculdade de Ciências Farmacêuticas, Araraquara. Dados fornecidos pelo autor(a).

Essa ficha não pode ser modificada.

JEFFERSON FERREIRA-FERREIRA

Influence of flood dynamics on forest carbon stocks, litterfall seasonality and net primary productivity in amazonian várzea fores ts

Tese de Doutorado apresentada ao Instituto de Geociências e Ciências Exatas do Câmpus de Rio Claro, da Unversidade Estadual Paulista "Júlio de Mesquita Filho", como parte dos requisitos para obtenção do título de Doutor em Geografia.

Comissão Examinadora

Prof. Dr. Thiago Sanna Freire Silva - Orientador
IGCE/UNESP/Rio Claro (SP)

Dr. Luiz Eduardo de Oliveira e Cruz de Aragão
INPE/São José dos Campos (SP)

Dra. Evlyn Márcia Leão de Moraes Novo
INPE/São José dos Campos (SP)

Dr. Conrado de Moraes Rudorff
CEMADEN/São José dos Campos (SP)

Profa. Dra. Leonor Patricia Cerdeira Morellato
IB/UNESP/Rio Claro (SP)

Conceito: APROVADO

Rio Claro/SP, 29 de Outubro de 2018

Resumo

Dois macro-ambientes podem ser distinguidos entre os tipos de vegetacionais da Amazônia: áreas de terra firme, predominantemente florestadas e não suscetíveis a inundações, e as áreas úmidas. A extensão total das áres úmidas na Amazônia é de cerca de 30% da bacia amazônica, das quais mais de 25% são constituídas por planícies fluviais. Na Amazônia, a amplitude das variações sazonais do nível da água pode atingir até 16 m na Amazônia Ocidental, 10 m na Amazônia Central e 6 m na Amazônia Oriental, com extensão e duração da inundação local dependendo da interação entre precipitação, descarga fluvial e geomorfologia. Os processos ecológicos e ambientais nessas planícies são amplamente controlados pelo pulso de inundação - um conceito teórico que postula que a amplitude, duração, frequência e periodicidade (previsibilidade) dos pulsos de inundação são os principais fatores que mantêm o equilíbrio ambiental dinâmico. As planícies fluviais amazônicas desempenham um papel importante nos ciclos biogeoquímicos regionais e na manutenção da biodiversidade, além de fornecer importantes serviços ecossistêmicos para as sociedades humanas. No entanto, esses ambientes permanecem largamente negligenciados em relação às estimativas dos ciclos biogeoquímicos na escala da bacia hidrográfica. Assim, o presente estudo tem como objetivo avançar nossa compreensão de como a heterogeneidade espacial em termos de diferentes fitofisionomias florestais e padrões de inundação nas florestas de várzea controla três aspectos ecológicos principais: estoques de carbono, produção e dinâmica de serapilheira e produtividade primária líquida. Usando imagens multitemporais de sensoriamento remoto de radar de abertura sintética (SAR) combinadas com dados de campo, derivamos mapas de fitofisionomias e de duração da inundação na área de estudo. Também desenvolvemos um método empírico de modelagem de inundação baseado em modelagem logística para nos permitir estender as capacidades atuais de prever padrões espaciais de inundação. Em seguida, exploramos como a heterogeneidade espacial gera padrões de estoques de carbono acima do solo usando métodos de inventário florestal. Monitorando um ano de queda de serapilheira, analisamos como a produção e a dinâmica da serapilheira variam entre comunidades florestais distintas sob diferentes regimes de inundação e também estimamos a produtividade primária líquida e discutimos como ela varia no espaço.

Palavras-chave: Várzeas Amazônicas; Sensoriamento remoto por radar; Estoques de carbono; produtividade primária líquida; serrapilheira.

Abstract

Two macro-environments can be distinguished among Amazonian vegetation types: upland areas, predominantly forested and not susceptible to flooding, and wetland areas. The full extent of wetlands in the Amazon is about c.a. 30% of the Amazon basin, where floodplains comprise more than 25% of wetland areas. In the Amazon, the amplitude of seasonal water level variations can reach up to 16 m in Western Amazon, 10 m in Central Amazon, and 6 m in Eastern Amazon, with local flood extent and duration depending on the interaction among precipitation, river discharge and geomorphology. Ecological and environmental processes in floodplains are largely controlled by the flood pulse - a theoretical concept which postulates that amplitude, duration, frequency and periodicity (predictability) of flood pulses are the major factor maintaining the dynamic environmental equilibrium in floodplains. Amazonian floodplains play an important role in the regional biogeochemical cycles and biodiversity maintenance, and provide important ecosystem services to human societies. However, these environments remain greatly overlooked regarding basin-scale estimates of biogeochemical cycles. Therefore, the present study aims to advance our understanding of how spatial heterogeneity in terms of different forest subtypes and flood patterns of várzea forests controls three key ecological aspects: carbon stocks, litterfall production and dynamics, and net primary productivity. Using multitemporal synthetic aperture radar (SAR) remote sensing imagery combined with field data, we derived vegetation structure and flood duration classes in the study area. We also developed an empirical flood modeling method based on logistic modeling to allow us to extend the current capabilities in predict spatial patterns of flooding. Then we explored how spatial heterogeneity drives patterns of aboveground carbon stocks using standard forest inventory methods. Monitoring one full year of litterfall, we asked how litter production and dynamics vary among distinct forest communities under different flood regimes and we also estimated net primary productivity and discussed how it varies in space.

Keywords: Amazonian várzeas; Radar remote sensing; Carbon stocks; Net primary productivity; litterfall.

List of Figures

2.1 Conceptual cross-section diagram showing the three main forest subtypes . . . 6
2.2 Location of the study area . . . 8
2.3 Visual interpretation key used to select training and validation samples for vegetation mapping . . . 13
2.4 Mean water stage and shaded 95% confidence interval for the 1991-2011 period, measured at the Mamirauá Lake gauge . . . 15
2.5 Major vegetation types and habitats of the southeastern portion of the Mamirauá Sustainable Development Reserve . . . 17
2.6 Temporal variation of ALOS/PALSAR backscattering coefficients for the three main woody vegetation classes . . . 18
2.7 Extent of estimated flood duration classes (in days), based on ALOS/PALSAR imagery . . . 19
2.8 Estimated flood duration based on a time series of ALOS/ PALSAR image data . . . 20
2.9 Relative area for each combination of land cover and flood duration classes derived from ALOS/PALSAR image time series . . . 21

3.1 Localization of study area . . . 29
3.2 Installed leveloggers to flood monitoring in the Southeastern portion of Mamirauá Sustainable Development Reserve . . . 32
3.3 Root mean squared errors (RMSE) of the 4-fold cross validation 35
3.4 Flood modeling results . . . 36
3.5 Histograms of flood duration as predicted by the logistic model, by year. . . . 37

4.1 Association between flood heights and flood duration recorded at leveloggers . . . 45
4.2 Aboveground forest carbon by forest type . . . 49
4.3 Aboveground forest carbon proportion by diametric classes and forest subtype . . . 49
4.4 Relationship between aboveground forest carbon and flood duration 50
4.5 Relationship between input parameters of allometric models used to estimate aboveground forest carbon and flood duration . . . 51
4.6 Relationship between metrics related aboveground forest carbon distribution at plot-level and flood duration . . . 52

5.1 Total litterfall and water level heights . . . 60
5.2 Total litterfall and water level heights by vegetation type . . . 61

5.3 Relationship between litterfall seasonality and water level variation 62
5.4 Relationship between mean annul litter production and flood duration . . . 63
5.5 Relative contribution of bi-weekly production of different litterfall components and water level heights . . . 64
5.6 Relationship between bi-weekly production of litterfall components and water stage . . . 65
5.7 Relative contribution of bi-weekly production of different litterfall components to total fine litterfall by forest subtypes . . . 66
5.8 Photosynthetic and reproductive components of fine litterfall by vegetation types . . . 67
5.9 Relative investment into reproductive and photosynthetic components of fine litterfall by forest subtypes . . . 68
5.10 Mean annual production of fine litter components by forest subtypes 70
5.11 Association between mean annual production of fine litterfall components and flood duration . . . 71
5.12 Association between mean annual production of fine litterfall components and flood duration controlling for forest subtype . . . 72
5.13 Relationship between investment in photosynthetic organs relative to reproductive organs (RL ratio), flood duration and forest subtypes . . . 73
5.14 Relationship between net primary productivity and flood duration 75

6.1 Spatial distribution of net primary productivity as a linear function of flood duration. . . . 82
6.2 Spatial distribution of net primary productivity as a function of flood duration controlling for forest subtype. . . . 83

List of Tables

1.1 Above-ground carbon and structural metrics of inventoried forest sample plots . . . 2

2.1 ALOS/PALSAR synthetic aperture radar images acquired . . . 11
2.2 Water stage for each map of inundation extent, and corresponding flood duration classes . . . 14
2.3 Confusion matrix and accuracy indices for the classification of vegetation types . . . 16
2.4 Comparison of flood duration estimates as determined in situ using temperature gauges and as derived from ALOS/PALSAR images . . . 19

3.1 ALOS-1/PALSAR images acquired for different water levels to map flood extent in the Mamirauá Sustainable Development Reserve (Central Amazon, Brazil). The range of captured water stages comprises 70% of the maximum historical amplitude for this location. . . . 30
3.2 Best logistic models to estimate the flood duration. . . . 34
3.3 Comparison of historical and 2016 water levels. . . . 35

4.1 Sample design of forest sample plots . . . 43
4.2 Allometric models to estimate the aboveground biomass . . . 44
4.3 Floristic summary of inventoried forest plots . . . 47
4.4 Above-ground carbon and structural metrics of inventoried forest sample plots . . . 48
4.5 Paired differences in mean aboveground carbon between forest subtypes . . . 49

5.1 Bi-weekly maximum (Max), minimum (Min), mean and mean annual fine litterfall . . . 61
5.2 Paired differences in mean annual fine litter production between forest subtypes . . . 62
5.3 Paired differences in mean annual production of fine litterfall components between forest subtypes . . . 69
5.4 Estimates of total Net Primary Productivity (NPP) by forest type 74
5.5 Paired differences in net primary productivity between forest subtypes . . . 74
5.6 Comparison of fine litterfall production of different Amazonian forests . . . 76

Contents

1 INTRODUCTION **1**

2 COMBINING ALOS/PALSAR DERIVED VEGETATION STRUCTURE AND INUNDATION PATTERNS TO CHARACTERIZE MAJOR VEGETATION TYPES IN THE MAMIRAUÁ SUSTAINABLE DEVELOPMENT RESERVE, CENTRAL AMAZON FLOODPLAIN, BRAZIL **5**

2.1 Introduction 5
2.2 Methods 7
2.2.1 Study Area 7
2.2.2 Remote sensing data and processing 10
2.2.3 Image segmentation and classification 11
2.2.4 Flood extent mapping 14
2.3 Results 16
2.4 Discussion 22
2.4.1 Management implications 23
2.4.2 Conclusion 24

3 MODELING THE SPATIAL AND TEMPORAL DYNAMICS OF INUNDATION IN AMAZONIAN FLOODPLAINS USING RADAR REMOTE SENSING AND LOGISTIC MODEL **26**

3.1 Introduction 26
3.2 Methods 28
3.2.1 Remote sensing data and flood mapping 28
3.2.2 Flood monitoring 31
3.2.3 Flood modeling with logistic regression 32
3.3 Results and discussion 34

4 ABOVEGROUND CARBON STOCKS IN AMAZONIAN VÁRZEA FORESTS: THE ROLE OF FOREST SUBTYPES AND FLOOD REGIME **41**

4.1 Introduction 41
4.2 Methods 42
4.2.1 Sample Design 42
4.2.2 Data Analysis 43
4.3 Results 45
4.3.1 Forest inventory 45
4.3.2 Aboveground carbon stocks (AGC) 48
4.4 Discussion 53

5 LITTERFALL AND NET PRIMARY PRODUCTIVITY IN AMAZONIAN VÁRZEA FORESTS: THE ROLE OF FOREST SUBTYPES AND FLOOD REGIME **55**
5.1 Introduction 55
5.2 Methods 57
5.2.1 Sample Design 57
5.2.2 Data Analysis 58
5.3 Results 60
5.3.1 Fine litterfall production and dynamics 60
5.3.2 Production and dynamics of fine litterfall components . . 64
5.3.3 NPP estimates from fine litterfall 74
5.4 Discussion 75

6 SYNTHESIS AND CONCLUSION **80**

Chapter 1

INTRODUCTION

Throughout the relatively long Amazonian natural history, the changing climatic, biotic, and landscape configurations (Hoorn and Wesselingh 2011; Mertes and Dunne 2007) have established complex environmental mosaics. As result, the uneven spatial distribution of current geologic, climatic, edaphic and ecological conditions (Anderson 2012; Mertes and Dunne 2007; Saatchi et al. 2007; Silva et al. 2013a) create an heterogeneous mosaic of plant communities.

Two macro-environments can be distinguished among Amazonian vegetation types: upland areas, predominantly forested and not susceptible to flooding, and wetland areas. Amazonian wetlands play an important role in the regional biogeochemical cycles and biodiversity maintenance, and provide important ecosystem services to human societies (Luize et al. 2018; Melack and Forsberg 2001; Mitsch and Gosselink 2000; Pangala et al. 2017; Wittmann et al. 2012).

However, Amazonian wetlands remain greatly overlooked regarding basin-scale estimates of biogeochemical cycles. For instance, it has been estimated that the flooded forests of the Amazon basin can contribute to carbon accumulations of about 0.04±0.01 Pg[1] C $year^{-1}$ in living aboveground biomass (Aragão et al. 2014). Nonetheless this value is still considered highly uncertain (Aragão et al. 2014) and depends on better estimates based on wetland habitat and vegetation maps such as those conducted by Silva et al. 2010 and Ferreira-Ferreira et al. 2015. Such estimates do not consider, for instance, the ecogeographical differences between várzea and igapó forests, determined by the different nutritional status of these floodplains, nor the average time that each forested region remains flooded annually.

Junk et al. 2011 developed a comprehensive classification of Amazonian wetlands, using climatic, hydrological, botanical, and limnological parameters. The authors estimate that, including riparian forests along lower-order rivers (1 to 5 in river order) and floodable interfluves (white-sand vegetation known as *campinas* and *campinaranas*), the full extent of wetlands in the Amazon is about c.a. 30% of the Amazon basin, where floodplains comprise more than 25% of wetland areas (Table 1.1).

The oligotrophic river floodplains of black- and clear-water rivers are called *igapó*, being poor in nutrients, while eutrophic white-water river floodplains are rich in nutrients and locally and scientifically known as *várzea* (Junk et al. 2012;

[1] 1 Petagram (Pg) = 1 Gigatonne (Gt) = 10^3 Teragram (Tg) = 10^6 Megagram (Mg) = 10^6 grams (g).

Table 1.1: Classification and coverage of Amazonian wetland environments according to Junk et al. 2011.

Wetland Environments	Area (km^2)	% of Basin	% of wetlands	% of wetlands (excluded *)
Várzea Floodplains†	275,000	3.93	13.62	27.00
Blackwater Floodplains‡	118,000	1.69	5.85	11.59
Clearwater Floodplains	126,100	1.80	6.25	12.38
Interfluvial Wetlands	488,374	6.98	24.20	47.96
Mangroves§	10,900	0.16	0.54	1.07
Riparian Wetlands of Low-Order Rivers*	1,000,000	14.29	49.54	
Total	2,018,374	28.83		
Basin area (approx)	7,000,000			

† excluding paleo-várzea environments $\approx 125,000 km^2$).

‡ only Negro River catchment considered.

§ Brazilian Mangroves = 10,000 km^2 + 900 km^2 in Guiana

Sioli 1954).

Sioli 1954 developed the first scientific classification of Amazonian rivers to explain their limnological characteristics and relate them to the geological and geomorphological properties of their respective catchments. According to Sioli's classification, the black-water rivers (e.g. Negro, Jutaí, and Tefé rivers) drain the Precambrian Guyana Shield, bordering the northern Amazon basin. Their waters have transparencies of 60-120cm (Secchi disk depth) with low amounts of suspended matter and moderate acidity (pH<5), and both the water and the substrate are relatively nutrient-poor, with large amounts of humic acids that result in reddish-brown water colors. Clear-water rivers (e.g. Branco, Tapajós, and Xingu rivers) mostly drain the Brazilian Central Plateau which borders the Amazon basin to the south. Their waters have transparencies of >150 cm, low amounts of suspended sediment and dissolved solids, variable pH (between 5 and 8), and water and substrate of low to moderate fertility, with transparent to greenish shades. Finally, white-water rivers (e.g. Solimões/Amazonas, Juruá, and Madeira rivers) have their headwaters in the Andeans foothills, transporting large volumes of suspended and dissolved sediments, and thus being rich in nutrient content. Water transparencies are low, between 20 and 60cm, and pH nearly neutral. The large sediment loads give them a characteristic whitish-brown color.

Sioli's classification was later supported by botanical studies such as from Prance 1979 and Kubitzki 1989, which attributed the ecogeographic differentiation among floodplain forests to water chemistry. Nutritional conditions imposed by the different water types lead to ecological and structural differences between várzea and igapó forests. In both forest types, tree species richness tends to increase with decreasing flood height and duration, i.e. with reduced intensity of the environmental filter imposed by the flood (Wittmann et al. 2010b). However, in várzea forests tree densities decrease as flood duration and height decrease along the flood gradient, while in igapó forests the opposite occurs - tree densities increase with the decreasing stress caused by flooding

(Wittmann et al. 2010b). The oligotrophic status of waters and soils in igapó floodplains are also responsible for much slower tree radial growth. For example, the same tree species (*Macrolobium acaciifolium*, Leguminosae), subject to the same flooding regime in different environments, had an average diameter increment of 3.04±0.76 mm $year^{-1}$ in the igapó, while its radial growth was on average 5.32±1.34 mm $year^{-1}$ in the várzea (Schöngart et al. 2005). Aboveground woody biomass can be as large in igapó forests (227-304 Mg ha^{-1}) as in várzea forests (230-270 Mg ha^{-1}) (Schöngart et al. 2010), but the annual productivity of várzeas is approximately three times higher (Schöngart et al. 2010; Worbes 1997).

About 75% of these várzeas are covered by forests, while 25% of the remaining areas correspond to water bodies (channels, rivers and lakes), herbaceous vegetation, and non-vegetated sandy bars (Melack and Hess 2010). The combination of annual variation in water levels along the Solimões River (7-13 meters) and the essentially flat topography results in an active floodplain that can span from 20 to 100 km away from the main channel, favoring the establishment of várzea ecosystems (Goulding et al. 1995; Melack and Hess 2010).

The flood pulse is a theoretical concept relating the flood regime of river-floodplain systems with the distribution and dynamics of the associated biota and biogeochemical processes. Junk et al. 1989 define the regular annual "pulse" of river discharge as the major force controlling these systems, governing the lateral exchange and recycling of nutrients and causing biotic responses that ultimately lead to morphological, anatomical, physiological, and phenological/ behavioral adaptations. Each location in a floodplain is positioned along a flood gradient, and distinct plant species will have their "optimum" along the gradient, so that local plant communities are assembled according to the flood regimes. Although this "optimum" can be modulated by other factors such as stability, structure, and fertility of the substrate, groundwater table height, and biotic processes (Junk et al. 1989), the spatial heterogeneity of flood duration is the most important factor for forest differentiation in várzeas, having a crucial influence on floristic composition and species diversity (Assis et al. 2015; Luize et al. 2015; Wittmann et al. 2010b, 2006a).

Prolonged flooding imposes constraints on gas exchanges in plants. The diffusion resistance of most gases in the water is about 10,000 times greater than in the air and there is a *c.a.* 30-fold reduction in oxygen concentration between the gaseous and dissolved states (Mitsch and Gosselink 2015). Oxygen depletion under inundation may be even more severe in the tropics, as higher temperatures enhance the microbial oxygen demand and reduces its solubility, which is of about 14 mg l^{-1} at 0°C and about 7 mg l^{-1} at 35°C (Parolin et al. 2010). In Amazonian várzea forests, sedimentation rates are an additional cause for oxygen depletion in the rhizosphere. In areas close to the river mainstems, the annual floods can lay up to 19.8 cm $year^{-1}$ of sediments (Wittmann et al. 2004), rapidly leading to anoxia in the root system and, consequently, to a decline in the energy supply of roots, eventually interrupting CO_2assimilation (Junk and Piedade 2010; Parolin 2000).

The modulating effect of flooding on carbon assimilation in várzea forests is known for many tree species (Parolin 2000; Parolin et al. 2010; Parolin and Wittmann 2010; Schöngart et al. 2010). However, landscape-scale estimates of carbon stocks and net primary productivity that take into account the spatial heterogeneity of várzea forests and its different hydrological regimes are

still missing. This spatial heterogeneity of várzea forests in carbon stocks and productivity has not been considered in the estimates of carbon fluxes for the Amazon basin, nor in dynamic global vegetation models that are coupled to biogeochemical and climate models (Cox 2001; Galbraith et al. 2010; Joetzjer et al. 2013; Marengo et al. 2012; Prentice et al. 2007; Sitch et al. 2013; Zhang et al. 2015).

Therefore, the present study aims to advance our understanding of how spatial heterogeneity in terms of different forest subtypes and flood patterns of várzea forests controls three key ecological aspects: carbon stocks, litterfall production and dynamics, and net primary productivity.

The present study is divided in four main chapters, each one addressing specific questions of the above goal. Chapter 2, published in Ferreira-Ferreira et al. 2015, uses multitemporal synthetic aperture radar (SAR) remote sensing imagery combined with object-based image analysis, and field data to derive vegetation structure and flood duration classes in the study area. This chapter provides the basis to assess the spatial heterogeneity in terms of distribution of vegetation and spatial patterns of inundation. In Chapter 3, we go a step further in spatial inundation characterization, moving from flood duration classes to temporally continuous and pixel-based estimation of flood duration. In this chapter we used the same SAR imagery as the previous chapter and a logistic model to develop an empirical flood modeling method which allow us to extend current capabilities in predict spatial patterns of flooding. Chapter 4 address two questions: (i) How much and in which direction aboveground carbon stocks vary depending on forest subtypes and flood regimes? And (ii) which of the factors influencing AGC are most affected by flood duration? We answered these questions using field inventory methods combined with results from previous chapters. Monitoring one full year of litterfall, in Chapter 5 we ask three scientific questions: (i) Does fine litterfall production and dynamics differ among forest subtypes and flood regimes? (ii) Do distinct forest types and flood regimes reveal different community-level signals of varying plant investment strategies into reproductive organs versus photosynthetic organs? (iii) Assuming that litterfall production can be used as a proxy for forest total NPP, what we can infer about how the primary productivity of várzea forest could respond to hydrological variability and changes? In this chapter, we estimate net primary productivity from litterfall production and discuss how it varies in space. Finally, in Chapter 6 we emphasize the main remarks of the complete study and relate them to form a more comprehensive picture of how the present work advances our understanding of the ecology and carbon biogeochemistry of várzea forests.

Chapter 2

COMBINING ALOS/PALSAR DERIVED VEGETATION STRUCTURE AND INUNDATION PATTERNS TO CHARACTERIZE MAJOR VEGETATION TYPES IN THE MAMIRAUÁ SUSTAINABLE DEVELOPMENT RESERVE, CENTRAL AMAZON FLOODPLAIN, BRAZIL[1]

2.1 Introduction

The Amazon várzea comprises the eutrophic floodplains influenced by the sediment-rich white-water rivers of the Amazon basin (Junk et al. 2012; Prance 1979; Sioli 1954). These environments cover an area of about 275,000 km2, or between 13% and 27% of all wetlands in the basin, contributing significantly to the regional carbon balance and biodiversity (Junk et al. 2011; Melack and Hess 2010; Melack et al. 2009a). The Solimões/Amazon River várzeas are characterized by an annual flood regime described as the "flood pulse" (Junk et al. 1989). Average maximum flooding depths can reach up to 16 m in Western Amazon, 10 m in Central Amazon, and 6 m in Eastern Amazon, and local flooding extent and duration depends on the interaction between precipitation, river discharge and topography (Bonnet et al. 2008; Junk et al. 1989; Lesack and Melack 1995; Ramalho et al. 2009).

The flood pulse is the main ecological forcing in the floodplain, controlling the occurrence and distribution of plants and animals, life-history traits, primary and secondary production, and also influencing carbon respiration, decomposition and nutrient cycles in water and soils (Junk 1997b). Together with geomorphological characteristics, the flood pulse is also directly related to ero-

[1]Published as FERREIRA-FERREIRA, Jefferson et al. Combining ALOS/PALSAR derived vegetation structure and inundation patterns to characterize major vegetation types in the Mamirauá Sustainable Development Reserve, Central Amazon floodplain, Brazil. Wetlands Ecology and Management, v. 23, n. 1, p. 41–59, 2015.

sion, transport and deposition processes (Irion et al. 1997). Most floodplain environments have a flooding gradient from aquatic to terrestrial conditions, resulting in a complex mosaic of habitats (Junk 1997b). Hydrogeomorphological dynamics such as migrating channels and evolving lakes are also an important feature of the várzea landscape, influencing habitat characteristics and vegetation distribution (Peixoto et al. 2009; Wittmann et al. 2004).

Ducke and Black 1954, Rodrigues 1961, and Takeuchi 1962 identified different habitat types, flooding regimes, nutrient availability and biogeographical history as factors influencing the composition, distribution, and diversity of species. Prance 1979 offered the first classification of Amazonian wetland forests, based on hydrological and hydrochemical parameters, and Pires and Koury 1959 and Hueck 1966 described a zonation of plant communities along the flooding gradient in eastern and central Amazonn várzeas. Plants subject to waterlogging have a variety of evolutionary adaptation strategies for coping with the anaerobic soil conditions, and flooding is considered to be the major driver of local-scale habitat zonation, a selective force influencing evolutionary processes (Parolin and Wittmann 2010; Wittmann et al. 2010b).

Junk 1989 reported associations between tree species and topographic heights, with inundations lasting 140 or less days per year, 140-230 days per year, and 230-270 days per year. Applying the nomenclature used by the local population, Ayres 1993 described different várzea forest types according to the mean inundation depth along the lower Japurá River. He described the chavascal as a vegetation community of dense shrubs with small trees occurring in areas where the water column depth ranged between 5 and 7 m; the low restinga as the vegetation community of forest occupying low land where the seasonal maximum inundation depth ranged between 2.5 and 5 m; high restinga as the vegetation community of forest occupying higher land where water column depth ranged from 1 to 2.5 m. Wittmann et al. 2002 updated this classification, modifying the terminology to várzea alta (high várzea) and várzea baixa (low várzea), to avoid confusion with the term *restinga* as used for coastal vegetation in the Brazilian literature (Figure 2.1).

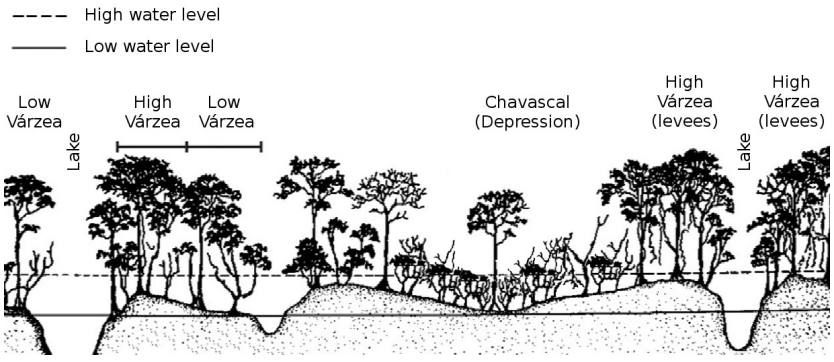

Figure 2.1: Conceptual cross-section diagram showing the three main forest subtypes present in Mamirauá Sustainable Development Reserve (Central Amazon, Brazil). Adapted from Ayres 1993

Recently, Junk et al. 2012 have proposed a comprehensive classification of

várzea habitats, based on a combination of hydrological, geomorphological and botanical characteristics. However, given the large extent and heterogeneity of várzea landscapes, little is currently known about the distribution, extent and relative proportion of each of these habitats within the Amazon Basin.

Remote sensing methods have been successfully used to study vegetation cover and hydrologic dynamics in wetland environments, and recent advances have allowed the characterization and quantification of multiple wetland ecological processes (Costa et al. 2013; Ozesmi and Bauer 2002). A few contributions to the understanding of ecological and anthropogenic processes in várzea habitats have been derived from optical remote sensing studies (Mertes et al. 1995; Renó et al. 2011; Wittmann et al. 2002), but most advances have been based on the use of synthetic aperture radar (SAR) sensors, given their ability to detect flooding under plant canopies, and its capacity to acquire images even under cloudy conditions (Henderson and Lewis 2008; Kasischke et al. 1997). Early SAR studies in the floodplain were supported by the SIR-C/X-SAR mission (Hess et al. 1995), and the launch of the Japanese JERS-1 L-band orbital sensor fostered studies on flooding dynamics, habitat mapping, water level height, and biomass estimation (Alsdorf et al. 2007a; Martinez and Letoan 2007; Rosenqvist et al. 2002). More recently, the combination of new processing methods such as object-based image analysis (OBIA) and imagery provided by the new crop of polarimetric SAR systems (ALOS/PALSAR, Radarsat-2, TerraSAR-X and Cosmo/Skymed) has allowed researchers to assess vegetation properties and ecological processes in the Amazon floodplain at the landscape scale (Arnesen et al. 2013; Hawes et al. 2012; Silva et al. 2013a).

Still, most of these studies are limited either temporally or spatially, and the distribution and spatial configuration of várzea habitats remains poorly known, limiting management, monitoring, and conservation initiatives and leaving these areas open to anthropogenic degradation and overexploitation. In this sense, remote sensing monitoring may not only offer a valuable scientific tool, but also contribute directly to the identification of priority areas for protection and conservation, as well as contributing to the proper management of these areas. For this reason, the present study demonstrates how L-band ALOS/ PALSAR imagery can be utilized to (i) identify the distribution and relative proportion of different vegetation types, and (ii) produce landscape-scale estimates of flooding extent and duration, within the context of management and conservation needs of the Mamirauá Sustainable Development Reserve protected area, in the Central Amazon floodplain.

2.2 Methods

2.2.1 Study Area

First of its kind, the Mamirauá Sustainable Development Reserve (MSDR) is located on a floodplain region at the confluence of the Solimões and Japurá Rivers, near the town of Tefé and approximately 600 km upstream from the city of Manaus, in the Central Amazon floodplain (Figure 2.2).

Covering approximately 11,240 km^2, the MSDR is one of the largest Brazilian protected areas dedicated to wetland environmental conservation, and one of the few functional protected areas in the Brazilian várzea forests (Queiroz

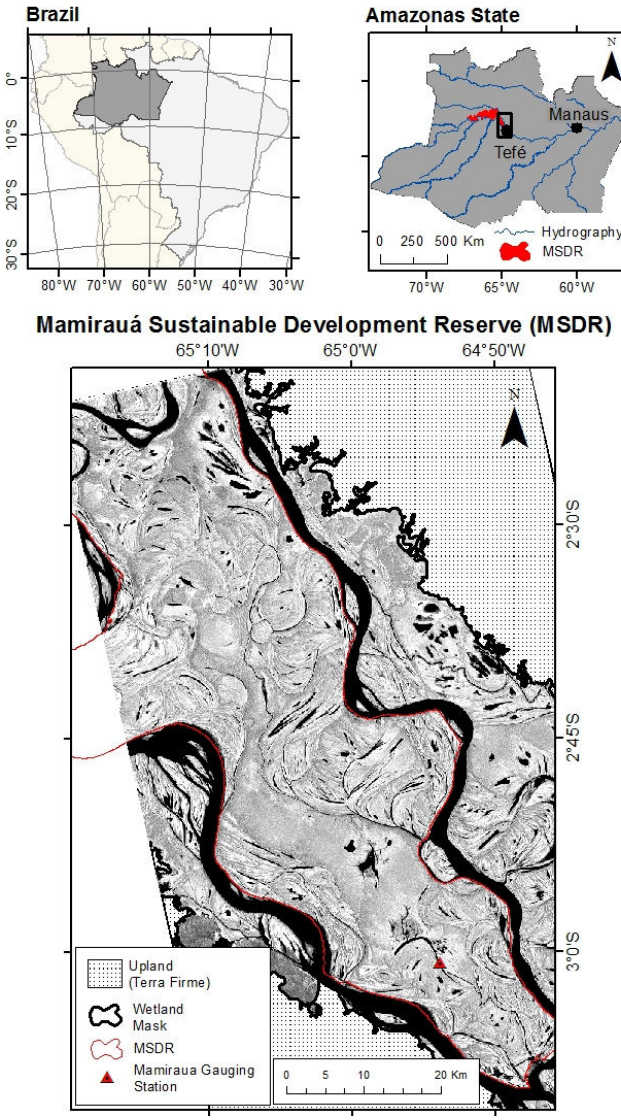

Figure 2.2: Mamirauá Sustainable Development Reserve (MSDR) location, in the Central Amazon floodplain, Brazil. On the right, the southeastern portion of MSDR, located between the Solimões and Japurá rivers, and its adjacent wetlands. The underlying image is a temporal average from a set of 13 HH ALOS/PALSAR image mosaics. The wetlands mask shown was derived from Hess et al. 2003, geometrically corrected by Rennó et al. 2013 and manually edited by Ferreira et al. 2013.

and Peralta 2006). Recognized as a World Heritage site by UNESCO (http://whc.unesco.org/en/list/998), the MSDR is also currently the only RAMSAR site representing Amazon wetlands (Secretariat 2013). Since 1992, active research programs and community-based management projects have been developed in the reserve to understand the biology and conservation of IUCN listed species, such as the Amazonian manatee (*Trichechus inunguis* - vulnerable),

the jaguar (*Panthera onca* - near threatened), the Black Caiman (*Melanosuchus niger* - lower risk/conservation dependent), and the white uakari monkey (*Cacajao calvus* - vulnerable), while promoting sustainable use and protecting the traditional livelihoods of riverine communities. Supporting a range of socio-economic and biological studies on forestry, agriculture, fisheries and ecotourism, the reserve is a key center for research on sustainable development and conservation in Amazonian environments (Queiroz and Peralta 2006; Schöngart and Queiroz 2010).

Flooding dynamics at the MSDR are characterized by a large monomodal flood pulse, reaching about 10 m in amplitude (Ramalho et al. 2009). The high water phase (cheia) starts in May, extending to mid-July, followed by a receding water phase (vazante) that lasts until September. The low water phase (seca) occurs from September to November, when the rising water phase (enchente) phase starts, lasting from December to May (Ramalho et al. 2009).

The main vegetation types observed in the reserve are the chavascal, low várzea, and high várzea, in addition to herbaceous vegetation stands. The chavascal name is given to poorly drained alluvial relicts developing in old depressions, abandoned channels, and shallow lakes, filled with large proportions of clay deposited during the aquatic phase and covered by a dense and species-poor shrub/tree community (Wittmann et al. 2010b). The flood duration in these habitats is reported as lasting about 180-240 days per year, with water heights varying between 5 and 7 m. Individual density may exceed 600 individuals ha^{-1}, with characteristic species such as *Symmeria spp.*, *Calyptranthes multiflora*, *Eugenia ochrophloea*, *Buchenavia oxycarpa* and *Pseudobombax munguba* (Wittmann et al. 2010b).

Low and high várzea habitats are differentiated by floristic and structural features induced by the hydroperiod, sharing between them only 12% of the tree species (Wittmann et al. 2002). Due to the stronger flooding pressure, low várzea areas have the fewest and smallest species, and higher individual density. Early successional stages are usually formed by dense and often monospecific stands of *Cecropia latiloba*, which decrease hydrodynamic energy, induce sedimentation, and provide the necessary shading to support the establishment of other species (Wittmann et al. 2010a,b). Late-successional stages usually contain 70-90 species per ha, such as *Piranhea trifoliata*, *Tabebuia barbata*, *Hevea spp.*, *Pouteria spp.*, *Oxandra spp.* and *Duroia duckei*. These forests tolerate flood durations of 120-180 days every year, with a water level of 2.5-5 m (Wittmann et al. 2010b).

On high várzea communities, population dynamics and canopy architecture are more complex, with higher biomass, species richness and diversity values than low várzea. In a survey conducted by Wittmann et al. 2002 in the same study area as ours, 177 species were found in a single 1 ha plot, where 101 species were represented by a single individual. These communities occur in the highest elevations, with a geomorphological context of relative stability, such as scrollbars and levees, and have a distinctive vertical stratification, with an upper canopy height of 30-35 m and emergent trees reaching heights of up to 45 m. Some representative species are *Pouteria procera*, *Malouetia tamaquarina*, *Aspidosperma riedelii*, *Guatteriopsis paraensis*, *Gustavia augusta* and *Pseudoxandra polyphleba*. Flood duration varies between 60 and 120 days per year, with maximum depths of 1-2.5 m. Depending on their position along the flooding gradient, some of these forests may experience less than 50 flooding days per year, and not

experience any flooding during exceptionally dry years (Schöngart et al. 2004).

In addition to woody vegetation, areas sometimes referred to as várzea fields (*campos de várzea*) are composed of low lying areas and shallow lakes that alternate seasonally between free water surface, exposed sediments and herbaceous vegetation (macrophytes), occupying areas with the longest flooding durations. These communities comprise several aquatic or palustrine grass species (e.g. *Echinochloa polystachya*, *Hymenachne amplexicaulis*, *Paspalum spp.*, *Oryza spp.*), as well as floating herbs such as *Eichhornia spp.*, *Pistia spp.*, *Salvinia spp.*, *Ludwigia spp.*, N*eptunia spp.*, *Nymphoides spp.* and *Victoria amazonica*. Most of these plants have very high growth rates, and can rapidly occupy available substratum, showing significant seasonal and interannual variation in distribution and coverage (Silva et al. 2013b).

2.2.2 Remote sensing data and processing

We acquired L-band (23.6 cm wavelength) SAR imagery from the Phased Array type L-band Synthetic Aperture Radar sensor on-board the Advanced Land Observation Satellite-1 (ALOS-1/PALSAR), operated by the Japanese Aerospace Exploration Agency (JAXA). Launched in January 2006 and decommissioned in April 2011, this was the first SAR mission to provide a systematic global image acquisition strategy, and it has since 2014 been followed by the ALOS-2 mission (Rosenqvist et al. 2014, 2010). Imagery for this study was provided by JAXA through the ALOS Kyoto and Carbon Initiative (K&C), later made freely available at different sources, e.g. NASA's Earth Observing System Data and Information System (`http://reverb.echo.nasa.gov/reverb/`).

Images were acquired in two polarization modes: fine beam single (FBS), with HH polarization, and fine beam dual (FBD), with HH and HV polarizations. The Fine Beam mode is characterized by a high resolution strip with a ≈70 km swath, a 38.7°of incidence angle (at the scene center) and 12.5 m pixel spacing (Rosenqvist et al. 2007). To better capture the flood pulse dynamics, a set of 26 scenes (Path 85, Frames 7120 and 7130) were acquired for several dates, chosen to provide the largest and most uniform range of water level conditions within the available imagery for the area. Water stage data was recorded at the Mamirauá Lake gauging station, located in the southern part of the study region (see Figure 2.2; IDSM 2013; Ramalho et al. 2009).

For each date, the corresponding adjacent scene pairs were mosaicked to provide complete coverage of the study area, resulting in a final set of 13 images (Table 2.1).

This acquisition pattern encompassed the southeastern portion of the MSDR, forming a seemingly triangular shape upstream of the confluence between the Japurá and Solimões rivers, where most management activities and research studies take place, and also encompassed adjacent wetlands contained within the selected scenes. The total area mapped comprises approximately 4,680 km^2. All images were acquired at the 1.5 processing level, which includes range and azimuth compression, multilooking, slant to ground range conversion and radiometric and geometric corrections (Japan Space Systems 2012), and converted to linear backscattering coefficients (σ^0) for statistical summarization. Final results were expressed in dB units, to allow comparisons with the previous literature. For PALSAR Fine Beam products, the conversion to σ^0 follows

Table 2.1: ALOS/PALSAR synthetic aperture radar images acquired at different dates and water stage levels, for mapping vegetation types and inundation extent within the Mamirauá Sustainable Development Reserve (Central Amazon, Brazil). *FBS* - fine beam single (HH polarization), *FBD* - fine beam dual (HH/HV polarization). Water level heights were obtained from Mamirauá gauge station. (IDSM 2013; Ramalho et al. 2009).

PALSAR acquisition date	Mode	Water stage height (masl)
2010-09-22	FBD	24.71
2007-10-30	FBS	27.00
2010-12-23	FBS	27.38
2008-12-17	FBS	30.02
2007-12-15	FBS	31.07
2010-03-22	FBS	32.72
2008-08-01	FBD	32.85
2007-07-30	FBD	33.37
2008-05-01	FBD	35.12
2010-05-07	FBD	35.65
2007-06-14	FBD	36.06
2010-06-22	FBD	36.28
2009-06-19	FBD	38.32

Equation 2.1:

$$\sigma^0 = 10 \times log_{10}(DN^2) - 83 \tag{2.1}$$

where DN is the backscattering amplitude expressed in digital numbers, and -83 is the calibration coefficient for PALSAR standard products (Shimada et al. 2009).

In addition to PALSAR images, georeferenced multispectral sensor mosaics with 5 m spatial resolution of RapidEye (multiple dates between 2009 and 2011) and 2.5 m spatial resolution of SPOT-5 (acquisition (acquisition on 2012-11-08) images were utilized as aid for visual interpretation of the land cover classes in the study area. These images were acquired and provided by the Mamirauá Sustainable Development Institute, who manages the MSDR (www.mamiraua.org.br).

2.2.3 Image segmentation and classification

Our study follows a similar approach to Silva et al. 2010 and Arnesen et al. 2013 to map land cover and inundation status in várzea environments, combining multitemporal SAR imagery and OBIA techniques. Standard image classification techniques work solely on a pixel-by-pixel basis, ignoring both the spatial context and the multi-scale information (texture) contained within the image elements, and are overly susceptible to SAR speckle. OBIA methods start by segmenting the image into homogeneous groups of pixels (objects), ideally

corresponding to homogeneous land cover features, and allow the use of multiple descriptive statistics and contextual information during the classification process (Blaschke 2010).

Prior to image segmentation, temporal composite images were produced, following Arnesen et al. 2013: temporal average backscattering (TAB), comprising the average backscattering of the entire image series; temporal standard deviation (TSD), comprising the per-pixel standard deviation for all observed values in the series, and lowest water level backscattering (LWB), simply defined as the scene with the lowest observed water stage level (2010-09-22). These seasonal descriptors allow the segmentation and classification to identify groups of pixels with similar time series of PALSAR backscatter coefficients. The measures chosen enable vegetation communities to be defined as a combination of vegetation structure and inundation dynamics. These images were filtered using three consecutive passes of a 3 x 3 Gamma filter (Shi and Fung 1994) and converted to an 8-bit radiometric scale, to reduce speckle heterogeneity and increase computational efficiency during segmentation.

The TAB, TSD and LWB images were used as inputs for the multi-resolution segmentation algorithm implemented on eCognition 8.0 (Definiens 2009), together with a vector file of the Amazon wetland mask produced by Hess et al. 2003, geometrically corrected by Rennó et al. 2013 and manually edited by Ferreira et al. 2013. This is a region-merging algorithm that begins with a single pixel and a pairwise comparison with its neighbors, with the goal of minimizing the resulting calculated heterogeneity. After iterative testing, the parameters of scale = 150, shape = 0.1 and compactness = 0.5 were selected.

After segmentation, the mean and standard deviation of σ^0 were computed for each image object, separately for all 15 available layers (single date images plus TAB and TSD), resulting in a total of 50 object attributes across all dates and polarizations available. For the TAB and TSD seasonal descriptors, the original unfiltered and unscaled images were used to ensure comparability with the single date imagery. Using vegetation type information from 86 survey plots provided by the Mamirauá Institute for Sustainable Development, and supported by Rapid Eye, SPOT-5 and Google Earth™ high resolution imagery, 360 objects were selected as training samples (72 objects per class) for subsequent radiometric analysis and classification, based on a multi-sensor interpretation key (Figure 2.3).

Five land cover classes recognized in the literature (Ayres 1993; Junk et al. 2012; Wittmann et al. 2002) were defined for evaluation: three main arboreal vegetation types (Chavascal, Low Várzea and High várzea), permanently free water surfaces (Water Bodies), and transient areas that alternate seasonally between water, substratum and herbaceous vegetation (Herbaceous/Soil). Non-floodable uplands (terra firme) areas were excluded using the wetland mask from Hess et al. 2003, and not further evaluated. After sample selection, the temporal radiometric response of each class was graphically analyzed using boxplots.

To discriminate the defined classes, we used the random forests (RF) algorithm, proposed by (Breiman 2001), as implemented in the *randomForest* package of the R open source statistical programming environment (Liaw and Wiener 2002). A vector file containing all image objects identified as training samples, with the associated attribute table containing class labels and sampled backscattering responses for all images in the series, was submitted as input to the RF algorithm, to derive the classification tree ensemble. This ensemble was

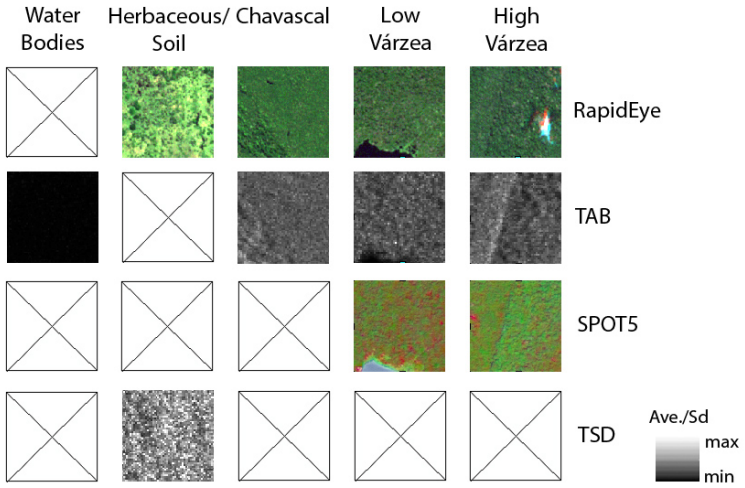

Figure 2.3: Visual interpretation key used to select training and validation samples for vegetation mapping at the Mamirauá Sustainable Development Reserve (Central Amazon, Brazil). TAB temporal average backscattering, TSD temporal standard deviation of backscattering, TAB and TSD were calculated using all available ALOS/ PALSAR images of the 2007-2010 time series.

then applied to the entire set of generated image objects, to produce the final classification.

The RF algorithm is an ensemble learning method based on classification and regression trees (CART), where instead of a single decision tree, a "forest" (i.e., ensemble) of individual trees is built through randomization of the training data. Final class predictions are based on using a majority voting scheme (consensus) among the trees in the ensemble, improving predictive accuracy. Independent trees are constructed using a bootstrap sample of the data set in a process called "bagging". In each bootstrap sample, approximately one-third of the reference data are left out. At the end of each iteration, the "out-of-bag" samples are then predicted using the ensemble derived from the bootstrap sample, and later aggregated to produce an out-of-bag (OOB) estimate of classification error for the entire "forest". The two main parameters of the classifier are the number of independent trees generated (n_{tree}) and the number of predictive variables that are randomly selected for choosing the best split (m_{try}). Multiple combinations of the two main parameters were tested until an optimal set of parameters was found.

The accuracy of the vegetation map was assessed using 142 validation points, randomly distributed within the study area using a Geographic Information System software. These points were manually classified based on the predefined interpretation key, using available high-resolution imagery. The resulting manual classification was compared to the RF classification to build a confusion matrix and derive overall accuracy, class accuracy, kappa statistics (Congalton 1991) and quantity and allocation disagreement measures (Pontius and Millones 2011). Quantity disagreement refers to the difference in area proportions be-

tween the reference data (training samples derived from field plots) and the classification. Allocation disagreement, on the other hand, is the proportion of misplaced objects from the classified map in comparison with positions in the reference data. A comparison between a reference map with two classes and a classification where every point is misclassified as the opposite class, for instance, would have 0% quantity disagreement and 100% allocation disagreement. Although Pontius and Millones 2011 condemn the use of the kappa index of agreement, we include it here to allow comparisons with previous literature.

2.2.4 Flood extent mapping

Flood extent maps were generated for all single date images based on the expected increase in SAR signals due to enhanced double-bounce scattering, where the radar beam is specularly reflected by the free water surface under the canopy, and then scattered back to the sensor by the standing vegetation, or vice versa (Hess et al. 1995; Silva et al. 2008). Flooded area for woody vegetation was determined based on simple thresholds, determined by the graphical analysis of backscattering values in each PALSAR scene.

Once flooded area was determined for each image in the time series, each flood map was associated to a corresponding water level, according to Table 2.2.

Table 2.2: Water stage for each map of inundation extent, and corresponding flood duration classes, in days, for the Mamirauá Sustainable Development Reserve (Central Amazon, Brazil).

Water stage height (masl)	Flood duration (days)
27.00	$>$ 295
30.02	175-295
31.07	175-295
32.72	125-175
33.37	105-125
35.12	40-105
35.65	$<$ 40
36.06	$<$ 40
38.32	$<$ 40

Water levels considered too similar in terms of flood extent were grouped into a single class, and the image acquired on 2010-09-22 was excluded from the analysis, since it had a very low water level and negligible flood extent outside of permanent water bodies. This resulted in nine different inundation extent maps, corresponding to each water level (27.0, 30.72, 31.07, 32.72, 33.73, 35.12, 35.65, 36.06 and 38.32 m).

Average flood duration was estimated by taking the average stage height for all available data from the Mamirauá gauge (1991-2011; meters above sea level), and determining the number of days per year where this average was equal or above the observed stage height at the moment of image acquisition. Flood duration categories were then established by taking this duration and extending it backwards until the previously observed duration category (see example on Figure 2.4).

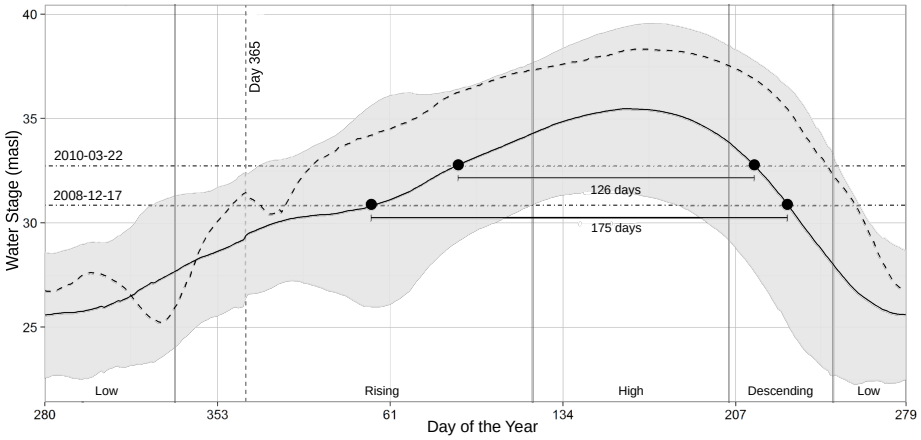

Figure 2.4: Mean water stage and shaded 95% confidence interval for the 1991-2011 period, measured at the Mamirauá Lake gauge, Mamirauá Sustainable Development Reserve (Central Amazon, Brazil) (IDSM 2013; Ramalho et al. 2009). The ordering of the Julian dates is offset, starting at the lowest mean water level to indicate the average onset date for the rising water period. The four stages of the flood pulse are indicated as low, rising, high and descending. The dashed line indicates the abnormally high water levels for the 2008-2009 hydrological year, when iButton inundation data was recorded (Affonso et al. 2011; Hess et al. 2011). Horizontal lines show the stage levels for two hydrologically consecutive image acquisition dates. According to our criteria, flood duration for the 2010-03-22 image is assumed to be between 175 and 125 days

Stage heights with very similar flood durations were again grouped into the same category, resulting in six flood duration classes. The single final map was derived by successively overlaying inundation maps of consecutive stage heights, and labelling all pairwise non-overlapping mapped areas as flooded between the levels observed for the first and second maps. Finally, all mapped Herbaceous/Soil areas were added to the map as belonging to the "$>$ 295 flooding days" class, and the mapped Water Bodies class was appended as a "365 flooding days" class.

Flood mapping validation was performed using temperature-based inundation data from Affonso et al. 2011; Hess et al. 2011, based on thermistor chains (Thermocron iButtons). These authors have recovered inundation data from 18 sites within the focal research area of the MSDR, for the 2008-2009 hydro- logical year. The location of each site was identified on the flood duration map, and the in situ duration of inundation was then compared to the estimated duration derived from the PALSAR time series.

Once both maps were validated, the co-occurrence of vegetation and inundation classes was determined by an overlay of both maps, quantifying the total area for each combination of vegetation type and flood duration.

2.3 Results

The best parameterization of the RF algorithm consisted of an ensemble of $n_{tree} = 5000$ decision trees, with $m_{try} = 20$ out of the 50 available predictor variables as candidates for a split. This resulted in an overall estimated OOB error of 10.6%. The highest prediction errors were observed for Chavascal, with a 20% prediction error composed mainly of misclassification with low várzea (12.5%) and high várzea (5.5%), and for low várzea with 13% prediction error, equally distributed between Chavascal and High Várzea. The remaining classes had prediction errors of 8% (Herbaceous/Soil), 6% (high várzea) and 2% (water bodies).

The resulting classification revealed a dominance of low várzea environments, and an overall complex mosaic of habitats resulting from the dynamic hydrogeomorphological characteristics of the area (Figure 2.5). Vegetative cover was distributed as 1,753 km^2 (37.7%) of low várzea, 873 km^2 (18.7%) of high várzea, 832 km^2 (18%) of Chavascal, 711 km^2 (15.3%) of Water Bodies, and 480 km^2 (10.3%) of herbaceous/soil. Independent validation of the vegetation cover classification based on comparison with high-resolution optical imagery yielded an overall accuracy of 83%, with a kappa index of agreement of 0.8 (Table 2.3). The worst results were again observed for the Chavascal and Low várzea classes, while the Herbaceous/Soil class had the largest spread of misclassification.

Table 2.3: Confusion matrix and accuracy indices for the classification of vegetation types using ALOS/PALSAR image time series and the random forests classification algorithm, for the Mamirauá Sustainable Development Reserve (Central Amazon, Brazil).

	Water Bodies	Várzea Fields	High Várzea	Low Várzea	Chavascal
Water Bodies	24	3	0	0	0
Várzea Fields	0	28	0	0	0
High Várzea	0	1	21	6	0
Low Várzea	0	3	1	18	7
Chavascal	0	0	1	2	27
N	24	35	23	26	34
% Error	0%	20%	8.7%	30.7%	20.5%
Overall accuracy 83%	Kappa: 0.8	Quantity disagreement	5%	Allocation disagreement	10%

Overall disagreement rates were of 5% for quantity and 10% for allocation. The highest allocation disagreement was observed for the Low várzea class, with 9% of misplaced objects, followed by Chavascal, with 8% and High várzea with 4%. Both Herbaceous/Soil and Water Bodies did not have a significant

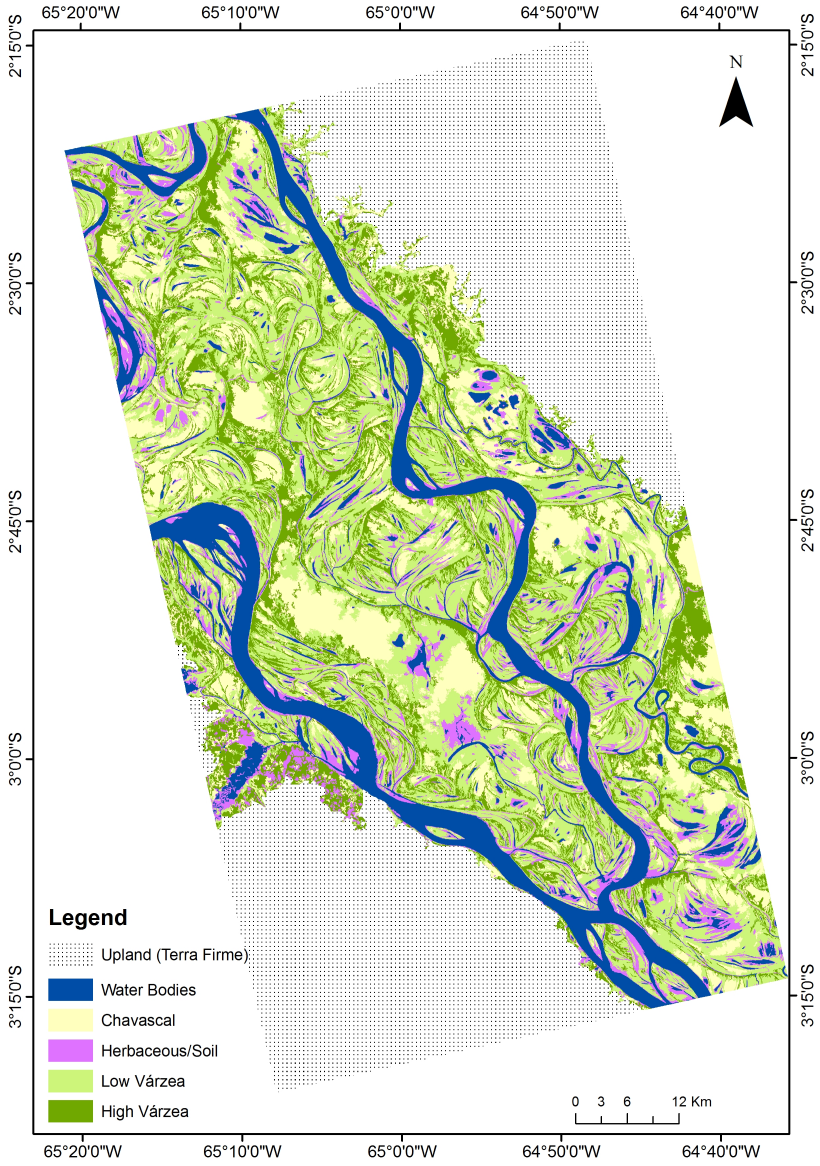

Figure 2.5: Major vegetation types and habitats of the southeastern portion of the Mamirauá Sustainable Development Reserve (Central Amazon, Brazil) and its surroundings, mapped using ALOS/PALSAR image time series, and the random forests classification algorithm.

amount of misplaced objects. Quantity disagreement indicated underestimation of Herbaceous/Soil (4%), resulting from confusion with Water Bodies, with negligible errors for the remaining classes (1-2%).

Graphical analysis of backscattering values showed the effect of flooding on the radar signal, emphasizing the different patterns of radar backscattering evolution that reflect different flood regimes for chavascal, low várzea and high várzea environments (Figure 2.6). The final image-specific thresholds selected

for inundation mapping varied between -6.57 and -5.85 dB, resulting in estimated flooding durations between less than 40 days and more than 295 days, in addition to the permanently flooded areas (Figure 2.8, Table 2.2). Overall, most areas were inundated for less than 40 days or for 125 to 175 days (Figure 2.7).

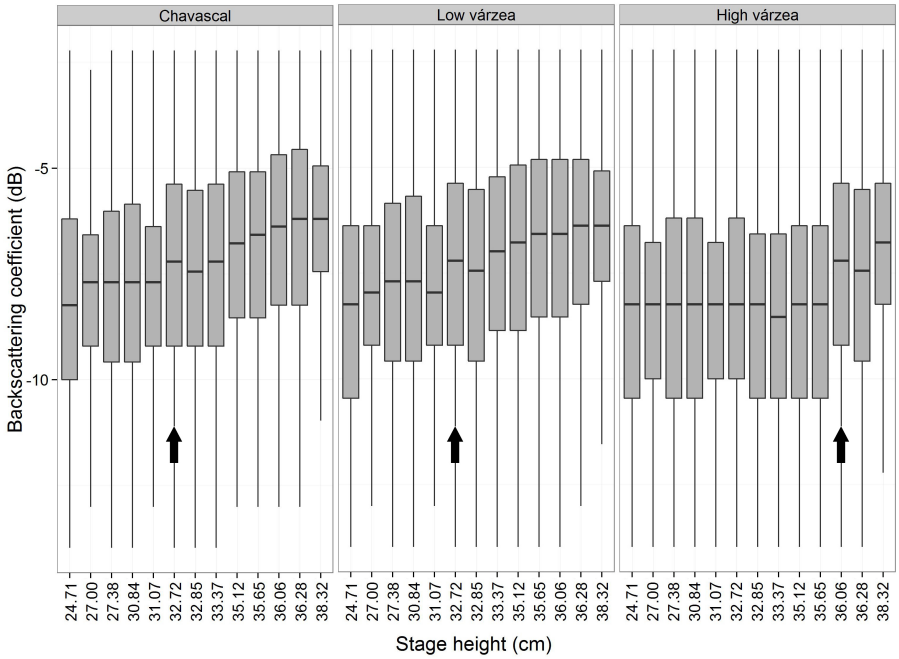

Figure 2.6: Temporal variation of ALOS/PALSAR backscattering coefficients for the three main woody vegetation classes occurring on the Mamirauá Sustainable Development Reserve (Central Amazon, Brazil). The arrows indicate the period where flooding begins. The different flooding onset and flooding patterns for each class are visible

The agreement between estimated flood durations and ground data from Affonso et al. 2011 was variable; from the 18 records, eight corresponded to the actual range of estimated flood duration, nine were off by one estimated class, and one was off by two classes (Table 2.4).

The intersection of vegetation types and flood duration classes showed that chavascal areas had the most varied inundation pattern, covering the entire range of estimated flood duration classes, with a higher frequency (49%) in the range of 105-125 days of flooding per year (Figure 2.9). Low várzea areas, on the other hand, occurred predominantly on the class labeled as 175-295 days of flooding, followed by the 125-175 days of flooding class. High várzea agreed more closely with the expected distribution across the flood duration classes, with the highest frequency being observed at less than 40 days of flooding per year. Moreover, about 181 km^2 of this class occurred in areas that were never mapped as flooded, considering the existing range of images (and which were added to the "<40 days of flooding class").

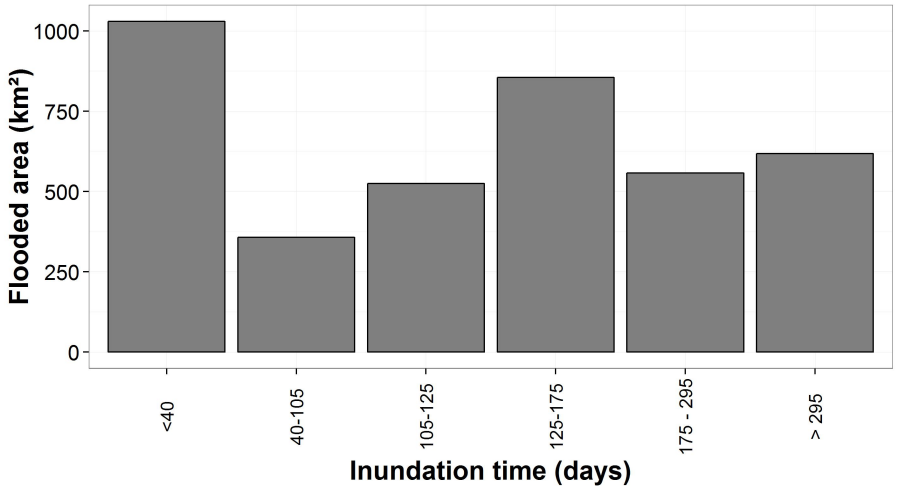

Figure 2.7: Extent of estimated flood duration classes (in days), based on ALOS/PALSAR imagery, for the Mamirauá Sustainable Development Reserve (Central Amazon, Brazil).

Table 2.4: Comparison of flood duration estimates as determined in situ using temperature gauges by Affonso et al. 2011 and Hess et al. 2011 and as derived from ALOS/PALSAR images for the Mamirauá Sustainable Development Reserve (Central Amazon, Brazil).

Station	Flood duration (days)	Flood duration PALSAR (days)
1	176	125-175
2	233	105-125
3	231	>295
4	217	125-175
5	241	>295
6	291	>295
7	219	175-295
8	237	175-295
9	239	175-295
11	238	175-295
13	240	>295
14	241	125-175
18	239	>295
19	176	175-295
20	238	125-175
21	244	175-295
22	249	>295
23	243	>295

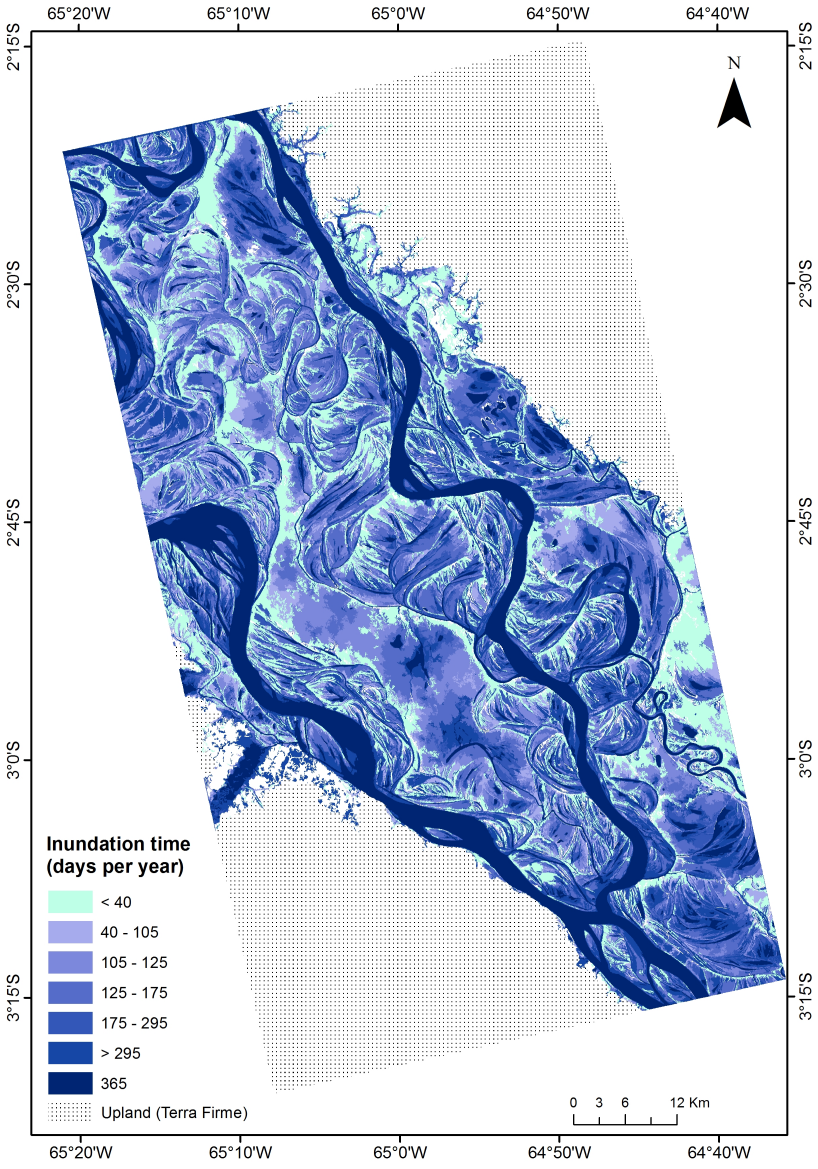

Figure 2.8: Estimated flood duration based on a time series of ALOS/PALSAR image data, for the southeastern portion of the Mamirauá Sustainable Development Reserve and surroundings, Central Amazon floodplain, Brazil.

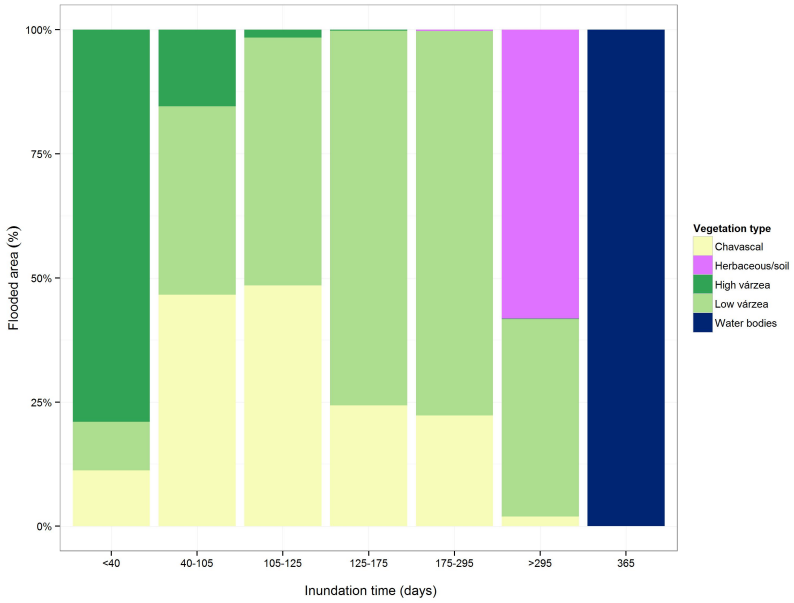

Figure 2.9: Relative area for each combination of land cover and flood duration classes derived from ALOS/PALSAR image time series for the Mamirauá Sustainable Development Reserve (Central Amazon, Brazil).

2.4 Discussion

The RF algorithm was a robust classification technique for várzea vegetation, when coupled with reliable and sufficient ground data and with OBIA methods. The availability of multitemporal information was paramount to obtain accurate class discrimination, as already shown by Martinez and Letoan 2007 and Silva et al. 2010. Due to their higher structural similarity, woody vegetation classes tended to share most of the misclassification errors, which may have led to the overestimation and erroneous allocation of Low várzea objects, compared to Chavascal and High várzea. While chavascal areas tend to form more homogeneous and densely packed stands and high várzea forests will often correspond to complex, relatively stable vegetation assemblies, low várzea regions can display a wide range of community composition and structural characteristics, depending on relative age and position along the flooding gradient. This variability was translated into well- defined class attributes for High várzea and Chavascal, while the larger variability of Low várzea samples increased classification error. L-band SAR data also led to confusion between Herbaceous/soil and water bodies, due the relative similar and smooth surface of these targets at this wavelength. The complementary use of shorter SAR wavelengths, such as C or X bands, could lower this error.

The dynamic geomorphological nature of the study area explains the naturally fragmented landscape mosaic evidenced by our mapping. In this context, high várzea forests can be seen as the narrowest and most disjoint landscape elements, while chavascal formations tend to form more aggregated, continuous fields. Noteworthy spatial associations were also observed, such as the interrelated distribution of water channels and flood duration, versus chavascal and high várzea distributions. As the chavascal occurs in poorly drained depressions or silted-up lakes, it tends to occupy the backswamps behind the levees covered by high várzea. Eventually, the establishment of pioneer vegetation will increase sediment deposition and raise the terrain level, reducing flood duration and allowing the establishment of other species, in a process of ecological and geomorphological co-evolution (Wittmann et al. 2010b). Given the well-known effect of landscape configuration on the conservation of plant and animal species (Lindenmayer et al. 2008), our detailed vegetation map can enable spatially aware decision making for conservation measures in the MSDR.

Virtually all of the study area was flooded when water levels were close to the peak of the high water phase. Results also showed that 22% of the evaluated areas were classified as "$<$ 40 days of flooding", followed by areas flooded for 125-175 days per year representing about 12% of the mapped area. The uneven distribution of flooded areas at different water levels results from the stepped nature of the floodplain terrain, where critical water stage heights result in large expansions of inundation area while other heights in the range have minimum effects. The best example of such as process is the water stage height at which transition from channel to overbank flow occurs, immediately inundating the backswamp depressions.

Although the comparison between flood duration and in situ temperature-based observations showed some disagreement, we believe that the maps obtained do represent the overall spatial distribution and variability of flooding in the studied system, and are similar to other products developed for floodplain forest environments in the Amazon (Forsberg et al. 2001; Rosenqvist et al.

2002). Three main sources of error can account for the observed disagreements: positional errors between in situ stations and image data; inherent variability of flood duration, as shown by the confidence intervals on Figure 2.3; and the fact that field data was acquired during the 2008-2009 hydrological year, the second largest flood of the last 50 years (Figure 2.4), whereas our imagery spans a broader time period. In response to our results, the Mamirauá Sustainable Development Institute is currently funding the installation of high precision level gauges, tied to surveyed altimetric transects and with accurate geolocation, to properly characterize flooding dynamics in the region. Once such data is available, the current results can be further validated and refined.

The intersection between vegetation and flood duration classes showed a wider range of combinations than expected based on the literature. Chavascal areas had shorter inundation periods than the usually recognized hydroperiod of 180-240 days of flooding (e.g. Ayres 1993; Wittmann et al. 2002), while low várzea was distributed between flood duration ranges that were higher than reported by the literature (120-180 days). This apparent inversion of results is likely owed to the higher misclassification errors between these two classes, implying that forests with a highly variable range of structural and taxonomic characteristics are distributed within the range of approximately 50-200 days of flooding. The graphical analysis of training samples based on actual ground data (Figure 2.6) suggests that inundation occurs at similar times for both classes, further adding to the differentiation problem.

While some of the unusual combinations of vegetation and flooding observed likely occurred due to classification errors, these results suggest that such combined information can be a good indicator of the complex gradient of habitats along the floodplain, including the identification of rare habitats. Further verification of these locations in the field could therefore suggest potential areas for special conservation measures, given their relative rarity in the landscape. For example, shrub-like vegetation occurring in areas flooded for short periods (mislabeled as chavascal) could indicate prevailing soil properties, such as high clay content and/or high phreatic levels, while forest communities growing at sites that were never mapped as flooded could indicate areas that only flood during extreme hydrological events, for short periods. As only 31% of várzea tree species are shared with upland forests, of which 67.5% are restricted to high várzea (Wittmann et al. 2006a), these areas could house species or assemblages that are currently rare in the landscape, but have the potential to become more prevalent under current scenarios of longer dry periods and more frequent extreme climatic events predicted for Amazonian environments (Malhi et al. 2008; Melack and Coe 2013). These areas can therefore have an important conservation role as vegetation refugia for maintaining current and future diversity in the floodplain (Ashcroft et al. 2009).

2.4.1 Management implications

The Amazonian várzeas are endangered ecosystems that require special protection initiatives (Junk et al. 2011). The composition and abundance of various components of the fauna are also associated to várzea environments and its vegetation types (Beja et al. 2010; Paim et al. 2013; Pereira et al. 2009). Detailed knowledge of the distribution and abundance of rare, endemic or threatened species in these environments is needed to define sensitive areas or areas that

should be addressed with additional efforts or special protection. The distribution and abundance of different endangered species, such as jaguars (*P. onca*), giant otters (*Pteronura brasiliensis*) and some primates such as the black squirrel monkey (*Saimiri vanzolinii*) or white uacari (*C. calvus*) are also associated with dominant types of forest formation, and the local regime of flooding (Da Silveira et al. 2010; Lima et al. 2012; Paim et al. 2013).

The flood predictability in the várzea environments is a key factor for a wide range of conservation initiatives and extractive activities of the local population that use the resources of these ecosystems. Large scale predictability already includes flood pulse intensity for some places of the Amazon, such as Manaus and Tefé (Schöngart and Junk 2007), but local scale information on flood dynamics and extent remains unavailable. Such information would allow adequate sustainable use of innumerous natural resources from the várzea ecosystems; for example, access to remote sites within the forest for extractive activities depends on previous information about flood dynamics at these sites. To plan timber exploitation on várzea forests, where there are no roads to transport the logs, local-scale flood predictability is crucial to allow wood transport by rafting during high-water periods (Schöngart and Queiroz 2010). Access to lakes and channels of exceptional productivity for Pirarucu (*Arapaima gigas*) fishing (Viana et al. 2007) and for caiman catching (Botero-Arias et al. 2009), both of which are forms of sustainable resource management in the floodplains at different stages of development, is also related to the predictability of flooding and hydrological dynamics in these locations. Therefore,providing habitat and flooding maps for the Amazon floodplain can significantly improve the efficiency in developing and managing conservation actions targeted towards these ecosystems.

2.4.2 Conclusion

Our results emphasize the potential contribution of SAR remote sensing to the monitoring and management of wetland environments, providing not only accurate information on spatial landscape configuration and vegetation distribution, but also important insights on the ecohydrological processes that ultimately determine this distribution. SAR systems are unique in their ability to map both vegetation distribution and flooding extent, and the combination of the two, together with a multitemporal approach, offers unique insight into the functioning of wetland ecosystems. Information derived from the present study also provides a solid basis for the study of plant and animal species distribution and habitat use, as well as an understanding of spatial variability of biogeochemical processes, and may ultimately support ecosystem modeling efforts and the forecasting of different ecological scenarios. It also provides an ideal database for testing the spatial implications of the "flood pulse concept" (Junk et al. 1989), a general theory of floodplain ecosystems which relates flood durations and other hydrological characteristics to the distribution and dynamics of aquatic flora and fauna. We believe our method could be successfully replicated for other seasonal wetland environments, using different kinds of SAR and optical image time series and available open-source remote sensing and statistical software. Given the rising availability of SAR sensors operating at multiple frequencies and spatial configurations, with a plethora of new systems planned or already scheduled for launch in the following years, multitemporal SAR studies could

become an affordable and reliable method for wetland ecological monitoring in the Amazon.

Chapter 3

MODELING THE SPATIAL AND TEMPORAL DYNAMICS OF INUNDATION IN AMAZONIAN FLOODPLAINS USING RADAR REMOTE SENSING AND LOGISTIC MODEL

3.1 Introduction

Flood regime and geomorphology are the prime factors modulating ecosystem structure and function in floodplain systems (Junk et al. 1989; Lewis et al. 2000). The broader paradigm regarding the function of flooding in river-floodplain systems is given by the flood pulse concept (Junk et al. 1989), which postulates that amplitude, duration, frequency and periodicity (predictability) of flood pulses are the major factor maintaining the dynamic environmental equilibrium in floodplains.

Major biogeochemical processes and the exchange of nutrients and organisms between different floodplain habitats are modulated by flooding regime (Jardine et al. 2015; Junk 1997a; Junk et al. 1989; Lake et al. 2006; Melack and Forsberg 2001; Mitsch and Gosselink 2015; Mitsch et al. 2010; Richey et al. 2002). The seasonal inundation regime also provides environmental connectivity that is critical for keeping long-term gamma diversity (Thomaz et al. 2007; Ward et al. 2002). In the community level of large river floodplains, birds and fishes have more stable communities in environments with rhythmic annual floods (Jardine et al. 2015; Luz-Agostinho et al. 2009). The occurrence, distribution, diversity, and densities of plant species is known to be strongly influenced by flood duration (Junk 1989; Luize et al. 2015; Silva et al. 2013b; Wittmann et al. 2002, 2006a). Furthermore, for many plant species living in floodplains, gaseous exchange rates are controlled by inundation, as it acts as a phenological trigger (Hawes and Peres 2016; Parolin et al. 2010).

In the Amazon, the amplitude of seasonal water level variations can reach

up to 16 m in Western Amazon, 10 m in Central Amazon, and 6 m in Eastern Amazonia, with local flood extent and duration depending on the interaction among precipitation, river discharge and geomorphology (Bonnet et al. 2008; Junk 1989; Lesack and Melack 1995; Ramalho et al. 2009). As ecological and biogeochemical processes in these systems are closely linked to climate and hydrology, they are the first to experience impacts when such conditions change (Mitsch et al. 2010). Results from numerical simulations to the end of the 21st century (2070-2099) predict increased mean (+9%) and maximum (+18.3%) inundation extent over Peruvian floodplains and the Amazon River in the western Amazon, while decreased river discharges (mainly in the dry season) are predicted for the eastern Amazon, reducing inundation extent during the low water season in the central (-15.9%) and eastern Amazon river (-4.4%) (Sorribas et al. 2016).

Guimberteau et al. 2017 included deforestation scenarios when modeling hydrological changes caused by climate change. While overall results agree with the contrasting regional changes above, the authors show that the expected decreases in river discharge for some catchments could be attenuated by increased runoff caused by deforestation, with a general consistent increase of 2.2% in runoff under the worst deforestation scenario (34% of forest loss). Climate-deforestation feedbacks in the intensely deforested southeastern Amazon basin have already caused significant hydrological changes in east-southern sub-basins (Coe et al. 2009; Coe et al. 2013).

Recent studies investigating hydrological changes in the Amazon basin have also shown that annual mean precipitation (from 1990 to 2015), wet season precipitation (from 1980 to 2015), and maximum river runoff (from 1980 to 2015) have increased, while dry season precipitation and minimum runoff have slightly decreased (Gloor et al. 2015). These changes have led to an increase in the frequency of extreme floods and "drier than usual" dry seasons in the last three decades (Gloor et al. 2015, 2013), agreeing with the expected increase in frequency and intensity of extreme events for the Amazon under climate change (Cook et al. 2012; Cox et al. 2008; Joetzjer et al. 2013; Marengo et al. 2012).

The lack of appropriate monitoring and management capacities for the large area comprising Amazonian floodplains makes them even more susceptible to changes in hydrological conditions (Castello et al. 2013). Throughout the Amazon basin, areas complying with the international criteria for wetland definition comprise between 14% and 30% of the lowland Amazon basin (Junk et al. 2011; UNEP/CBD 2003). Floodplains represent between 25 and 50% of Amazonian wetlands, or about 519,100 km^2 (Junk et al. 2011). This large uncertainty in wetlands and floodplains representativity results from methodological differences in the quantification of total wetland area (Hess et al. 2015; Junk et al. 2011; Melack and Hess 2010), mainly depending on whether small floodplains along the dense network of low-order rivers and streams are considered or not. These areas are difficult to detect either from optical or radar remote sensing, but according to Junk 1993 could reach one million squared kilometers, and were considered in the estimate by Junk et al. 2011.

One of the main current anthropogenic threats looming over Amazonian floodplain ecosystems is the construction of dams to satisfy energy demands. Brazilian Amazonian rivers have less hydroelectric plants than other biomes and incur in less compensation costs from permanent inundation of local communities and private lands, so that most of the planned hydropower plants for

Brazil are focusing on these rivers (Lees et al. 2016). According to Lees et al. 2016, Brazil will be the most impacted Amazonian country, with 143 dams already operational or under-construction, and 254 planned dams. Recently, Anderson et al. 2018 showed that Marañón and Ucayali river basins already lost about 20% of tributary network connectivity due to hydropower dams and that planned hydropower plants could decrease river connectivity up to 50%, isolating river reaches and imposing serious threatens to freshwater ecosystems. Analyzing the potential impacts of six planned hydropower dams on Andean forelands, Forsberg et al. 2017 estimated a total reduction of 64% in basin-wide sediment supply, 97 and 83 % in phosphorus and nitrogen supply and impacts to fish yeld, greenhouse gas emissions and flood pulse dynamics downstream.

Given these threats, and the critical role of the flood pulse as a driver of environmental dynamics in Amazonian floodplains, it is critical that we improve our understanding of the spatial and temporal behavior of flooding at finer scales, and its impacts on ecological systems. Important efforts have been made using hydrological models (Rudorff et al. 2014a,b; Trigg et al. 2009; Wilson et al. 2007). Although these mechanistic approaches offer many advantages in represent high-fidelity flood dynamics, accurate modeling largely depends on high quality terrain models, still unavailable for most of the Amazon basin.

Synthetic aperture radar (SAR) remote sensing has been used as an alternative to characterize landscape-level inundation extent and behavior over Amazonian floodplains (Alsdorf 2004; Alsdorf et al. 2007b; Arnesen et al. 2013; Chapman et al. 2015; Hawes et al. 2012; Martinez and Letoan 2007; Rosenqvist et al. 2002). Most of these studies, however, are limited by the temporal resolution of SAR satellites and/or by the availability of regular time-series in their ability to provide detailed spatially-explicit estimates of flood duration, the key hydrological variable for ecosystems response and adaptation.

Ferreira-Ferreira et al. 2015 was one of the first studies to combine SAR imagery with historical records of water level to estimate not only flooding extent, but also flood duration. However, the lack of regular and continuous time series of SAR data limited the predictions to semi-quantitative estimates of flood duration classes. To date, fully quantitative and spatially explicit estimates of flood duration and dynamics based on remote sensing are still lacking. Thus, the present study addresses this issue developing a method to spatially estimate flood duration using a logistic model.

3.2 Methods

3.2.1 Remote sensing data and flood mapping

The flood mapping performed in the Section 2.2.4 (Figure 3.1) was used in this study and briefly summarized here. We acquired a set of 26 ALOS-1/PALSAR scenes (Path 85, Frames 7120 and 7130), and mosaicked consecutive frames of the same date, resulting in 13 images/dates. These dates were chosen to better capture the flood pulse dynamics, providing the largest and most uniform coverage of water level conditions within the available imagery (Table 3.1). The acquired images captured a stage height range from 24.71 to 38.32 meter above sea level (masl), as recorded in the Mamirauá lake gauging station, or about 70% of the historical maximum amplitude for this gauge.

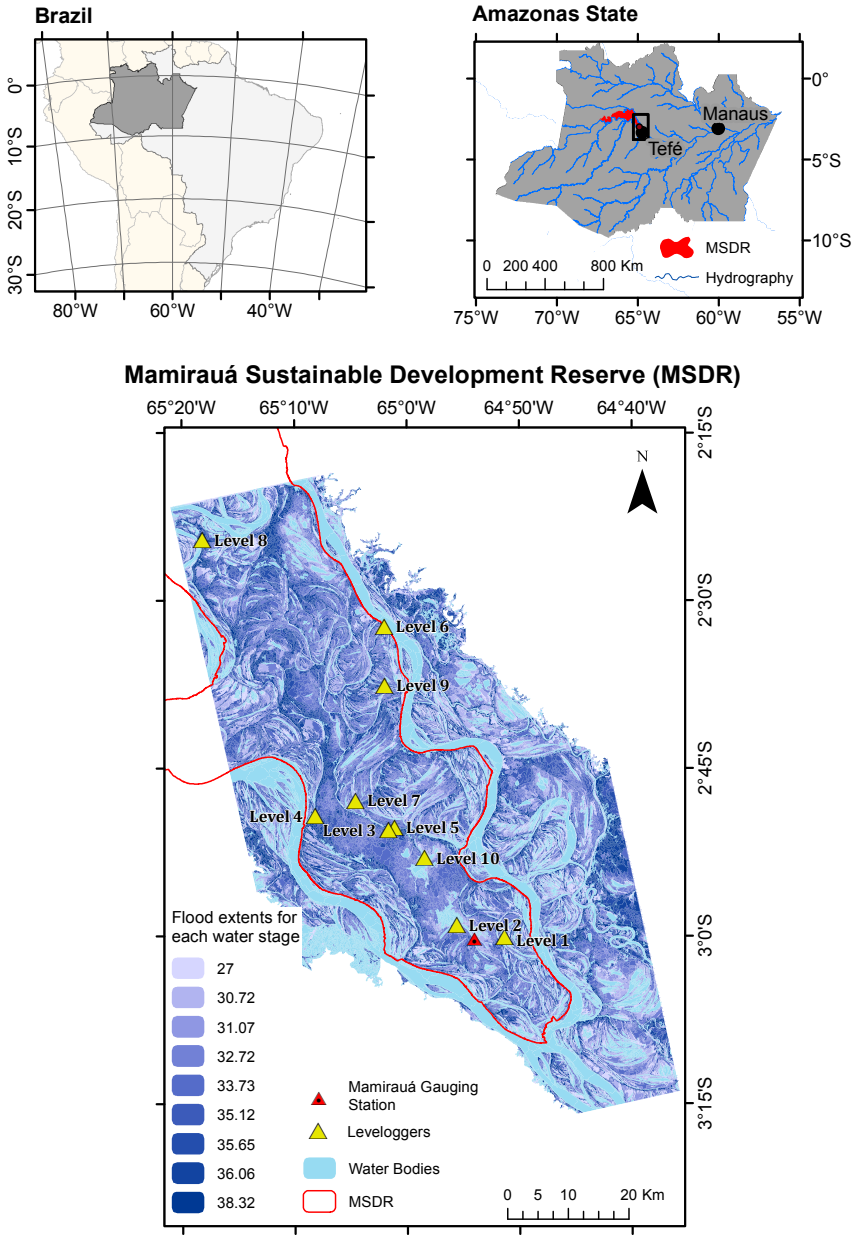

Figure 3.1: Southeastern portion of Mamirauá Sustainable Development Reserve (MSDR), in the Central Amazon floodplain, Brazil. The underlying map is the flood extent for each water stage recorded in Mamirauá gauging station for the dates of ALOS-1/PALSAR imagery used (see Chapter 2)

.

Table 3.1: ALOS-1/PALSAR images acquired for different water levels to map flood extent in the Mamirauá Sustainable Development Reserve (Central Amazon, Brazil). The range of captured water stages comprises 70% of the maximum historical amplitude for this location.

PALSAR acquisition date	Mode	Water stage height (masl)
2010-09-22	FBD	24.71
2007-10-30	FBS	27.00
2010-12-23	FBS	27.38
2008-12-17	FBS	30.02
2007-12-15	FBS	31.07
2010-03-22	FBS	32.72
2008-08-01	FBD	32.85
2007-07-30	FBD	33.37
2008-05-01	FBD	35.12
2010-05-07	FBD	35.65
2007-06-14	FBD	36.06
2010-06-22	FBD	36.28
2009-06-19	FBD	38.32

FBS - fine beam single (HH polarization), *FBD* - fine beam dual (HH/HV polarization). Water level heights were obtained from Mamirauá gauge station. (IDSM 2013; Ramalho et al. 2009).

Water stage heights were recorded at the Mamirauá Lake gauging station, located in the southern portion of the study area (see Figure 3.1; IDSM 2013; Ramalho et al. 2009) and paired with image acquisition dates to determine the expected water levels at the time of acquisition of each image. This data is freely available at http://mamiraua.org.br/pt-br/pesquisa-e-monitoramento/monitoramento/fluviometrico/. Based on backscattering thresholds, Ferreira-Ferreira et al. 2015 mapped flooded areas in each of the 13 images. As some water levels were considered too similar, some flood maps were disregarded resulting in flood extent maps for nine water stages: 27.00, 30.72, 31.07, 32.72, 33.73, 35.12, 35.65, 36.06 and 38.32 masl (see Figure 3.1).

To support the empirical inundation modeling, we obtained the Shuttle Radar Topography Mission Digital Elevation Model (SRTM-DEM) version 3.0 with 1 arc second spatial resolution (about 30 meters; Available at http://reverb.echo.nasa.gov/reverb/). From SRTM-DEM we derived , (1) the terrain Height Above the nearest drainage (HAND), (2) euclidean distance from the nearest drainage (EDND), (3) slope (SLP), (4) terrain curvature (TC), (5) profile curvature (PC), (6) planform curvature (PLANC) and (7) accumulated precipitation 15 days prior to each image acquisition date (PCP).

HAND is a locally and hydrologically coherent terrain descriptor that normalizes the topography in respect to the drainage network, applying two sequential procedures on a DEM. First, the algorithm creates a hydrologically coherent DEM, by defining flow paths and delineating channels and lake basins.

Then, it uses local flow directions and the estimated drainage network to derive the nearest drainage map, which will then guide the HAND algorithm in calculating the normalized topography (Nobre et al. 2011; Rennó et al. 2008). The HAND algorithm is implemented in the TerraView GIS Software (http://www.dpi.inpe.br/terraview/index.php). The resulting HAND model was resampled using nearest neighbor assignment to 12.5 meters to match the flooding map resolutions.

EDND was determined using the "gdal_proximity.py" python routine implemented in Geospatial Data Abstraction Library (GDAL; http://www.gdal.org/gdal_proximity.html). The output cell size was also set to 12.5 meters.

SLP, TC, PC and PLANC were calculated using algorithms available in ArcMap 10.3, an implementation of the methods by Zevenbergen and Thorne 1987 and whose detailed procedures are described in the official documentation, available at http://desktop.arcgis.com/en/arcmap/10.3/tools/spatial-analyst-toolbox/an-overview-of-the-surface-tools.htm. SLP was processed to express angles in degrees. TC is the second derivative of the vertical dimension of the raster surface with respect to slope (i.e. "the slope of the slope"). A positive cell value indicates the surface is upwardly convex at that cell, while a negative curvature indicates the surface is upwardly concave. A flat surface is assigned a value of 0. PC is the terrain's curvature in the direction of maximum slope - i.e. the rate of change in slope - which affects the acceleration and deceleration of water flow. Finally, PLANC is the curvature of the land surface in the perpendicular direction of the slope, influencing flow convergence and divergence. Both TC, PC and PLANC units are in hundredths (1/100) of the vertical unit (meters). Reasonable expected values for all three output variables for an area of moderate relief can vary from -0.5 to 0.5.

We also used daily precipitation estimates from the 3B42-v7 product of TRMM (Tropical Rainfall Measuring Mission), at 0.25° spatial resolution, downloaded from http://mirador.gsfc.nasa.gov/. From this dataset, we extracted the accumulated precipitation 15 days prior to the acquisition date of each SAR image used to map flood extent (see Table 3.1), resulting in nine accumulated precipitation observations to be included in our model.

3.2.2 Flood monitoring

We monitored *in-situ* flood dynamics to calibrate the flooding model, using ten pressure transducers ("leveloggers", *Level Logger Edge Solinst®* model M20) and two barometers (*Barologger Edge Solinst®*). These transducers are equipped with Hastelloy type piezoresistive sensors, measuring the total absolute pressure above the sensor, i.e. atmospheric plus hydrostatic pressure when submerged. Expected accuracies are within ±1 cm for levelogers, and ±0.05 kPA for barologgers.

All loggers had their internal systems codified with unique identifiers and were programmed to collect data every 8 hours (8, 16 and 24h, GMT -4). Cylindrical supports of galvanized steel, bored and open at the ends were built to allow free water movement and prevent sediment accumulation on the sensor (Figure 3.2 and Figure 3.1).

Logger distribution was planned in a GIS environment, to ensure coverage of all flood duration classes mapped by Ferreira-Ferreira et al. 2015. Following the manufacturer's recommendations, no leveloggers were installed beyond 30 Km

(a) (b)

Figure 3.2: Installed leveloggers to flood monitoring in the Southeastern portion of Mamirauá Sustainable Development Reserve (MSDR), in the Central Amazon floodplain, Brazil. (a) Leveloggers have about 16cm and it was fixed in (b) cylindrical supports of galvanized steel, bored and open at the ends to allow free water movement and prevent sediment accumulation. Leveloggers were attached to the base of large trees, at about 5 cm from the ground.

from a barologger, thus preventing compensation errors from horizontal atmospheric pressure variations. The devices were installed in two field campaigns during the dry season (December/2013 - January/2014). GIS planned logger locations were loaded in a Trimble® ProXRT double-frequency (L1/L2) GNSS receiver. Each levelogger was attached to the base of a large tree, at about 5 cm from the ground, and the barologgers were positioned above the maximum flood water marks left on the trunks. Logger geographic positions were determined with an average planimetric precision of 90 cm (Figure 3.1).

Water level data was retrieved for 4 full hydrological cycles, from December/January of 2014 to October 2017. Exceptions are the leveloggers 8 and 9 which could not be accessed due to low water conditions in October 2017 and which data extends until January 2017. The raw measures made by the leveloggers were subsequently compensated for atmospheric pressure using the barologger measurements, using the Levelogger Series Software (`http://www.solinst.com/downloads/`). Final measures were expressed in centimeters of water column above the sensor.

As we had three water stages measurements per day, we filtered the data series to include only the daily maximum water stage. Considering the expected accuracies, leveloggers were labeled as "flooded" when a water column $\geq$2 cm was recorded. After labeling all observations as either "flooded" or "non-flooded", we then determined flood start and end dates, as well as flood height and duration, for each levelogger and hydrological season.

3.2.3 Flood modeling with logistic regression

The basic rationale of our proposed method is to be able to predict *per pixel* flooding probability based on daily observations of water stage level, and then use probability thresholds to determine if it could be considered flooded for the given water level. Daily model predictions obtained for a full hydrological cycle would then allow us to estimate the spatial distribution of flood durations.

To describe the relationship between flood probability and predictor variables we used a logistic regression model. Logistic regression uses the log odds-

ratio as link function (Equation 3.1) and the anti-logit to transform logit-scaled values in probabilities ($0 \geq p \leq 1$; 3.2) (Kleinbaum and Klein 2010).

$$log_e \left(\frac{p}{1-p} \right) = \alpha + \beta_1 x_1 + \beta_2 x_2 + ... + \beta_i x_i \tag{3.1}$$

$$p = \frac{e^{\beta_0 + \beta_1 x}}{1 + e^{\beta_0 + \beta_1 x}} \tag{3.2}$$

where p would be the flooding probability, β_i are the model coefficients, and x_i are observed values of predictor variables.

We first converted our flood maps into binary rasters representing observations of flooded and non-flooded pixels (1/0) for our nine water stages mapped through ALOS/PALSAR imagery. According to Silvapulle 1981, a certain degree of overlap in the response variable is necessary so as there be sufficient conditions for the existence of maximum likelihood estimates for a binomial response model, otherwise at least one coefficient estimate diverges to $\pm\infty$ (Heinze and Schemper 2002). The nature of our analyzed phenomenon (floods) did not show any overlap, i.e. there was always a water stage value that perfectly separates whether a given pixel was flooded or not. To fit the model under this restriction, we used the *logistf* R package (Heinze et al. 2013), which implements the Firth 1993 solution for bias reduction on coefficient estimation using a penalized maximum likelihood scheme (see Heinze and Schemper 2002).

We started by fitting a full model including all predictor variables, and successively tested all possible variable combinations. For each model, we generated predictions of *per-pixel* flooding probability using water level data from the Mamirauá gauging station spanning 2014 to 2017, the same observation range of the levelogger water level data. To compute annual flood duration, we converted probability values to binary values (flooded-non/flooded). The probability threshold defining if a pixel was labeled as "flooded" was determined through a 4-fold cross-validation.

First, we defined every hydrological year as starting at the minimum water level of a given calendar year, and ending at the next year's minimum. We looked at the probability values of the first hydrological year (2014) in each of the ten levelogger pixels when the devices were first submerged and calculated its mean value. This one-year mean probability was then used as threshold to define flooded/non-flooded pixels (0/1) of the remaining years for the entire study area.

The process was repeated for all years, using one year to define the flood probability threshold and the three remaining years for validation. The predicted annual flood duration of the remaining years were compared to levelogger data to compute the RMSE (root mean squared error), finally resulting in 12 RMSE values (4 years used to thresholds definition x 3 remaining years each of these 4 years). Yearly thresholds defined in the cross validation were then averaged and used to generate models results, i.e. daily flood maps and annual flood duration computation. Final model selection was based on the smallest mean RMSE.

3.3 Results and discussion

The best inundation prediction model used only water stage (WS) from the Mamirauá gauging station and the HAND terrain descriptor as predictor variables, with one interaction term (model 1, Table 3.2). Mean probability threshold defining if pixels were flooded or non-flooded was 0.942. The model had a mean RMSE of 44.73 days (range: 28.71 to 84.74, see Figure 3.3a) whereas the next three best models achieved RMSE of 47.55, 61.03 and 70.86 days, respectively.

Table 3.2: Best logistic models assessed to predict flood duration in the Mamirauá Sustainable Development Reserve (Central Amazon, Brazil).

	Model	Average RMSE	SE
1	$-0.28 + (5.087WS) + (0.039HAND) + (-0.120(WS \times HAND))$	44.73	4.48
2	$-0.197 + (5.101WS) + (0.060HAND) + (-0.0001EDND) + (-0.119(WS \times HAND))$	47.55	5.89
3	$0.421 + (4.809WS) + (-0.047HAND)$	61.03	10.17
4	$0.584 + (4.810WS) + (-0.020HAND) + (-0.0001EDND)$	70.86	12.50

Average RMSE - average root mean square errors among 4-fold cross validation folds; *SE* - standard errors of the averaged RMSE.

Results from 4-fold cross validation showed that flood duration errors were mostly influenced by flood onset errors when compared to flood ebb (Figures 3.3b and 3.3c). Flood onset RMSE ranged from 21.35 to 63.23 days whereas flood ebb ranged from 8.06 to 23.68 days.

In general, 2016 was the year presenting large errors when using another year mean probability threshold to predict 2016 flood duration. This is probably due to the exceptional water levels recorded by the gauging station of that year, which recorded values close to the minimum historical levels (1991-2017; Table 3.3). The largest RMSE of the cross validation was achieved using 2015 (maximum water level of 36.93 m.a.s.l.) mean probability threshold, the highest water level in the 4-year series, to predict 2016 (maximum water level of 32.74 m.a.s.l.) flood duration, the lowest maximum water level on our series.

Outputs from flood duration modeling resulted in maximum flood durations of 152, 222, 174, and 199 days for 2014, 2015, 2016, and 2017, respectively (Figure 3.4). Pixels presenting these maximum flood duration values per year represented 43% of the total pixels in the mapped area, except for 2016 whose pixels with maximum flood duration represented 19% of the total (Figure 3.5).

Prediction errors can be mainly associated with two sources of uncertainty: (i) inaccuracies in the flood extent maps from Ferreira-Ferreira et al. 2015 used

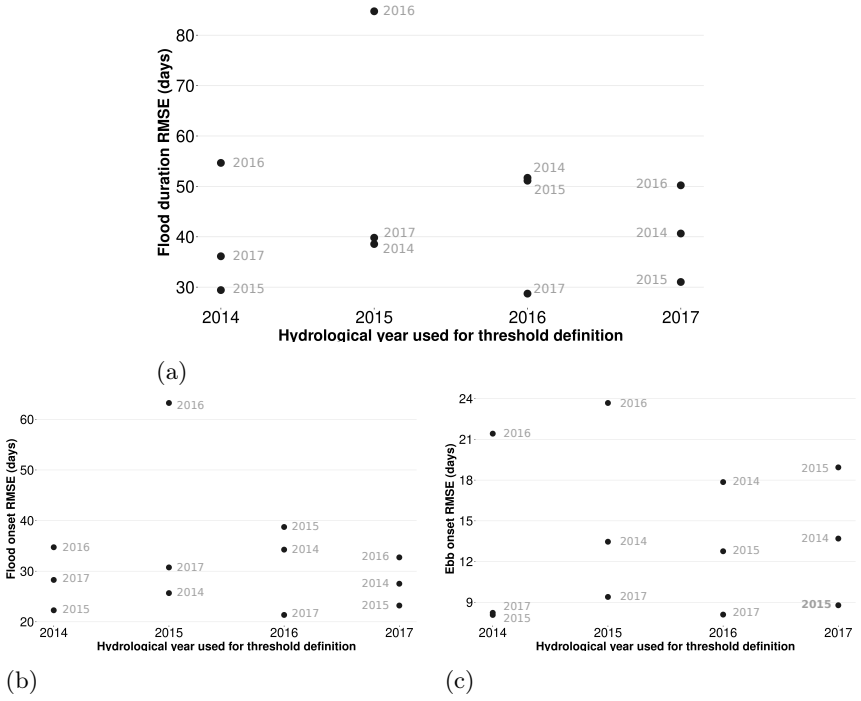

(a)

(b)

(c)

Figure 3.3: Root mean squared errors (RMSE) of the 4-fold cross validation by yearly mean probability threshold used to predict flood duration(3.3a), onset (3.3b) and ebb (3.3c) of the remaining years (dots) in the southeastern portion of Mamirauá Sustainable Development Reserve (MSDR), Central Amazon floodplain, Brazil.

Table 3.3: Comparison of historical and 2016 water levels as recorded by Mamirauá lake gauging station in the Mamirauá Sustainable Development Reserve (Central Amazon, Brazil). Statistics presented for the historical records are the minimum of the minima, the minimum of the maxima, the minimum recorded amplitude and of the mean records.

	historical	2016
Min	21.71	22.47
Max	31.10	32.74
Ampl	03.86	10.27
Mean	26.96	27.94

to fit the model and (ii) coarseness and inaccuracy of the terrain (SRTM) data, from which HAND and other terrain descriptors were derived. Additionally, an issue influencing predicted flood durations is the actual HAND inability to represent topographical levels below the nearest drainage level, cases where a value equal to zero is assigned, thus contributing to the concentrations of predicted values towards maximum flood durations. Slightly modifications on the HAND algorithm to allow negative values may also contribute to improve

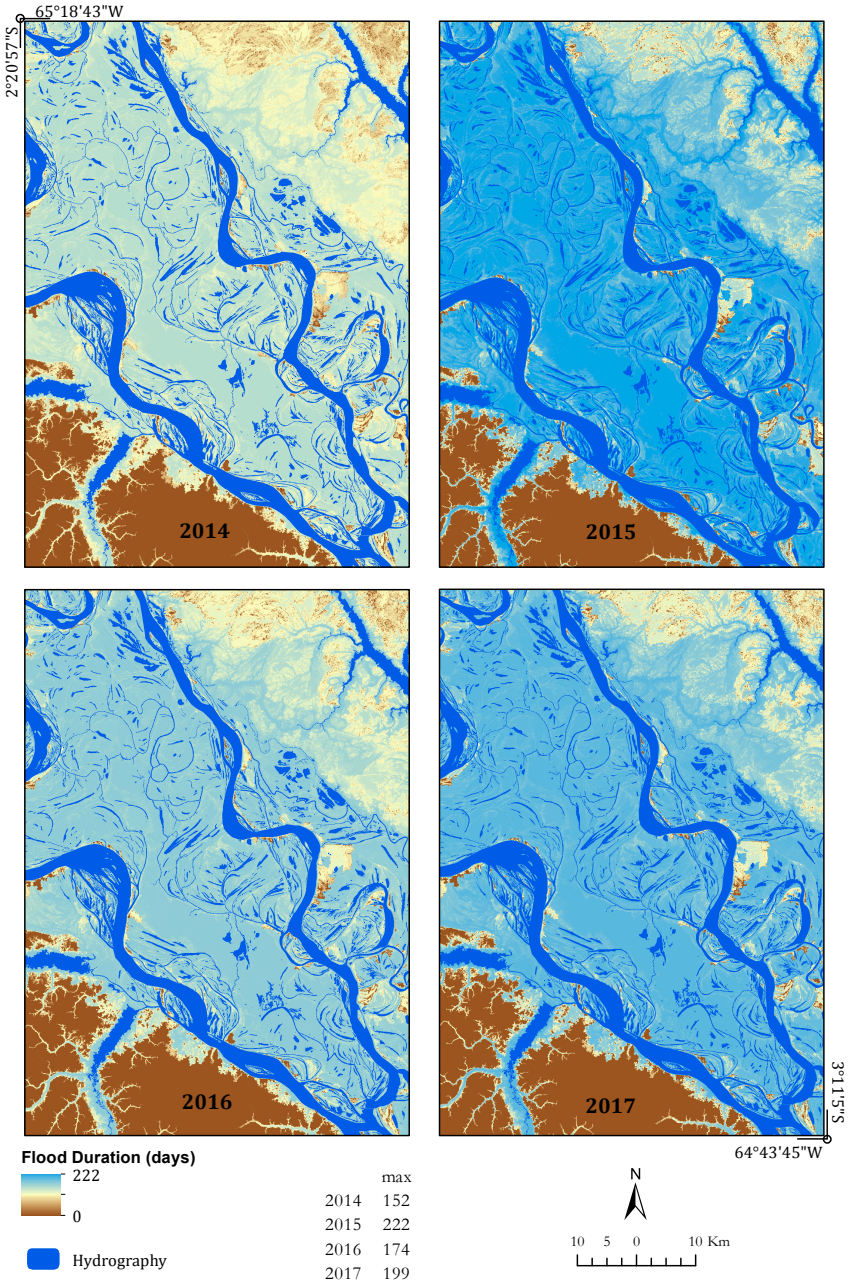

Figure 3.4: Flood duration as predicted by the logistic model applied in the southeastern portion of Mamirauá Sustainable Development Reserve (MSDR), Central Amazon floodplain, Brazil. Maximum flood duration predicted in days by year is showed in the legend.

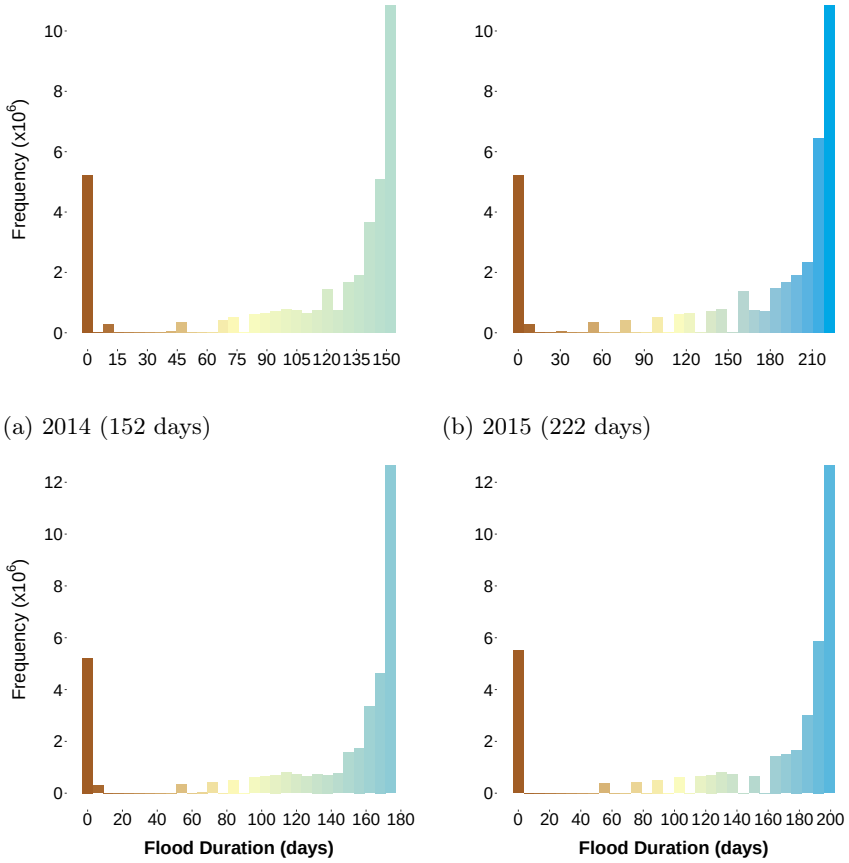

(a) 2014 (152 days)

(b) 2015 (222 days)

(c) 2016 (179 days)

(d) 2017 (199 days)

Figure 3.5: Histograms of flood duration as predicted by the logistic model, by year, applied in the southeastern portion of Mamirauá Sustainable Development Reserve (MSDR), Central Amazon floodplain, Brazil. Maximum flood duration predicted by year is showed.

our model.

Ferreira-Ferreira et al. 2015 identified backscattering threshold values separating flooded and non-flooded areas, and applied this value to each image in their timeseries to obtain flood extent maps. Although the method has been widely used (e.g Chapman et al. 2015; Martinez and Letoan 2007), it is subject to errors due to the complex backscattering response resulting from different combinations of incidence angles and vegetation structure. There is a strong correlation between SAR backscattering and vegetation structure (Henderson and Lewis 1998; Silva et al. 2015; Townsend 2002), so that the signal scattered back to the SAR antenna from the flooded areas respond slightly different under distinct vegetation types (Arnesen et al. 2013; Hess et al. 1995; Silva et al. 2010). Therefore, is plausible that flood extraction using an unique threshold applied to the whole image could under or overestimate flooded areas, hence introducing bias in flood duration estimates of our model.

It is worth to mentioning that we used flood maps from nine water stages depicted in available ALOS-1/PALSAR imagery to fit the models. Yet unavailable higher temporal resolution L-band imagery could probably improve these results as more flooded pixels from more water stages (samples) would be available.

Regarding coarseness and inaccuracy of SRTM data (ii), a global assessment of SRTM identified a coherent long wavelength height error of the order of ±10 meters across the South America related to interferometric baseline roll oscillation (Rodriguez et al. 2006). In addition, SRTM elevations are estimated to be located around 40% of the C-band's path from the top of the canopy towards the ground, on average, with increasing uncertainties related to increasing SRTM roughness (measured as the standard-deviation of elevations in a 3x3 array) (Carabajal and Harding 2006). SRTM spatial resolution may also introduce errors due to the complex local geomorphology, in many places formed by narrow and elongated scroll bars.

These complex spatial and temporal patterns of water movement across the floodplain are also difficult to capture in hydraulic models based on SRTM data (Alsdorf et al. 2007b). Incomplete hydrological processes derived from errors in topographic data significantly decrease the accuracy of hydraulic models between high and low water seasons (Wilson et al. 2007). Until more precise topographic data are available for large areas of the Amazonian floodplains (Rudorff et al. 2014a), hydrological processes within floodplains will still be misrepresented. This is especially true in the low, mid-rising and receding water seasons, when water flow stops being hydraulically influenced and starts to be bathymetrically/topographically controlled (Alsdorf et al. 2007b).

Since the JERS-1 and ALOS-1 spaceborne L-band SAR missions, remote sensing-based studies aiming to provide spatially explicit flood duration estimates for floodplains has been demonstrated as a feasible alternative (Ferreira-Ferreira et al. 2015; Hawes et al. 2012; Martinez and Letoan 2007; Rosenqvist et al. 2002; Silva et al. 2015). There is, however, an important "trade-off" between hydrological modeling and empirical flood duration estimation using SAR remote sensing. While the first is capable of simulating daily or hourly water stages during the passage of the flood waves, its capacity to estimate water permanence within floodplains is still severely constrained by yet unavailable high-quality terrain models, even at sub-basin scale. On the other hand, C and L-band SAR imagery are able to detect the presence of water under vegetation canopies (Hess et al. 1995; Silva et al. 2008), but the ability to mapping the water movement across floodplains is strongly limited by two factors: (i) the temporal resolution satellites are able to reach and/or (ii) regularity of available image time series.

The best estimates derived from SAR remote sensing mapped flood duration classes within 44-day intervals using regular image timeseries of coarse resolution SAR imagery (Rosenqvist et al. 2002), or average time intervals combining irregular image time series with historical water stage records (Ferreira-Ferreira et al. 2015; Hawes et al. 2012). Our current approach improves on these limitations by providing a high-resolution, spatially explicit flood duration estimate that can be derived for each individual hydrological year or period of interest, and allows for back- and forecasting using historical or modeled stage height inputs.

Since flood dynamics are the key driver of ecological and biogeochemical processes in floodplain ecosystems, this capability for spatially estimating flood

duration offers new opportunities for understanding landscape-level processes. For example, Nahlik and Mitsch 2011 and Villa and Mitsch 2014 have recently demonstrated that variations in methane emissions rates from tropical and subtropical wetlands are strongly correlated with flood depth and duration,being higher at intermediate water levels and lower at shallower and deeper water depths.

In the Amazon main-stem and their fringing floodplains, annual methane emissions is estimated to vary between 0.67 Tg C yr^{-1} and 2.4 Tg C yr^{-1} between minimum and maximum total flooded areas (Melack et al. 2004). But explicit evaluations of spatial heterogeneity in methane emission rates are still lacking. Bousquet et al. 2006 suggest that the negative trend in global natural emissions of methane between 1993 and 2001 was mainly in response to a detected decrease in total flooded area worldwide.

Our method offers the possibility to improve previous landscape-scale estimates through the production of annual flood duration maps which can support more precise predictions of biogeochemical processes and its alteration by hydrological shifts due to climate change.

Primary productivity is also linked to the inundation period. Many tree species reduce their atmospheric CO_2 uptake by about 10% to 50% during the aquatic phase (Parolin 2000; Parolin and Wittmann 2010), while highly productive aquatic grass stands occurring in low-lying areas have their stem elongation and horizontal expansion strongly influenced by flood duration and amplitude (Silva et al. 2013b). These grasses can contribute with up to half of floodplain productivity in some areas (Engle et al. 2007), and hydrological variability could lead differences in annual grass productivity of up to 50% (Silva et al. 2013b). Therefore, once we are able to spatially predict flood duration, new possibilities arise to estimate community-level carbon stocks and fluxes in these environments.

Flood duration is also a major force driving plant species occurrence, distribution, and diversity, as well as individual densities in Amazonian floodplains (Junk 1989; Luize et al. 2015; Silva et al. 2010; Wittmann et al. 2002, 2006a). As partial or complete submergence tolerance varies between plant species and ecotypes, floodplain communities present local-scale habitat zonation along the flood gradient and form a complex environmental mosaic across floodplains (Junk 1997a; Wittmann et al. 2010b).

Lewis et al. 2000 studied population dynamics, biogeochemistry and river-floodplain exchanges, controls of consumers community structure, and food webs and energy flows over 15 years in the Orinoco basin. The authors proposed that most major ecological complexity of the floodplains in the Orinoco basin can be explained by geomorphological and hydrological factors, suggesting the biotic predictability of this system led by its surprisingly degree of environmental order and repetition.

Amazonian floodplains and their counterparts in Orinoco basin were separated ca. 10.5 million years ago and possibly episodic connections occurred afterwards as currently occurs at Cassiquiare canal (Wesselingh and Hoorn 2011). This explains the striking similarity between their floodplains' biota as well as their hydrological, geomorphological, and ecological processes (Junk 1997c). So it is likely we can take the same assumptions to the Amazonian floodplains and use flood duration estimates to better understand their ecological spatial patterns.

Our method to estimate flood duration spatial heterogeneity extends our capability to answer relevant scientific questions regarding Amazonian floodplains ecological structure and functioning as well as biogeochemical processes. The uncertainties in flood modeling we report shows that further development is needed. This prevented us to use flood duration predictions in the following sections. However, the method proved feasible, applied the necessary corrections in the HAND model and in the flood extent maps given as input in the model. It also offers possibilities of make predictions about different ecological and biogeochemical scenarios under climate change. As we used global coverage, high-resolution, and readily available ALOS-1/PALSAR data our empirical modeling methodology can be replicated to other large tropical floodplains where water stage records are available. Additionally, at least three spaceborne L-band sensor should be available around 2020: the US-India joint mission NISAR (L- and S-band), the Japanese ALOS-4, and the Italy-Argentina joint mission SAOCOM-1 and 2, besides the first spaceborne P-band SAR, the European BIOMASS mission.

Chapter 4

ABOVEGROUND CARBON STOCKS IN AMAZONIAN VÁRZEA FORESTS: THE ROLE OF FOREST SUBTYPES AND FLOOD REGIME

4.1 Introduction

The quantitative assessment of how much carbon is stored in the living biomass and how it varies in space and time is paramount to understand biogeochemical cycles (Carvalhais et al. 2014), how human activities affect them (Baccini et al. 2012), and to develop better environmental policies (Freitas et al. 2018). The estimated carbon stored among all kingdoms of the global biosphere is 550 Pg C, of which approximately 80% (450 Pg C) are plants (Bar-On et al. 2018). Tropical forests alone store 247 Pg C, of which 121 Pg C (49%) are estimated to belong to tropical forests of South America (Saatchi et al. 2011), and nearly 85% of South American carbon stocks are estimated to be stored in the Amazonian forests (107.5±12.5 Pg C; Baccini et al. 2012; Gibbs et al. 2007; Malhi et al. 2006).

Wetlands cover c.a. 30% of the Amazon basin (Junk et al. 2011). However, most studies on biogeochemical cycling and carbon stocks have been concentrated on the Amazonian non-floodable (*terra firme*) forests, overlooking the extent and significance of the Amazonian wetlands in these processes (Junk et al. 2012; Sousa Jr et al. 2011). Eutrophic floodplain (várzea) environments comprise between 13% and 27% of Amazonian wetlands, and 75% of its area is covered with forests (Junk et al. 2011; Melack and Hess 2010). These forests experience seasonal water level variations of 10-13 meters (Junk 1989; Ramalho et al. 2009), strongly influencing tree establishment and growth, and many biogeochemical and ecological processes in general (Junk 1997a; Melack and Forsberg 2001; Mitsch et al. 2010).

The broader theory regarding the function of inundation in floodplain systems is given by the flood pulse concept (Junk et al. 1989), which postulates that amplitude, duration, frequency and periodicity (predictability) of flood pulses are the major factor influencing ecosystem processes. The modulating effect of flooding is known to strongly influence occurrence, distribution, diversity, and densities of várzea plant species, creating a typical zonation along the

flood gradient (Junk 1989; Luize et al. 2015; Silva et al. 2013b; Wittmann et al. 2002, 2006a). Seasonal flooding also acts as a phenological trigger, controlling gaseous exchange rates (Chapter 5, Hawes and Peres 2016; Parolin et al. 2010) and carbon assimilation in many várzea tree species (Parolin 2000; Parolin and Wittmann 2010).

The biomass stocks of várzea forests can vary depending on forest subtypes (high várzea, low várzea, chavascal). Schöngart et al. 2010 estimated the aboveground coarse wood biomass (AGWB) in várzea forests of different successional stages in Central Amazon, reporting values ranging from 55.99±4.23 Mg C ha^{-1}(low várzea) to 112.33±5.17 Mg C ha^{-1}(high várzea). Nebel et al. 2001 estimated aboveground carbon stocks in three forest subtypes in Peru, reporting values of 116.05 (chavascal) to 91.37 Mg C ha^{-1}(high várzea). However, little is still known about the influence of the flood regime on aboveground carbon stocks in the Amazon várzeas, and whether patches of the same forest subtype under different flood durations may have significant differences in carbon stocks, since the phenology, structure and species composition of each patch can be strongly influenced by the hydrological regime.

This chapter advances our understanding of how aboveground carbon (AGC) stocks can vary as a function of landscape heterogeneity and spatial hydrological variation. Specifically, we address the following questions: (i) How much and in which direction aboveground carbon stocks vary depending on forest subtypes and flood regimes? (ii) Which of the factors influencing AGC are most affected by flood duration?

4.2 Methods

4.2.1 Sample Design

We established 18 forest plots of 0.25 ha (50 x 50 meters; total of 4.5 ha). The forest plots were distributed within the study area in a stratified sample design by forest subtype (high várzea, low várzea and chavascal forests). For each forest subtype, 6 forest plots were installed, covering a range of topographical levels to capture distinct flood regimes. The sites were chosen over a six-day expedition conducted in January 2017, surveying about 34 floodplain sites and observing the general forest structure and composition to determine the subtype, supported by a trained parabotanist.

As flood height is directly related to flood duration, we recorded watermarks left on tree trunks by the last flood season (2016), choosing five trees distributed at the four corners and the center of each plot, to determine the different flood regimes per forest subtype (considering that flooding height is a direct proxy of flood duration (Table 4.1).

We then inventoried all living trees with diameter at breast height ≥10 cm, in all plots. Palms, epiphytes and hemi-epiphytes were not included in the inventories. All inventoried trees were tagged with unique identifier numbers using aluminum plates. Botanical identification was made for all tagged trees in the field by a botanist and a parabotanist, and botanical vouchers were collected for species whose identification was not possible by direct observation. Vouchers were transported to the herbarium at the National Institute of Amazonian Research (INPA), Manaus, where they were identified to the lowest taxonomic

Table 4.1: Sample design of forest sample plots triplicates for estimates of aboveground biomass and monitoring of seasonal litterfall under different flood regimes and forest types in várzea forests of Mamirauá Sustainable Development Reserve (Central Amazon, Brazil). Mean watermark height (WM) and its standard error of the mean (SE) refers to measurements taken in the field.

Plot ID	Forest type	WM (±SE)
Plot 1a	High várzea	1.76±0.06
Plot 1b	High várzea	1.36±0.04
Plot 1c	High várzea	1.10±0.06
Plot 2a	High várzea	2.34±0.11
Plot 2b	High várzea	2.96±0.12
Plot 2c	High várzea	1.52±0.24
Plot 3a	Low várzea	3.54±0.34
Plot 3b	Low várzea	1.86±0.03
Plot 3c	Low várzea	2.62±0.19
Plot 4a	Low várzea	4.79±0.38
Plot 4b	Low várzea	5.06±0.28
Plot 4c	Low várzea	4.36±0.60
Plot 5a	Chavascal	4.33±0.08
Plot 5b	Chavascal	3.86±0.21
Plot 5c	Chavascal	3.85±0.09
Plot 6a	Chavascal	5.25±0.25
Plot 6b	Chavascal	3.56±0.23
Plot 6c	Chavascal	5.29±0.31

level possible. According to herbarium regulations, only fertile voucher material was permanently deposited.

For each inventoried tree, we measured diameter at breast height (DBH) and total tree height (h). DBH was measured using a diametric tape and h was estimated by trigonometry (Equation 4.1) using the distance from the observer to the tree (d), elevation angle to the tree top (θ) and eye height of the observer (h_{eye}). Distance from the observer to the tree (d) was measured with a laser range finder (*Bosch*® GLM 80), and elevation angle (θ) was measured using a clinometer (*Suunto*® PM-5).

$$h = d \times tan\theta + h_{\text{eye}} \tag{4.1}$$

4.2.2 Data Analysis

All numerical analyses was conducted in R statistical programming language (R Core Team 2018). Binomial taxonomic names were checked using the Taxonomic Name Resolution Service (TNRS) provided in the *correctTaxo* function of "BIOMASS" R package (Rejou-Mechain et al. 2017). For each plot we calculated the α parameter of Fisher's logarithmic series used as a diversity index (referred as α diversiy; Fisher et al. 1943) and the Berger-Parker dominance index (D; Berger and Parker 1970), simply defined as the proportional abundance of the most abundant species relative to the total number of individuals in the plot.

To evaluate the β diversity of all pooled plots we used the Sørensen index of dissimilarity (Sørensen 1948).

Data on wood specific gravity (ρ, hereinafter wood density) were compiled from the Global Wood Density Database (GWDD; http://datadryad.org/handle/10255/dryad.235), which currently represents the best available source of wood density values (Chave et al. 2009; Flores and Coomes 2011; Zanne et al. 2009). Wood density values were matched to each tree individual using binomial taxonomic names. When inventoried species were absent from GWDD, we used the mean wood density from the lowest taxonomic level available (genus or family). When even the taxonomic family of inventoried species were absent from the GWDD, we used the mean wood density of all recorded species in the plot.

There are currently no allometric models specifically developed to estimate aboveground biomass (AGB) in várzea forests. However, an evaluation of seven general allometric equations was conducted by Schöngart et al. 2010. The average of three of these empirically tested models showed a good agreement to várzea forests of different ages (Table 4.2).

Table 4.2: Allometric models whose average will be used to estimate the aboveground biomass (Mg ha $^{-1}$), incorporating the DBH (d in cm), wood specific gravity (ρ in g cm^{-3}) and tree height (h in m), according to Schöngart et al. 2010.

	Allometric Model	Source
1	$0.6 \times \rho \times h \times \pi \times \left(\frac{d}{2}\right)^2$	Cannell 1984
2	$0.112 \times (\rho \times h \times d^2)^{0.916}$	Chave et al. 2005
3	$0.0509 \times \rho \times h \times d^2$	Chave et al. 2005

AGB was estimated to individual trees as the mean result from the three allometric models and then summed at plot level and converted to Mg C ha^{-1}. We then converted AGB to carbon fraction assuming the proportion of 47% of carbon in dry mass (Aalde et al. 2006), reported as aboveground carbon (AGC).

We also calculated the plot-level AGC per unit of basal area (Mg C m^{-2}), defined as the structural conversion factor. Baker et al. 2004 found that SCF seems to better explain spatial variations in biomass than basal area itself.

The flood duration was estimated for each plot based on ten levelogger devices installed in the study area to monitor flood dynamics (see Figure 3.1). Each levelogger recorded 3 full hydrological years from 2014-02-01 to 2017-01-13, storing flood heights in centimeters above the sensor, three times per day (Details on Section 3.2.2). For each levelogger and hydrological year, we computed the maximum flood height and the flood duration in days per year. We then used a simple linear model to relate maximum flood heights (independent variable) to flood duration (dependent variable). The watermarks left on trunks by the last flood season (2016) was then used as input in this model to predict flood durations in our forest plots.

Flood duration and maximum flood heights per year as recorded in the

leveloggers had a strong linear association (slope $= 2.86, r^2 = 0.93, p = 2^{-16}$; Figure 4.1). The recorded water mark heights left on trunks at our forest sample plots ranged from 1.10 to 5.29 meters aboveground, so that we estimated flood durations ranging from 87 to 207 days.

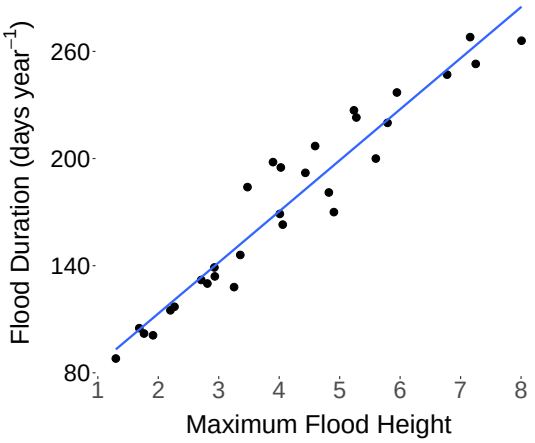

Figure 4.1: Association between flood heights and flood duration recorded at leveloggers installed in the várzea forests of Mamirauá Sustainable Development Reserve (Central Amazon, Brazil). Data points consist of 10 devices with records for three years (N = 30).

To investigate differences in AGC per forest subtype we used an one-way analysis of variance (ANOVA) followed by the post-hoc Tukey's honestly significant difference (HSD) test (James et al. 2013). All errors are reported as standard errors of the mean, except when indicated.

We investigated the association between flood duration and AGC using a simple linear model. The same method was applied to investigate the association between flood duration and the parameters given as inputs to the allometric models. We also used this approach to investigate the relationship between flood duration and plot-level metrics related to ACG: (i) mean basal area; (ii) mean wood density, (iii) mean tree height; (iv) SCF; (v) number of stems; and (vi) species richness. To evaluate the effect of flood duration on AGC and on the above parameters and metrics, while controlling for forest subtype controlling for forest subtype, we used an analysis of covariance (ANCOVA).

The coefficients of linear fits were reported as standardized coefficients to allow comparisons with future studies. Standardized coefficients were obtained by centering the numerical variables on the mean and scaling them by their standard deviation.

4.3 Results

4.3.1 Forest inventory

We inventoried 2022 stems of 1848 individuals belonging to 184 morphospecies. The minimum and maximum number of stems inventoried per plot

ranged from 67 (high várzea) to 213 (chavascal). Among the inventoried morphospecies, 14 taxa could only be taxonomically identified to the genus level, and 1 morphospecies was not identifiable at all, resulting in a total of 165 valid species identified, belonging to 124 genera and 42 families. Fischer's α diversity per plot varied by one order of magnitude, from 4.7 (chavascal) to 42.5 (high várzea). Mean α diversity per forest subtype was 34.1 for high várzea, 19.7 for low várzea, and 7.1 for chavascal forests. The Sørensen index of dissimilarity (β-diversity) for the pooled inventoried area was 0.74. β-diversity by forest subtype was 0.65 for high várzea, 0.62 for chavascal and 0.61 for low várzea forests.

We recorded 46 singletons, representing 2.3% of inventoried stems and 27.9% of all identified species. The three most abundant species accounted for 26.3% of all recorded stems and were *Buchenavia oxycarpa* (Mart.) Eichler, *Pseudobombax munguba* (Mart. & Zucc.) Dugand, and *Triplaris weigeltiana* (Rchb.) Kuntze, corresponding to 105, 185, and 242 stems, respectively. Chavascal and high várzea plots had the three highest and the three lowest Berger-Parker Dominance index, respectively (Table 4.3).

Table 4.3: Floristic summary of inventoried forest sample plots in the várzea forests of Mamirauá Sustainable Development Reserve (Central Amazon, Brazil). For = Forest subtype (high várzea, low várzea, and chavascal), S = Species richness, A = Number of stems, α = Fischer's alpha diversity, Most Abundant *spp* = The most abundant specie(s), I = Number of individuals of the most abundant specie(s), D = Berger-Parker Dominance Index (%), Single = Number of singletons, Flood = Flood duration as estimated from leveloggers data.

Plot	For	S	A	α	Most Abundant *spp*	I	D	Single	Flood
1a	HV	42	72	42.2	*Pseudoxandra leiophylla*	7	10	27	106
1b	HV	39	70	36.3	*Couepia chrysocalyx* *Theobroma cacao*	6	09	22	95
1c	HV	41	69	42.5	*Apeiba glabra* *Pouteria procera*	4	06	23	87
2a	HV	50	130	29.7	*Iryanthera laevis* *Mouriri myrtifolia*	8	06	17	123
2b	HV	39	107	22.1	*Mouriri myrtifolia*	14	13	16	141
2c	HV	36	67	31.7	*Apeiba glabra* *Nectandra hihua* *Pseudoxandra leiophylla*	5	07	20	99
3a	LV	42	114	24.0	*Oxandra riedeliana*	18	16	19	157
3b	LV	50	111	35.0	*Discocarpus essequeboensis*	9	08	27	109
3c	LV	36	101	20.0	*Mabea nitida* *Mouriri myrtifolia*	8	08	11	131
4a	LV	28	94	13.5	*Piranhea trifoliata*	11	12	7	193
4b	LV	26	88	12.5	*Oxandra riedeliana* *Piranhea trifoliata*	16	18	10	201
4c	LV	28	97	13.2	*Piranhea trifoliata*	15	15	8	181
5a	CH	17	170	4.7	*Buchenavia oxycarpa*	42	25	4	180
5b	CH	22	155	7.0	*Buchenavia oxycarpa* *Triplaris weigeltiana*	46	30	8	166
5c	CH	23	213	6.5	*Triplaris weigeltiana*	84	39	10	166
6a	CH	23	125	8.3	*Pseudobombax munguba*	26	21	6	206
6b	CH	18	137	5.5	*Pseudobombax munguba*	47	34	6	158
6c	CH	25	102	10.6	*Triplaris weigeltiana*	34	33	11	207

4.3.2 Aboveground carbon stocks (AGC)

Our AGC estimates per forest plot varied from 46.75 to 234.46 Mg C ha^{-1} (Table 4.4). Mean AGC estimated for the entire inventoried area was 114.01±11.63 Mg C ha^{-1}. Low várzea forests had higher AGC estimates than high várzea forests, while chavascal had the lowest estimates (Figure 4.2). Mean AGC estimates per forest subtype were 143.49±12.14, 128.01±23.03, and 70.51±10.49 Mg C ha^{-1} for low várzea, high várzea, and chavascal forests, respectively.

We detected small differences in mean AGC between paired forest subtypes mostly between chavascal and other subtypes, although the differences could not be statistically confirmed (Table 4.5).

Table 4.4: Above-ground carbon and structural metrics of inventoried forest sample plots in the várzea forests of Mamirauá Sustainable Development Reserve (Central Amazon, Brazil). Plot = plot ID, Forest = forest subtype, Flood = Estimated flood duration, AGC = Estimated above-ground carbon (Mg C ha^{-1}), BA = Mean basal area (m^{-2} ha^{-1}), SCF = Structural conversion factor (Mg C m^{-2}), Tree H = mean tree height, ρ = mean wood specific gravity (g cm^{-3}).

Plot	Forest	Flood	AGC	BA	SCF	Tree H	ρ
1a	HV	106	102.28	65.24	1.56	16.44	0.57
1b	HV	95	95.06	64.04	1.48	19.43	0.60
1c	HV	87	145.75	102.15	1.42	18.92	0.56
2a	HV	123	108.84	77.20	1.41	17.12	0.62
2b	HV	141	234.46	123.99	1.89	19.04	0.68
2c	HV	99	81.68	57.49	1.42	19.89	0.58
3a	LV	157	168.80	103.49	1.63	17.52	0.71
3b	LV	109	126.41	87.41	1.45	17.06	0.66
3c	LV	131	122.54	88.23	1.39	17.18	0.65
4a	LV	193	122.40	67.16	1.82	14.90	0.62
4b	LV	201	128.53	71.76	1.79	18.56	0.73
4c	LV	181	192.29	94.24	2.04	18.81	0.68
5a	CH	180	48.80	76.57	0.64	12.83	0.54
5b	CH	166	63.72	79.86	0.80	14.52	0.58
5c	CH	166	65.02	100.54	0.65	13.44	0.51
6a	CH	206	115.50	108.01	1.07	15.47	0.52
6b	CH	158	83.28	133.92	0.62	14.79	0.43
6c	CH	207	46.75	60.58	0.77	14.03	0.49

The main contrast between forest subtypes was the AGC distribution over DBH classes. While in high várzeas 42% of the AGC was concentrated in 18 trees with DBH $\geq$ 70 cm (3.5% of its trees), in low várzeas a similar proportion of their AGC (41%) belonged to 70 stems with DBH between 40 and 69.99 cm (11.6% of its tree stems). In chavascal forests, half of the total AGC (52%) was distributed over 90.8% of its tree stems with 10 $\leq$ DBH $\leq$ 39.99 cm, while the remaining AGC belonged to 83 tree stems $\geq$ 40 cm (9.2% of its tree stems; Figure 4.3).

AGC did not have a linear relationship with flood duration, either for all pooled forest plots or when controlling for forest subtype in our dataset (Figure 4.4). Although the ANCOVA revealed an expressive portion of the variance explained by flood duration when controlling for forest type, the slope of high

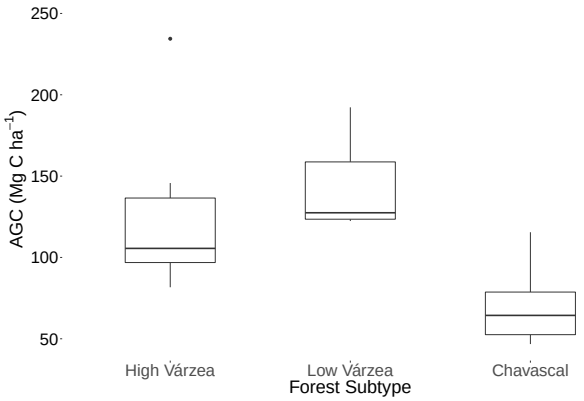

Figure 4.2: Aboveground forest carbon by forest type estimated in the inventoried forest sample plots in the várzea forests of Mamirauá Sustainable Development Reserve (Central Amazon, Brazil).

Table 4.5: Paired differences in mean aboveground carbon (ΔAGC) between forest subtypes (in Mg C ha^{-1} $\pm$ confidence interval at 95% significance) in the Mamirauá Sustainable Development Reserve (Central Amazon, Brazil). Difference between means were tested with one-way ANOVA and post-hoc Tukey's honestly significant difference (HSD) test.

Forest subtypes	ΔAGC	p_{adj}
Low Várzea - High Várzea	16.47±63.32	0.78
Chavascal - High Várzea	-61.17±63.32	0.06
Chavascal - Low Várzea	-77.6±63.32	0.02

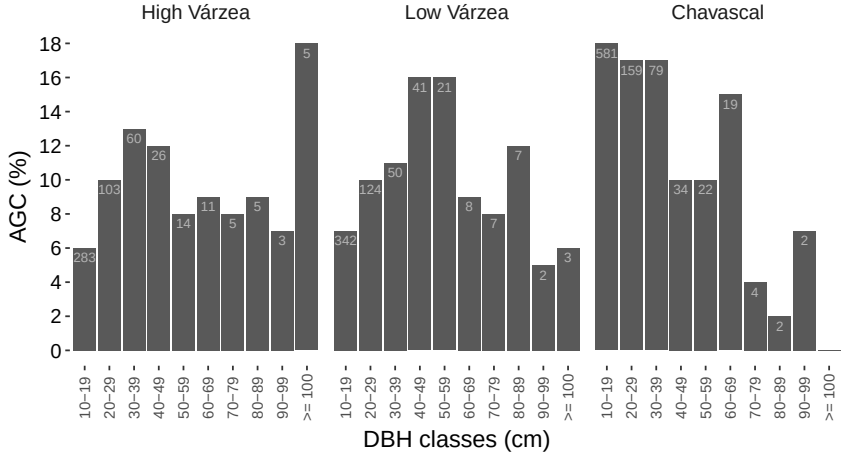

Figure 4.3: Aboveground forest carbon proportion according to diametric classes (DBH) and forest subtypes in the inventoried forest sample plots of Mamirauá Sustainable Development Reserve (Central Amazon, Brazil). Light-gray numbers inside bars refers to the number of stems in each diametric class.

várzea AGC was influenced by a single extreme value, and the remaining slopes are all near zero.

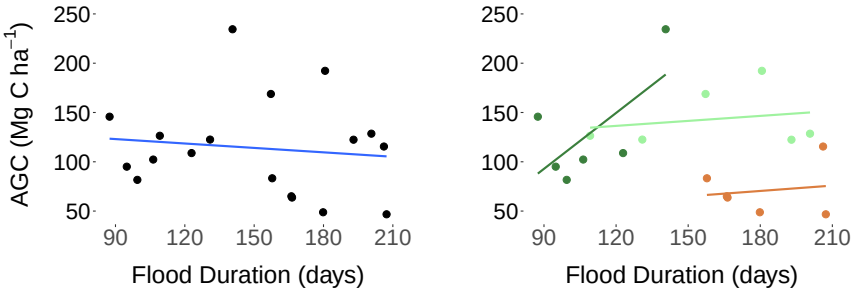

(a) Pooled forest plots. Linear fit; standartized slope $= -0.12, r^2 = 0.01, p = 0.63$

(b) Controlling for forest subtype. ANCOVA; $r^2 = 0.60, p = 0.03$

Figure 4.4: Relationship between aboveground forest carbon and flood duration in forest sample plots established in Mamirauá Sustainable Development Reserve (MSDR), Central Amazon floodplain, Brazil.

When forest subtypes were not considered, mean tree height per forest plot showed a strong inverse association with flood duration, while remaining parameters did not show any relationship (Figures 4.5a, 4.5c, and 4.5e). The effect of flood duration controlling by forest subtype showed evidences that basal area in high várzea and chavascal forests had stronger associations with flood duration compared to low várzea. While flood duration positively affected basal area in high várzea forests, we found an opposite effect for chavascal forests (Figure 4.5b). In high várzea forests, mean wood density and mean tree height per forest type showed, respectively, clear positive and negative associations with flood durations. In low várzea and chavascal forests slopes were close to zero, thus revealing no relationship in our dataset (Figures 4.5d and 4.5f).

We then assessed the effect of flood duration and forest subtype on plot-level metrics related to AGC. The effect of flood duration was strongly detected for species richness, while the number of stems and the SCF were weakly and not associated with flood duration, respectively (Figures 4.6a, 4.6c, and 4.6e). The effect of flood duration on the number of stems per plot controlling for forest subtype was positive and stronger on high várzea forests (Figure 4.6b). For chavascal forests, there was some evidence of an inverse relationship between the number of stems and flood period, while for low várzea the effect is negligible. The effect of flood duration on species richness was notably evident in low várzea forests, with a strong inverse association, while for high várzea and chavascal this relationship was positive, although weak (Figure 4.6d). For the amount of AGC per squared meter of basal area at the plot-level (SCF), the effect of flood was strong and positive for low várzea and chavascal forests, while for high várzea slope was influenced by one single extreme value (Figure 4.6f).

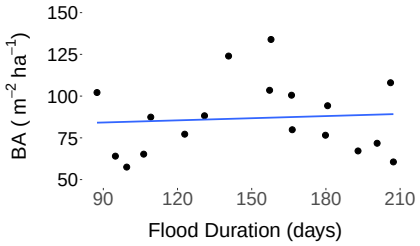

(a) Pooled forest plots. Linear fit; standartized slope $= 0.08, r^2 = 0.01, p = 0.76$

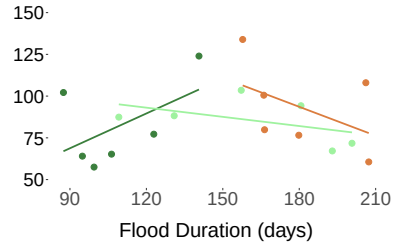

(b) Controlling for forest subtype. ANCOVA; $r^2 = 0.29, p = 0.48$

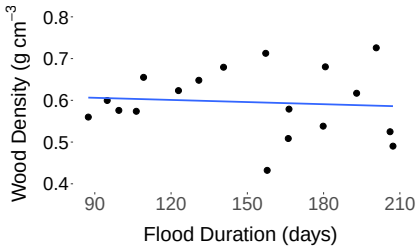

(c) Pooled forest plots. Linear fit; standartized slope $= -0.09, r^2 = 0.01, p = 0.73$

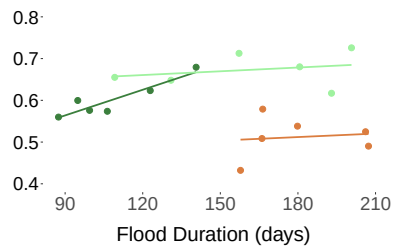

(d) Controlling for forest subtype. ANCOVA; $r^2 = 0.80, p = 0.0006$

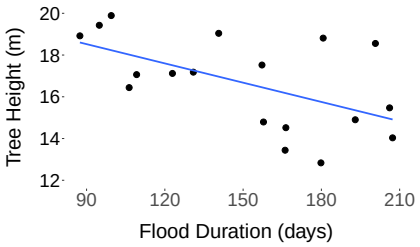

(e) Pooled forest plots. Linear fit; standartized slope $= -0.56, r^2 = 0.31, p = 0.01$

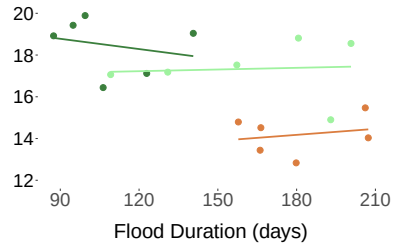

(f) Controlling for forest subtype. ANCOVA; $r^2 = 0.72, p = 0.004$

Figure 4.5: Relationship between the input parameters of allometric models used to estimate aboveground forest carbon and flood duration in forest sample plots established in Mamirauá Sustainable Development Reserve (MSDR), Central Amazon floodplain, Brazil. (a) and (b) - Mean basal area per plot; (c) and (d) - Mean wood density per pot; (e) and (f) - Mean tree height per plot.

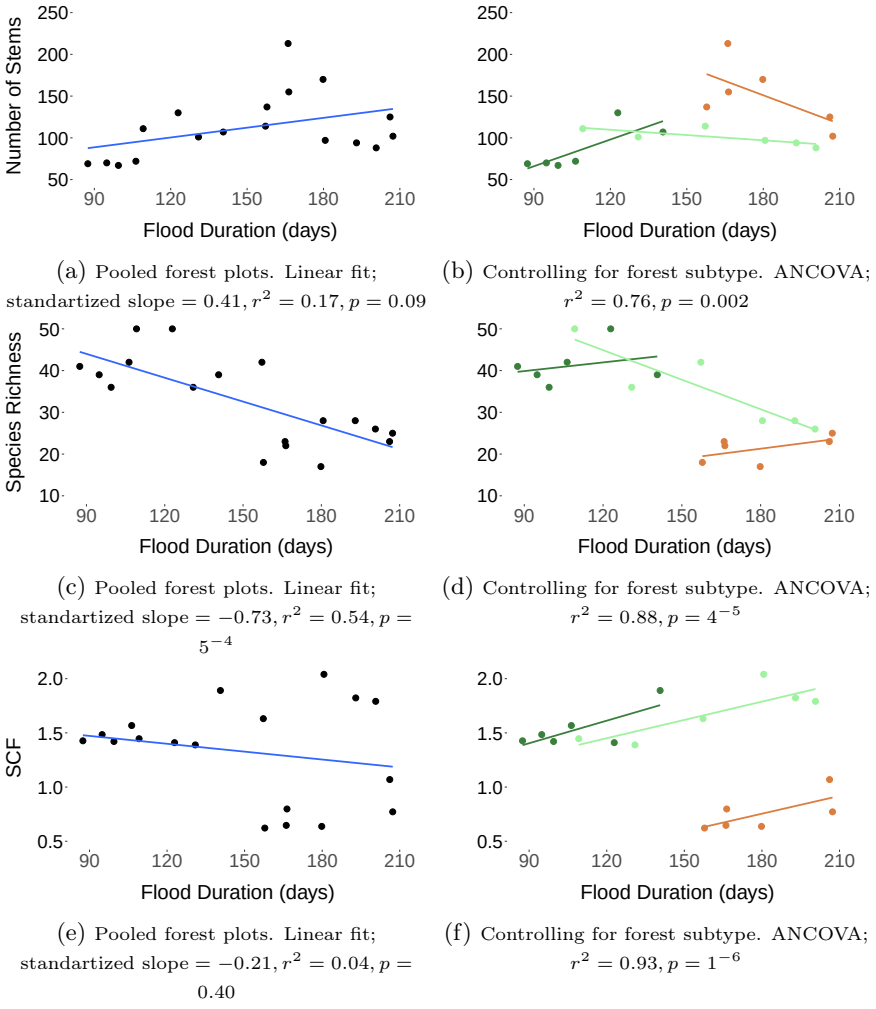

(a) Pooled forest plots. Linear fit; standartized slope $= 0.41, r^2 = 0.17, p = 0.09$

(b) Controlling for forest subtype. ANCOVA; $r^2 = 0.76, p = 0.002$

(c) Pooled forest plots. Linear fit; standartized slope $= -0.73, r^2 = 0.54, p = 5^{-4}$

(d) Controlling for forest subtype. ANCOVA; $r^2 = 0.88, p = 4^{-5}$

(e) Pooled forest plots. Linear fit; standartized slope $= -0.21, r^2 = 0.04, p = 0.40$

(f) Controlling for forest subtype. ANCOVA; $r^2 = 0.93, p = 1^{-6}$

Figure 4.6: Relationship between plot-level metrics related aboveground forest carbon stocks (AGC) distribution and flood duration in forest sample plots established in Mamirauá Sustainable Development Reserve (MSDR), Central Amazon floodplain, Brazil. (a) and (b) - Number of stems per plot; (c) and (d) - Species richness per pot; (e) and (f) - Structural conversion factor per plot, defined as the AGC by m^{-2}.

4.4 Discussion

There is weak evidence that flood duration differences cause expressive effects on AGC stocks among individual forest subtypes. Our results suggest that the dendrometric factors affecting stand AGC balance each other out, causing no clear trends in AGC per forest subtype.

Along the entire range of the flooding gradient, AGC does not vary linearly in response to flood duration, but it appears to have a non-linear inverted "U"-shape association with flooding, with high várzeas and chavascal forests, positioned at both ends of the flood gradient, having lower AGC stocks than low várzea, which had relatively higher stocks. Nebel et al. 2001, however, studying these three forest subtypes in Peru, reported the highest AGC stocks in chavascal forests, followed by low várzea. Hawes et al. 2012 also found higher AGC in longer flood durations, however in this case the authors aimed to compare terra firme forests with várzeas, not specifying forest subtypes and probably not sampling chavascal forests. Our results are, however, in line with previous findings from Schöngart et al. 2010 and Lucas et al. 2014 which found higher AGC stocks in intermediate levels of flood duration, where late secondary/intermediate succession stages (low várzeas) takes place.

The main factors concurring to this result seems to be the influence of flood duration on basal areas, wood density, and indirectly, species richness. The decreasing flood stress along the flood gradient results in habitat suitability for a greater number of species less adapted to survive flooding (Wittmann et al. 2002, 2010a). In general, high várzea forests stands in our study area are thought to be c.a. 240 years-old with trees up to 400 yeas-old (Schöngart et al. 2010; Worbes et al. 1992). Although, at first, older stand ages could mean higher stand biomass, the reduction in flood durations in high várzeas also implies in lower basal areas by the reduced total number of stems $\geq$10cm towards less flooded terrains. This decrease in the the number of stems under less flooded conditions is well documented in the literature (Luize et al. 2015; Wittmann et al. 2002, 2010b; Worbes 1997). Also, comparatively, low várzea forests show a higher number of species with denser woods.

We attribute the higher mean wood density of low várzeas to the shorter growing season, which encourages an accelerated growth rate when the conditions are favorable, resulting in densely packed growth rings and thus denser woods (Wittmann et al. 2006b). Chao et al. 2008 related wood density and diameter increment in terra firme forests and found that higher wood densities were generally associated with slow growing rates. However, Hacke et al. 2001 proposes that in some instances a denser wood may favor high growth rates under water shortage, creating thick-walled cells and fibres that protect vessels from implosion when the water deficit creates negative water potentials in the xylem. Hence, species with higher woods densities may indeed be an adaptation to hydric stress in low várzeas, allowing heavy-wooded trees to grow under conditions that could cause lighter-wooded trees to shutdown its water transport system (Chave et al. 2009).

Schöngart et al. 2010, Hawes et al. 2012, Nebel et al. 2001 and Lucas et al. 2014 report that biomass become more concentrated in a few number of large trees as we progress towards terrains with lower flood durations, along the flood/successional gradient. We also found this pattern, with AGC concentration distributed among more and smaller stems in chavascal forests, and

concentrated in fewer large trees for high várzeas. At continental scale of tropical South America, for instance, it is estimated that big trees (DBH ≥70 cm) represent only 1.5% of stems, but store 25% of total biomass (Slik et al. 2013). This stresses the importance in understanding how the predicted higher amplitude and severity of the flood pulse (i.e. strengthened seasonality; IPCC 2013; Ronchail et al. 2018; Zulkafli et al. 2016) may affect this trees that hold the largest portions of AGC in high várzeas.

In conclusion, we show that, within individual forest subtype, there is a small influence of flood duration to express a substantial variation in AGC stocks. The major influence of flood duration on AGC seems to be its ecological filtering effect, which ultimately results in the well known species zonation along the flood gradient (Luize et al. 2015; Wittmann et al. 2006a) with different carbon stock capacities depending on stand age and forest subtype (Hawes et al. 2012; Lucas et al. 2014; Schöngart et al. 2010). Our results thus raise evidence that AGC stocks do not vary substantially within forest communities under different flood regimes. However, given our limited sampling effort, this hypothesis should be confirmed by further studies within the Amazon várzea floodplains.

Chapter 5

LITTERFALL AND NET PRIMARY PRODUCTIVITY IN AMAZONIAN VÁRZEA FORESTS: THE ROLE OF FOREST SUBTYPES AND FLOOD REGIME

5.1 Introduction

Net Primary Production (NPP) is one of the major components of the global carbon cycle, defined as the amount (or rate) of produced organic material after subtracting autotrophic respiration (Houghton 2009). The Amazon biome alone contributes to about 14% of all fixed carbon in the terrestrial biosphere and accounts for about 66% of interannual variations of global NPP (Zhao and Running 2011). At the biome scale, the NPP of the Amazon varies between 18.6±2.6 and 34.0±2.8 Mg ha^{-1} $year^{-1}$, with a mean NPP of 25.6±1.8 Mg ha^{-1} $year^{-1}$(Aragão et al. 2009). Aragão et al. 2009 found that this almost two-fold variation in NPP was positively related to phosphorus availability, supporting the hypothesis that tropical forests are phosphorus-limited (Quesada et al. 2010; Vitousek 1984).

Given its higher nutritional status, eutrophic river floodplain ("várzea") forests tend to be more productive than upland non-floodable ("terra firme") forests and oligotrophic floodplain ("igapó") forests (Wittmann et al. 2010b). In várzea forests of western Amazon, Nebel et al. 2001 estimated aboveground NPP (ANPP) as ranging from 20.82 to 25.58 Mg ha^{-1} $year^{-1}$and Schöngart et al. 2010 estimated ANPP rates between 13.30 and 31.80 Mg ha^{-1} $year^{-1}$in central Amazon. Although these studies quantified only aboveground NPP components, they place várzea forest NPP at the upper limit of mature terra firme forests (Schöngart et al. 2010).

Várzea forests are primarily influenced by the strong Amazonian flood regime, which controls its structure and function (Junk 1997b; Junk et al. 1989; Wittmann et al. 2002). In the Central Amazon, maximum annual flood depths can reach 10-13 meters (Ramalho et al. 2009), with flood durations of up to 230-300 days in depressions and low-lying areas, a recurring process that has been called the "flood pulse" (Junk 1989). Várzea tree species have distinct morphological and

ecophysiological adaptations to waterlogging, and the flooding gradient from the river margins to the interior of the floodplains generally translates into a well-defined species zonation (Wittmann et al. 2002). Species richness, individual abundance, population dynamics, canopy stratification and canopy height are also known to be strongly related to flood gradients and sedimentation rates (Wittmann et al. 2010b).

Additionally, várzea forests are also among the most dynamic Amazonian forest types, undergoing relatively rapid changes due to the ever changing fluvial geomorphology (Fragal et al. 2016; Peixoto et al. 2009; Salo et al. 1986). River bank erosion and river channel migration can remove centuries-old mature várzea forests within short periods, while simultaneously depositing sediments in the opposite margin and triggering early successional stages of várzea forests, thus "reseting" the system (Mertes 1994; Mertes et al. 1995; Peixoto et al. 2009; Salo et al. 1986). The combined effects of annual variation in water levels and dynamic geomorphology leads to a markedly heterogeneous mosaic of forest communities and ages with differing species composition, diversity, and soil properties (Campbell et al. 1992; Pires and Koury 1959; Prance 1979; Salo et al. 1986; Wittmann et al. 2002).

Given that picture, it is not surprising that NPP comparisons among várzeas forests subtypes and among várzea, igapó, and terra firme forests are difficult, especially as they are dependent on stand age, forest type and flood duration (Schöngart et al. 2010; Wittmann et al. 2010b). Additionally, some components of total forest NPP are very challenging to measure in seasonally flood environments, and may be further restricted by high financial and/or logistic costs, such as autotrophic respiration or belowground NPP. Accurate and widespread NPP estimates are mainly available for aboveground components (Schöngart et al. 2010), hindering our detailed knowledge on the contribution of várzea and floodplains to regional NPP.

Bray and Gorham 1964 have proposed that litterfall could be a good estimator of forest NPP at the global scale, and this relation has been proven for old-growth terra firme forests in low-land Amazon (Aragão et al. 2009), Amazonian montane forests (Girardin et al. 2010) and for tropical forests in general (Malhi et al. 2011). Malhi et al. 2011 showed that canopy NPP estimated by fine litterfall consistently comprises 34±6% of total forest NPP (both aboveground and belowground). More importantly, litterfall is a relatively simpler component of forest NPP to estimate, and thus if the above findings indeed hold for Amazon forests in general, an increased effort in sampling litterfall within the still poorly studied Amazonian várzea forests could let us better understand its relation with the flood pulse, and its contribution to regional forest productivity.

In addition to being a reliable proxy for total NPP, litterfall itself is a key process in the functioning of tropical forest ecosystems, which has been clearly demonstrated by several observational studies and experimental manipulations worldwide (Sayer 2006, for a comprehensive review.). Forest productivity is largely controlled by seasonal litterfall dynamics, as leaf turnover influences photosynthetic production (Wu et al. 2016). Plant litter act as a major pathway of carbon supply to soils, and mediates physical changes between soil and atmosphere as a protective layer, plays a major role in soil respiration (Chen and Chen 2018; Sayer 2006). In floodplains, litterfall also plays a major role in sustaining a supersaturated CO_2 condition in the main Amazon rivers and floodplains (Melack et al. 2009b; Richey et al. 2002). This supply can fuel an

evasion of 1.26±0.3 Mg C ha^{-1} $year^{-1}$ back to atmosphere - an order of magnitude greater than fluvial export of organic carbon to the ocean - to which litterfall contribution is about 35% (Richey et al. 2002). Abril et al. 2014 estimated that half of the gross primary production of Amazonian wetlands is exported as dissolved $CO_2$and organic carbon to river waters. However, studies of litterfall dynamics in Amazonian floodplains are still few and very localized, and thus insufficient to provide a representative view of these heterogeneous forest mosaics.

Therefore, in the present chapter we analyzed fine litterfall production and dynamics at an undisturbed Central Amazon várzea forest landscape and estimated total NPP from fine litterfall as a function of landscape heterogeneity. Specifically, we address the following questions: (i) Does fine litterfall production and dynamics differ among forest subtypes and flood regimes? (ii) Do distinct forest types and flood regimes reveal different community-level signals of varying plant investment strategies into reproductive organs versus photosynthetic organs? (iii) Assuming that litterfall production can be used as a proxy for forest total NPP, what we can infer about how the primary productivity of várzea forest could respond to hydrological variability and changes?

5.2 Methods

5.2.1 Sample Design

We established 18 forest plots of 0.25 ha (50 x 50 meters; total of 4.5 ha). The forest plots were distributed within the study area in a stratified sample design by forest subtype (high várzea, low várzea and chavascal forests). For each forest subtype, 6 forest plots were installed and placed in different topographical levels to capture distinct flood regimes. We determined the forest subtype observing general forest structure and species composition with the support of a trained parabotanist. Within each forest subtype, we used watermarks left on trunks in the last flood season as a proxy of distinct flood regimes (see Section 4.2.1 for details on forest plots).

We installed 162 littertraps among the 18 forest plots, placing nine traps per plot distributed as a 3 x 3 grid, with traps equidistant 12.5 meter from each other and from plot edges. The area covered by each set of nine littertraps represented 18% of total plot area.

We then performed biweekly sampling to collect fine litterfall production over a full year, from 2017-02-15 to 2018-01-30. Fine litter was defined according to the RAINFOR (Amazon Network of Forest Plots) protocol (Marthews et al. 2014), as comprising any organic material fallen from the canopy, including woody material $\leq$2 cm in diameter. Littertraps were constructed following the design by Hawes and Peres 2016, using a fine polyester mesh (1-2 mm) and PVC tubes to form a square basket of 71 x 71 cm (0.5 m^2) suspended at about 1.0 m from the ground. Buoyancy was added to the littertraps by tying three watertight 2 liter plastic bottles as stacks, and then fixing them under two opposite corners of the basket, so that the polyester mesh was kept above water at all times during seasonal floods. The littertraps were tied loosely to long bamboo rods or upper branches of surrounding trees to stabilize each trap position within the sampled plots, as they moved vertically with the flooding.

When necessary tying was redone between visits to ensure proper positioning.

The sampled material was dried to constant mass at 60°C. Once dried, fine litterfall was separated into six components: (i) leaves, (ii) flowers, (iii) fruits, (iv) seeds, (v) twigs ≤2, and (vi) fine debris (unidentifiable debris), and then weighted. Weights were then converted to Mg $ha^{-1}$and the mean and standard error of bi-weekly fine litter production was computed for each plot. We also calculated mean annual production by adding up the bi-weekly production of each littertrap and computing the means and standard errors. This calculations were performed for pooled littertraps and by várzea forest subtype.

5.2.2 Data Analysis

We assessed the seasonality of fine litter production using the Wald-Wolfowitz runs test (Runs test; Caeiro and Mateus 2014; Wald and Wolfowitz 1940). This test is commonly used to evaluate the hypothesis that consecutive elements in a sequence are mutually independent (randomness). Each value along the sequence is coded as "+" or "-" if it lies above or below the overall median, respectively, and a *run* is defined as a sequence of equally coded elements. The expected number of runs in a sequence of elements independently drawn is defined as

$$E(\bar{R}) = \frac{2mn}{m+n} + 1 \tag{5.1}$$

where m is the number of positive values and n the number of negative values. A number of runs significantly higher or lower than $\bar{R}$ hence is incompatible with the null hypothesis that each element in a sequence of successive measurements is independently drawn from the same distribution. Thus, an evidence of strong seasonality can be inferred from the lack of independence of successive observations (e.g. Haugaasen and Peres 2005).

We evaluated the influence of water level variations on bi-weekly fine litter production with simple linear models. First, bi-weekly mean plot values were used as dependent variable and water stage heights, recorded at each bi-weekly collection date, were entered as explanatory variable. Water stages were recorded at the Mamirauá Lake gauging station (hereafter gauging station), located in a lake within the floodplain and approximately 25 km from the farthest forest plots. This data is freely available at http://mamiraua.org.br/pt-br/pesquisa-e-monitoramento/monitoramento/fluviometrico/.

The coefficients of the linear fits were standardized to allow comparisons with future studies, by centering and scaling the bi-weekly means and water stages by they standard deviation.

We also explored the relative investment into reproductive *versus* photosynthetic organs by computing the *RL* ratio, following Chave et al. 2010. The RL ratio consists in dividing the total production of reproductive organs (flowers, fruits and seeds) by the production of leaf litter. An RL ratio of 1 corresponds to an equal investment into reproductive and photosynthetic organs, and provided a baseline for comparison among forest subtypes and flood regimes. The RL ratio was computed bi-weekly to investigate seasonal variability of relative investment between photosynthesis and reproduction, and the mean annual values by forest subtype and for each forest plot were also calculated.

To estimate total forest NPP (aboveground and belowground) we used the tropical assessment of NPP allocation presented by Malhi et al. 2011, which analyzed 71 tropical forest plots (except African forests). The authors have shown that proportion of canopy NPP with respect to total NPP is almost invariant among studied sites, so that fine litterfall consistently represents an average of 34±6% of total forest NPP. We assumed, for the sake of analysis, that this finding also holds for várzea forests, and estimated total NPP based on fine litterfall data from our sites.

We used a Monte Carlo simulation approach, drawing 10,000 random realizations of the model in 5.2:

$$NPP = AL \times LP \tag{5.2}$$

where NPP is simulated net primary productivity, AL and LP are simulated annual litterfall and litterfall-NPP proportions, respectively, and such that $AL \sim N(\mu_{AL}, \sigma_{AL})$ and $LP \sim N(0.34, 0.06)$. Hence, annual litterfall was simulated as random draws from a normal distribution with mean μ_{AL} and variance σ_{AL} equal to the observed mean and variance of annual litterfall production in the present study, and LP was simulated as random draws from a normal distribution with mean and variance as given by Malhi et al. 2011. We carried out separate Monte Carlo simulations for total annual fine litter production and for annual fine litter production by forest subtype and for each plot individually.

To assess the possible differences among forest subtypes in terms of (i) mean annual fine litter production, (ii) mean annual production of each litter component, (iii) RL ratio, and (iv) NPP, we used an one-way analysis of variance (ANOVA) followed by post-hoc Tukey's honestly significant difference (HSD) test.

The flood duration in each plot was estimated based on ten levelogger devices installed in the study area to monitor inundations (see Figure 3.1). The leveloggers recorded 3 full hydrological years from 2014-02-01 to 2017-01-13, recording flood heights in centimeters above the sensor three times per day (Details on Section 3.2.2). For each levelogger in each hydrological year we computed the maximum flood height and the flood duration. We then used a simple linear model to relate maximum flood heights (independent variable) to flood duration (dependent variable). Then, the watermarks left on trunks in the flood season of 2017 as used as input in this model to predict flood durations in our forest plots.

To evaluate the effect of flood duration on (i) mean annual fine litter production, (ii) mean annual production of each litter component, (iii) RL ratio, and (iv) NPP controlling for forest subtype, we used an analysis of covariance (ANCOVA).

When convenient, we converted our estimates of NPP from biomass production to carbon fraction assuming the proportion of 47% of carbon in dry mass (Aalde et al. 2006). All numerical analyses were conducted in the R statistical programming language (R Core Team 2018).

5.3 Results

5.3.1 Fine litterfall production and dynamics

Mean annual fine litter production was 8.62±1.01 Mg ha^{-1}, distributed along the year with a clear seasonal pattern supported by the Runs test (runs $= 5, n = 24, p = 0.0008$). Water level variations explained substantial part of seasonality (standartized slope $= 0.54, r^2 = 0.28, p = 0.007$). This seasonal pattern is visible in the Figure 5.1. From this figure, we did noticed larger error bars from the end of the flood peak to the start of rising water phase, mostly due to different litterfall timings in each forest type (Figure 5.2).

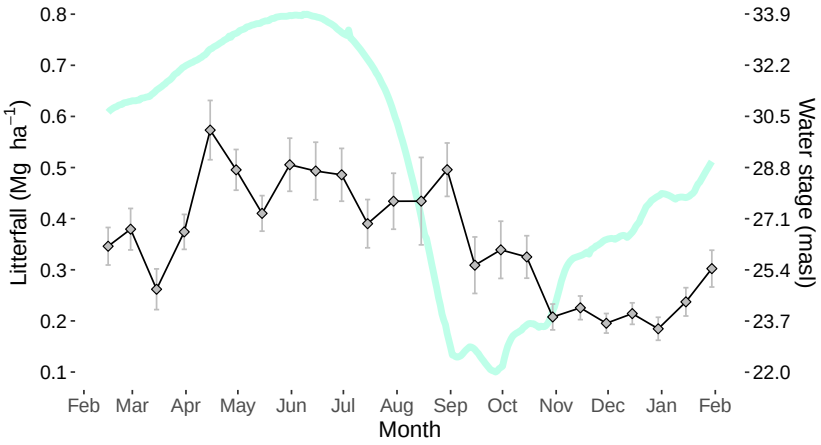

Figure 5.1: Bi-weekly total fine litterfall in the várzeas of Mamirauá Sustainable Development Reserve (Central Amazon, Brazil). Water stages (light blue line) were obtained from Mamirauá gauge station (IDSM 2013; Ramalho et al. 2009). Error bars are standard errors.

While fine litter production in low várzea forests peaked in the rising/high water phase (near April), high várzea forests presented its higher amounts approximately 4 months later, in the receding water phase (August). Chavascal environments, were synchronized with low várzeas and had higher litterfall rates during the rising/high water phase, followed by decreasing values along the flood pulse.

We found that litter production seasonality of low várzea and chavascal forests presented strong linear relationships with water levels throughout the year (Figures 5.3b and 5.3c). As could be inferred from the Figure 5.2, fine litter production in high várzea forests did not shown direct linear association with water levels (Figure 5.3a). Even so, a time lag of 60 days seems to exists between litterfall production and flood pulse in high várzeas (Figure 5.3d).

Mean annual litter production per forest subtype overlapped each other by their standard errors, although mean values indicated a slight decrease in litterfall production from high várzeas, to low varzeas, and to chavascal (Table 5.1). Therefore, we detected small differences between paired forest subtypes, mostly between chavascal and high várzeas, although not statistically confirmed (Table 5.2).

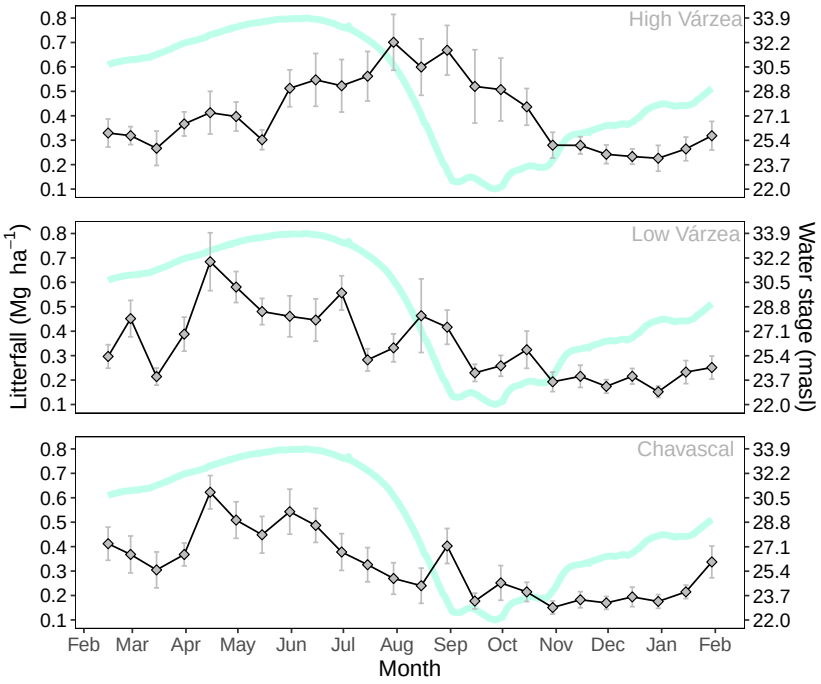

Figure 5.2: Bi-weekly total fine litterfall by forest type in the várzeas of Mamirauá Sustainable Development Reserve (Central Amazon, Brazil). Water stages (light blue line) were obtained from Mamirauá gauge station (IDSM 2013; Ramalho et al. 2009). Error bars are standard errors.

Table 5.1: Bi-weekly maximum (Max), minimum (Min), mean and mean annual fine litterfall (in Mg ha^{-1}± standard errors) by forest type in the Mamirauá Sustainable Development Reserve (Central Amazon, Brazil).

Vegetation	Max	Min	Bi-Weekly Mean	Annual
High Várzea	0.70	0.23	0.41±0.07	9.81±1.80
Low Várzea	0.68	0.15	0.35±0.06	8.30±1.44
Chavascal	0.62	0.15	0.32±0.06	7.75±1.39

Then we assessed the effect of flood duration on mean annual litter production using our estimates of flood duration based on leveloggers data (methods detailed on Section 4.2.2; see Table 4.3).

Without differentiating forest subtypes, annual litter production was inversely related to flood durations (Figure 5.4a). However, the ANCOVA analysis showed that this effect is dependent on forest subtype (Figure 5.4b). The effect of flood duration on mean annual fine litter production when controlling for forest subtype was strongly evident for low várzeas and chavascal, while no pattern was discernible for high várzeas.

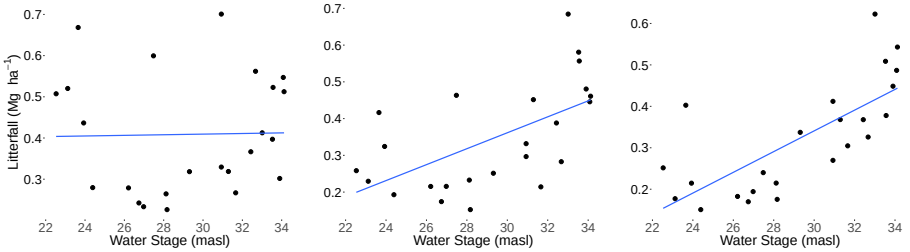

(a) High Várzea. Linear fit; standartized slope $= 0.02, r^2 = 4^{-4}, p = 0.93$

(b) Low Várzea. Linear fit; standartized slope $= 0.58, r^2 = 0.34, p = 0.003$

(c) Chavascal. Linear fit; standartized slope $= 0.73, r^2 = 0.54, p = 5^{-5}$

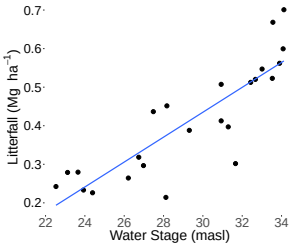

(d) High Várzea. Linear fit with litterfall lagged 60 days; standartized slope $= 0.86, r^2 = 0.73, p = 9^{-8}$

Figure 5.3: Relationship between bi-weekly fine litterfall and water stage by vegetation type in the Southeastern portion of Mamirauá Sustainable Development Reserve (MSDR), Central Amazon floodplain, Brazil. Water level heights for each collection date were obtained from Mamirauá gauge station (IDSM 2013; Ramalho et al. 2009). Data points are mean bi-weekly litter production per forest subtype (N=24).

Table 5.2: Paired differences in mean annual fine litter production between forest subtypes (in Mg ha^{-1}± confidence interval at 95% significance) in the Mamirauá Sustainable Development Reserve (Central Amazon, Brazil). Difference between means were tested with one-way ANOVA and post-hoc Tukey's honestly significant difference (HSD) test.

Forest subtypes	Difference	p_{adj}
Low Várzea - High Várzea	-1.51±2.80	0.36
Chavascal - High Várzea	-2.07±2.80	0.16
Chavascal - Low Várzea	-0.55±2.80	0.87

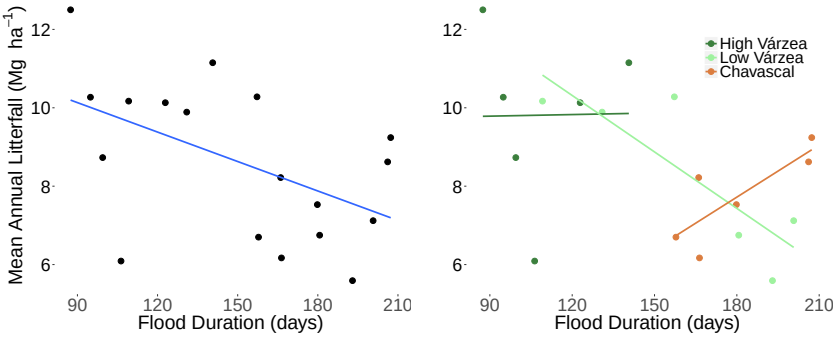

(a) Pooled forest plots. Linear fit; standartized slope $= -0.51, r^2 = 0.26, p = 0.03$

(b) Controlling for forest subtype. ANCOVA; $r^2 = 0.51, p = 0.09$

Figure 5.4: Relationship between mean annul litter production and flood duration in forest sample plots established in Mamirauá Sustainable Development Reserve (MSDR), Central Amazon floodplain, Brazil. Data points are mean annual liter production per forest plot (N=18).

5.3.2 Production and dynamics of fine litterfall components

Leaves comprised 68.22% of annual fine litterfall, while reproductive organs represented 15.42%. Mean annual leaf fall was 5.88 ± 0.37 Mg ha^{-1}. Likewise, 1.33 ± 0.37 Mg ha^{-1} were allocated to reproductive organs. The relative investment into reproduction versus photosynthesis (RL ratio) for the entire dataset had an annual average of 0.26, with bi-weekly RL values ranging from 0.09 to 0.64 throughout the year.

Leaves and reproductive parts comprised respectively 70.52% and 14.35% of litterfall production during peak flooding (mid-June), with RL ratio = 0.20, while during peak low water periods (mid-October) they represented 45.95% and 29.48%, respectively, with RL ratio = 0.64. The investment into reproductive organs was more intense during the three months between mid-August and mid-November, when water levels were between the receding and rising water phases. Twigs were an expressive and steady component of fine litterfall throughout the year, comprising 15.59% of the total (Figure 5.5).

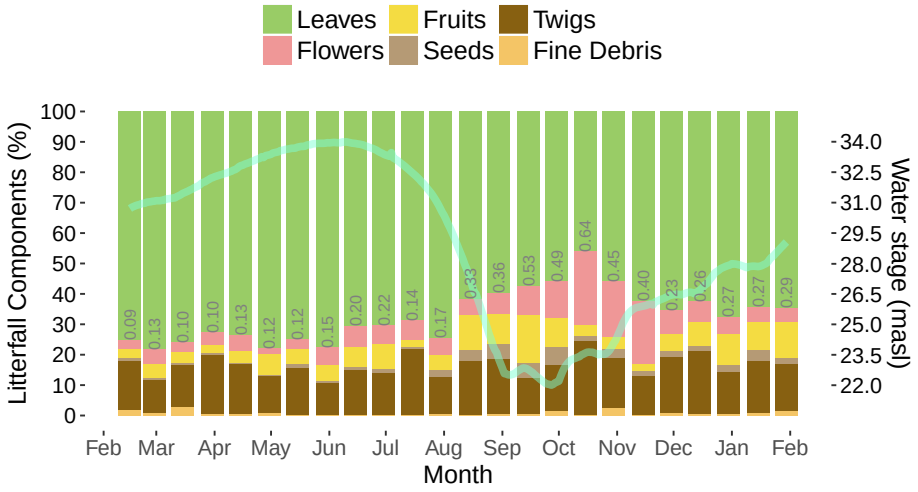

Figure 5.5: Relative contribution of bi-weekly production of different litterfall components in the forest sample plots established in the várzeas of Mamirauá Sustainable Development Reserve (Central Amazon, Brazil). Numbers inside bars represent the relative allocation of reproductive versus photosynthetic organs (RL ratio), where a value of 1 means an equal investment. Water level heights were obtained from Mamirauá gauge station (IDSM 2013; Ramalho et al. 2009).

Fruit fall was also steady throughout the year, with no clear association with water level variations (Figure 5.6c). We did notice, however, two main peaks of fruit fall activity during the low and rising water periods (August-September and January-February). Leaf, flower and seed fall amounts, on the other hand, had a clear association with the flood pulse. Flowers and seeds had a significant negative association with water stage (Figures 5.6b and 5.6d), while leaf fall values had a strong positive relation with the flood pulse (Figure 5.6a).

Still, the timing of litterfall production of each component was expressively different among forest subtypes (Figures 5.7 and 5.8). Leaf fall timing was

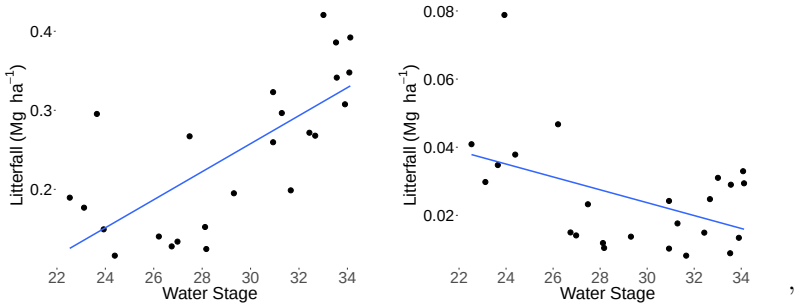

(a) Leaf fall. Linear fit; standartized slope $= 0.73, r^2 = 0.53, p = 0.00006$

(b) Flower fall. Linear fit; standartized slope $= -0.46, r^2 = 0.21, p = 0.02$

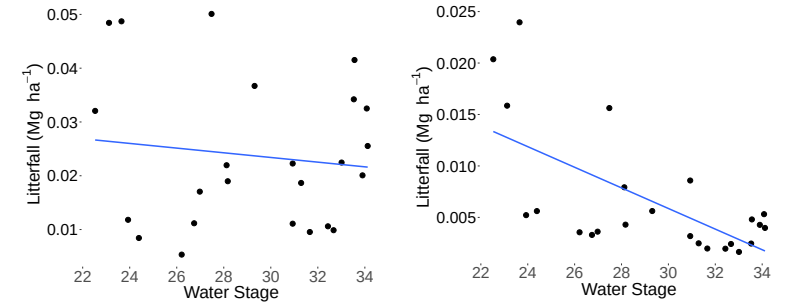

(c) Fruit fall. Linear fit; standartized slope $= -0.12, r^2 = 0.01, p = 0.6$

(d) Seed fall. Linear fit; standartized slope $= -0.64, r^2 = 0.41, p = 0.0007$

Figure 5.6: Relationship between bi-weekly production of litterfall components and water stage in the Southeastern portion of Mamirauá Sustainable Development Reserve (MSDR), Central Amazon floodplain, Brazil. Water level heights were obtained from Mamirauá gauge station (IDSM 2013; Ramalho et al. 2009). Data points are mean bi-weekly litter production (N=18).

clearly different in high várzea compared to low várzea and chavascal. While leaf litter production in low várzea and chavascal forests peaked in rising/high water phase (around April/May), in high várzea it occurred approximately 4 months later, in the receding water phase. Investment into reproductive organs of high várzea forests were more intense in a specific period when water levels were lower, from the end of the receding water phase (August) to the middle of rising water phase (February). These forests also had the highest RL ratio across the dataset (0.80), which were reached in the low water phase (October). The inverse timing between leaf fall and flower fall was also especially noticeable in high várzeas: the period when leaf fall reached minimum amounts (October-November) was the period of maximum flower fall (Figures 5.8a and 5.8b).

In chavascal forests, the timing of more intense reproductive fall was similar to high and low várzeas, but started 1.5 month earlier (mid-August). However, the investment into reproductive organs in chavascal forests was more evenly distributed along the year, and higher RL ratios were distributed through a longer period - between the flood peak and rising water phases - when compared

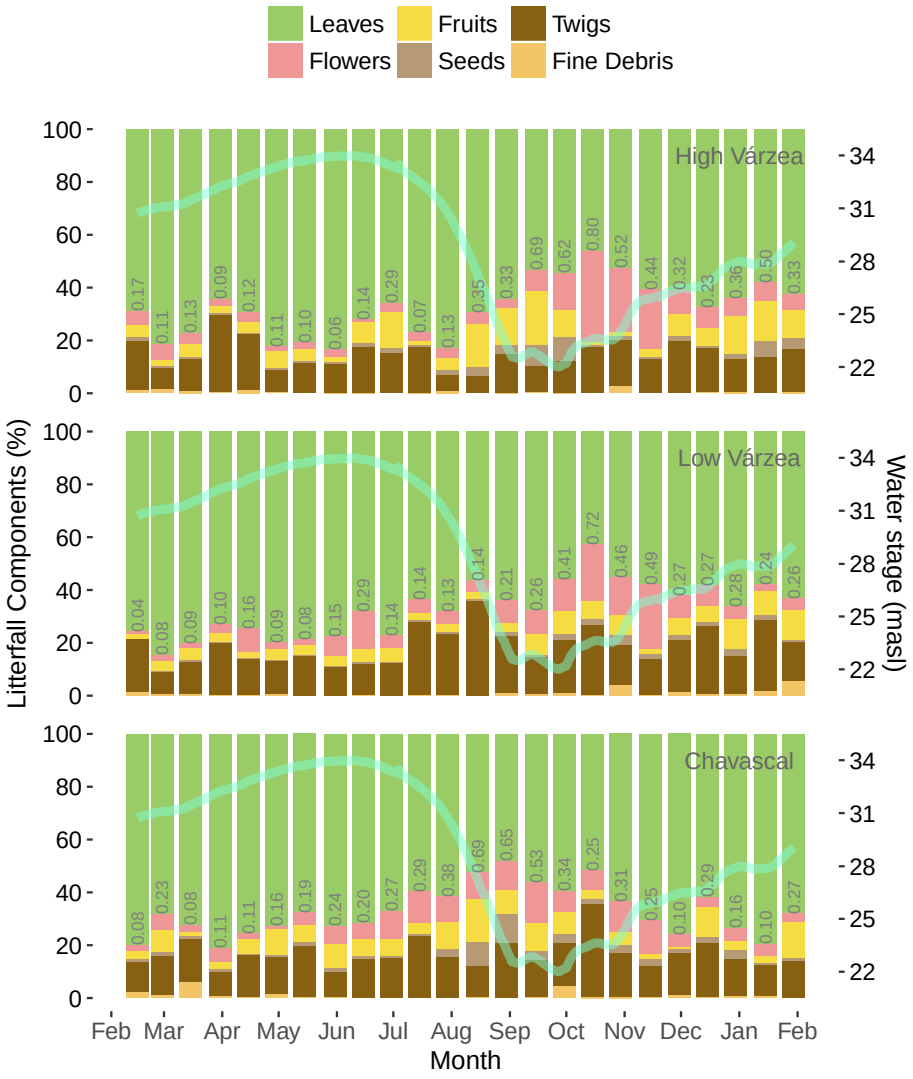

Figure 5.7: Relative contribution of bi-weekly production of different litterfall components to total fine litterfall by forest subtypes in the forest sample plots established in the várzeas of Mamirauá Sustainable Development Reserve (Central Amazon, Brazil). Numbers inside bars represent the relative allocation of reproductive versus photosynthetic organs (RL ratio), where a value of 1 means an equal investment. Water level heights were obtained from Mamirauá gauge station (IDSM 2013; Ramalho et al. 2009).

to high várzeas and low várzeas (Figure 5.9).

Assessing the mean annual production of fine litter components between paired forest subtypes, our results showed that differences were mostly statistically undetectable (Table 5.3), with only slight evidence that high várzeas have higher seed litter production than low várzeas, and more leaf litter production than chavascal (Figure 5.10).

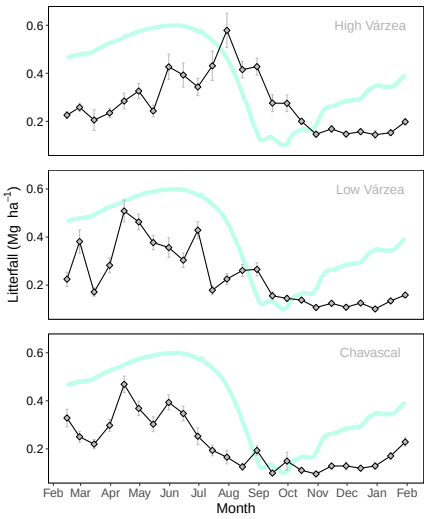

(a) Leaf fall.

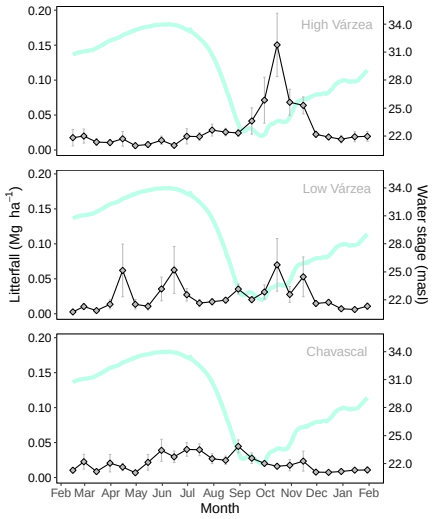

(b) Flower fall.

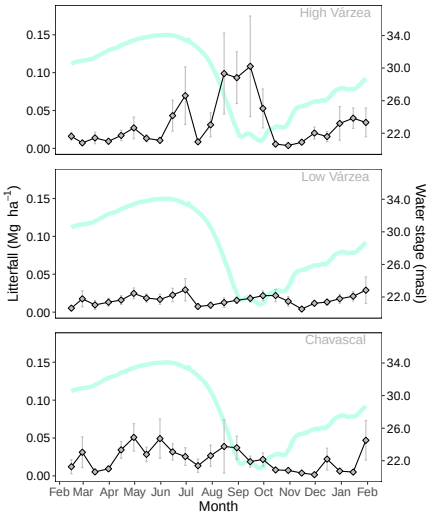

(c) Fruit fall.

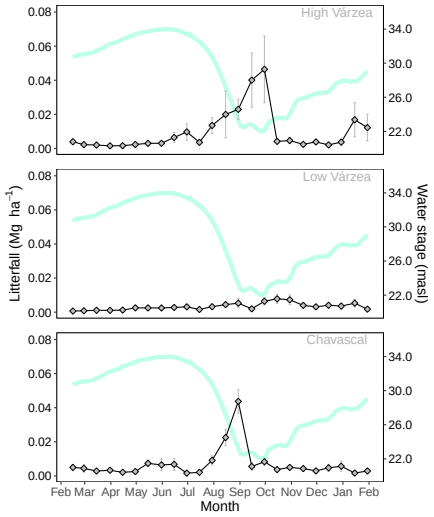

(d) Seed fall.

Figure 5.8: Photosynthetic and reproductive components of annual fine litterfall by vegetation types in the Southeastern portion of Mamirauá Sustainable Development Reserve (MSDR), Central Amazon floodplain, Brazil. Water level heights were obtained from Mamirauá gauge station (IDSM 2013; Ramalho et al. 2009).

Regarding the effect of flood duration on mean annual production of litterfall components, we found evidence that flood duration explains part of leaf litter production (Figure 5.11a). The mean annual production of remaining fine litter components are not associated with flood duration. Although the models show

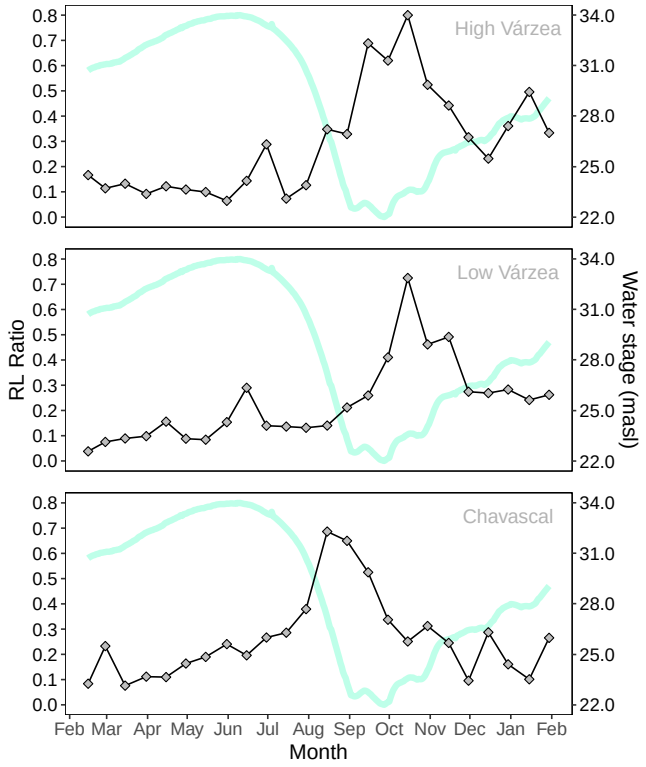

Figure 5.9: Relative investment into reproductive and photosynthetic components of fine litterfall (RL ratio) by forest subtypes in the forest sample plots established in the várzeas of Mamirauá Sustainable Development Reserve (Central Amazon, Brazil). An RL ratio value of 1 means an equal investment into reproduction and photosynthesis. Water level heights were obtained from Mamirauá gauge station (IDSM 2013; Ramalho et al. 2009).

that flower and seed fall had a small part of their variance explained by flood duration, this explanatory power is strongly influenced by the presence of an extreme outlier value in each of these components. If we remove outlier values, no evidence of linear association between mean annual production of flower, fruit, and seed litter with flood duration is apparent (Figures 5.11b to 5.11g).

ANCOVA analysis indicated that the effect of flood duration on mean annual production of litterfall components was dependent on forest subtype (Figure 5.4b). This effect was specially evident for leaf and seed components (Figures 5.12a to 5.12d). ANCOVA revealed stronger associations except for high várzea forests, especially since the extreme outliers identified belonged to this forest subtype in all components, biasing coefficient estimates (Figures 5.12e to 5.12h)).

When the RL ratio was summarized as the mean RL ratio per forest plot and the forest subtypes were paired to evaluate possible differences, we found that they were low and indistinguishable, ranging from 0.04 to 0.06; $F_{(2,15)} = 1.09, p = 0.36$). We found evidence that the relative investment into reproduction decreases under longer flood periods. However, when controlling for forest

Table 5.3: Paired differences in mean annual production of fine litterfall components between forest subtypes (in Mg ha^{-1}± confidence interval at 95% significance) in Mamirauá Sustainable Development Reserve (Central Amazon, Brazil). Differences between means were tested with one-way ANOVA and post-hoc Tukey's honestly significant difference (HSD) test.

Forest subtypes	Component	Difference	p_{adj}
Low Várzea - High Várzea	Leaf	-0.94±1.64	0.33
	Flower	-0.13±0.45	0.73
	Fruit	-0.39±0.77	0.41
	Seed	-0.16±0.20	0.15
Chavascal - High Várzea	Leaf	-1.40±1.64	0.10
	Flower	-0.22±0.45	0.43
	Fruit	-0.25±0.77	0.70
	Seed	-0.07±0.20	0.68
Chavascal - Low Várzea	Leaf	-0.46±1.64	0.75
	Flower	-0.09±0.45	0.87
	Fruit	0.14±0.77	0.88
	Seed	0.09±0.20	0.51

subtype, there was only weak evidence that this effect is dependent on subtype (Figure 5.13).

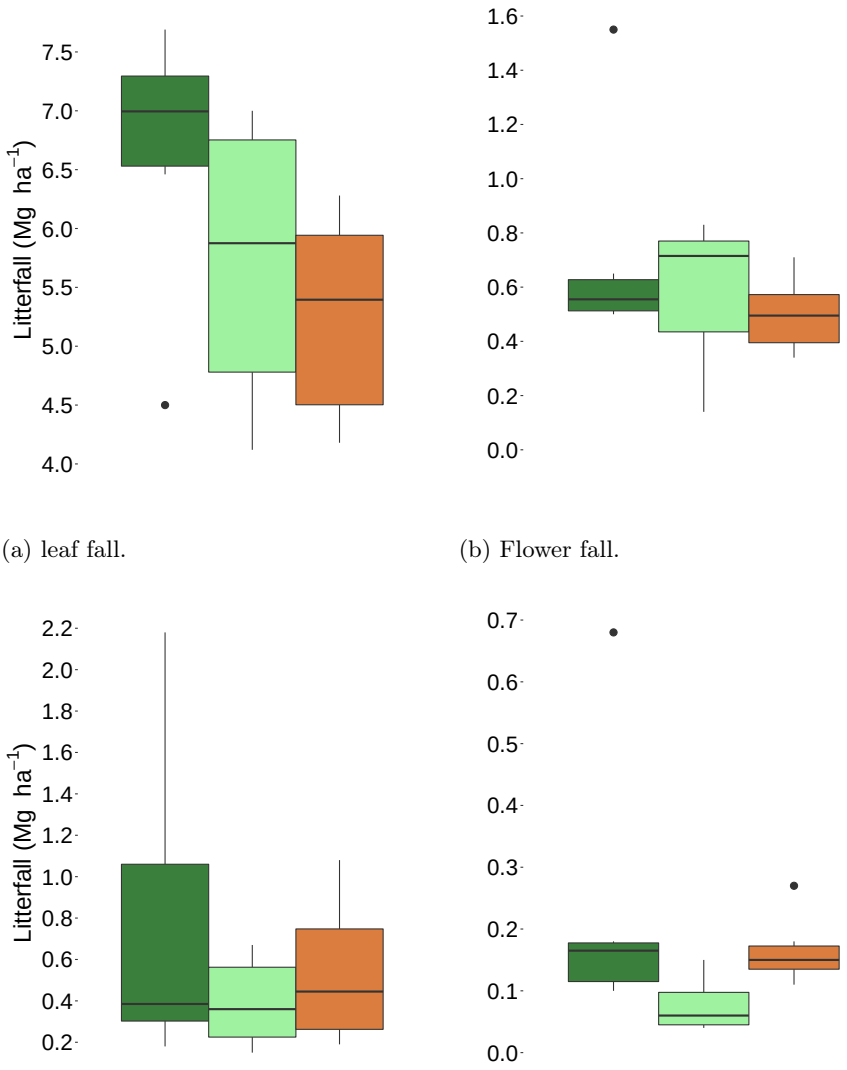

(a) leaf fall.

(b) Flower fall.

(c) Fruit fall.

(d) Seed fall.

Figure 5.10: Mean annual production of fine litter components by forest subtypes in Mamirauá Sustainable Development Reserve (MSDR), Central Amazon floodplain, Brazil. Dark green = High Várzea; light green = Low Várzea; orange = Chavascal.

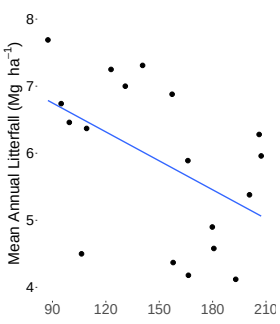

(a) Leaf fall. Linear fit; standartized slope = $-0.01, r^2 = 0.24, p = 0.04$

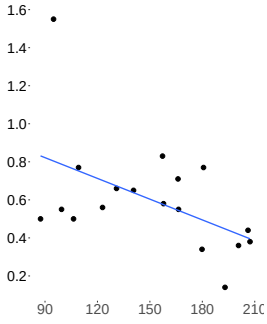

(b) Flower fall. Linear fit; standartized slope = $-0.01, r^2 = 0.25, p = 0.04$

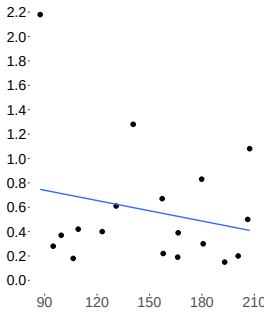

(c) Fruit fall. Linear fit; standartized slope = $-0.005, r^2 = 0.05, p = 0.04$

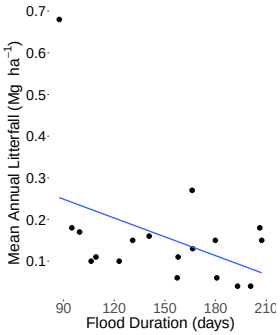

(d) Seed fall. Linear fit; standartized slope = $-0.01, r^2 = 0.18, p = 0.08$

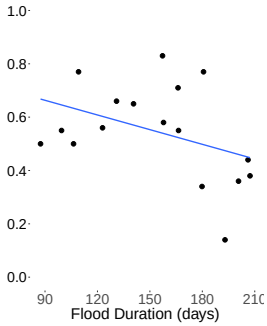

(e) Flower fall. One outlier removed. Linear fit; standartized slope = $-0.01, r^2 = 0.16, p = 0.11$

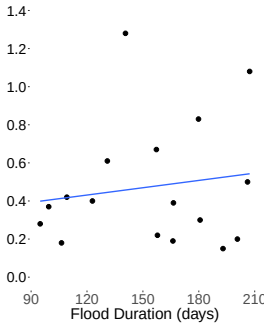

(f) Fruit fall. One outlier removed. Linear fit; standartized slope = $-0.004, r^2 = 0.02, p = 0.57$

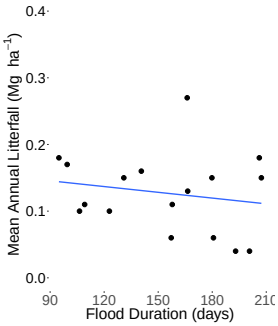

(g) Seed fall. One outlier removed. Linear fit; standartized slope = $-0.005, r^2 = 0.03, p = 0.48$

Figure 5.11: Association between mean annual production of fine litterfall components and flood duration on forest sample plots established in Mamirauá Sustainable Development Reserve (MSDR), Central Amazon floodplain, Brazil. Brazil. Data points are mean annual litter production per forest plot (N=18). Figures from (a) to (d) including the entire dataset; figures (e) to (g) excluding one extreme outlier in each component.

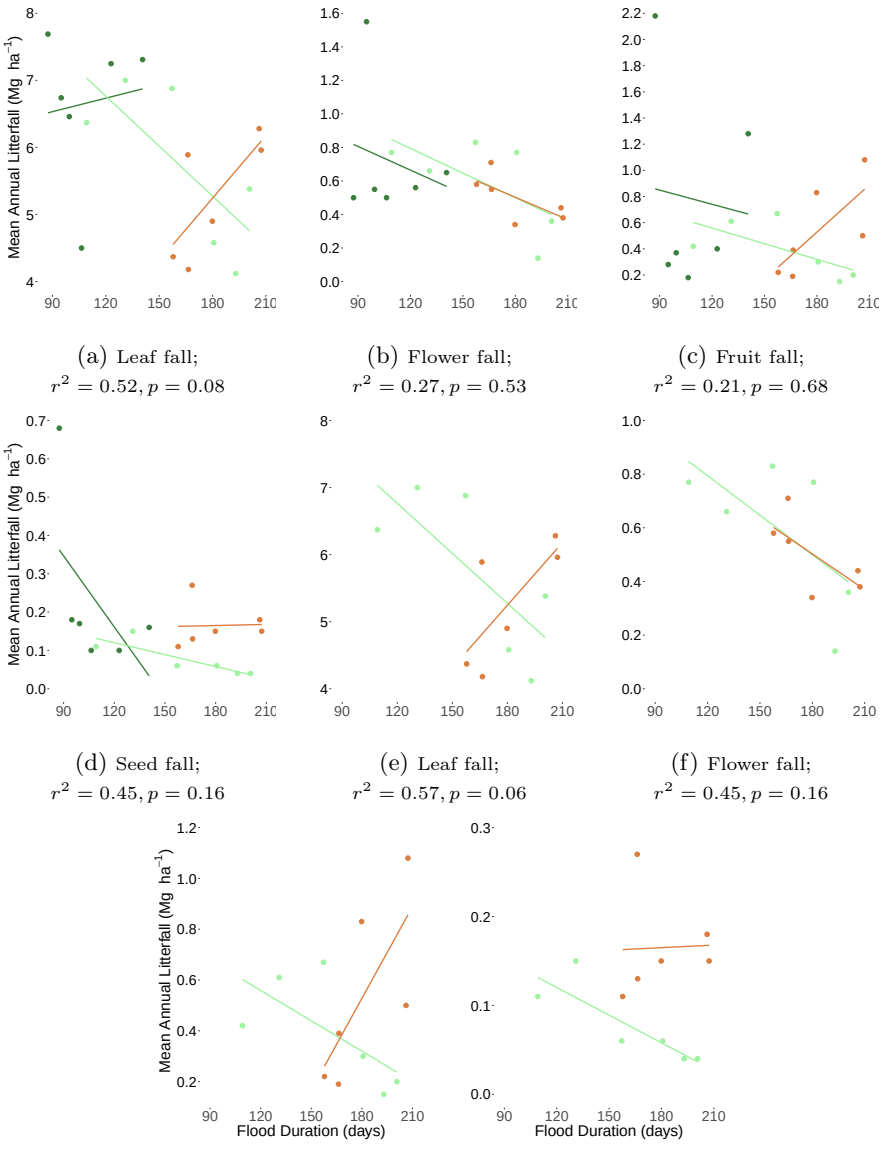

(a) Leaf fall; $r^2 = 0.52, p = 0.08$

(b) Flower fall; $r^2 = 0.27, p = 0.53$

(c) Fruit fall; $r^2 = 0.21, p = 0.68$

(d) Seed fall; $r^2 = 0.45, p = 0.16$

(e) Leaf fall; $r^2 = 0.57, p = 0.06$

(f) Flower fall; $r^2 = 0.45, p = 0.16$

(g) Fruit fall; $r^2 = 0.54, p = 0.08$

(h) Seed fall; $r^2 = 0.62, p = 0.04$

Figure 5.12: Association between mean annual production of fine litterfall components and flood duration controlling for forest subtype on forest sample plots established in Mamirauá Sustainable Development Reserve (MSDR), Central Amazon floodplain, Brazil. Data points are mean annual litter production per forest plot (N=18). Figures (a) to (d) including the entire dataset; figures (e) to (h) excluding high várzea, which presented extreme outliers for all fine litterfall components. Dark green = High Várzea; light green = Low Várzea; orange = Chavascal.

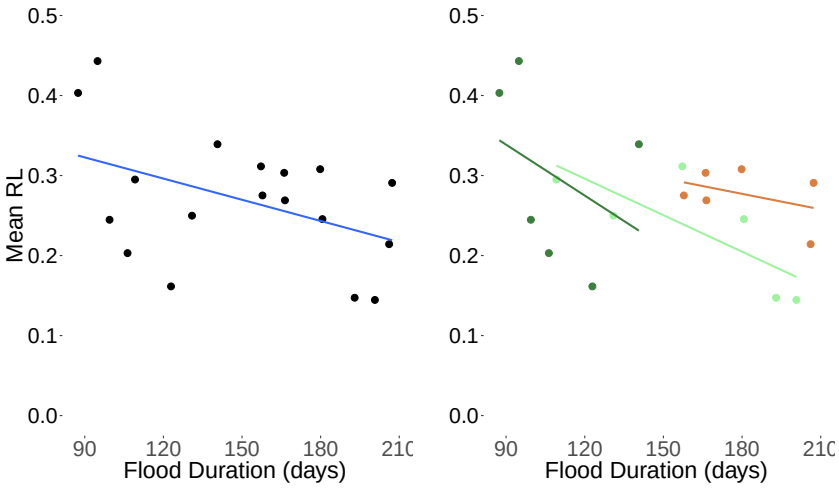

(a) Pooled forest plots. Linear fit; standartized slope $= -0.44, r^2 = 0.20, p = 0.07$

(b) Controlling for forest subtype. ANCOVA; $r^2 = 0.35, p = 0.32$

Figure 5.13: Relationship between investment in photosynthetic organs relative to reproductive organs (RL ratio), flood duration and forest subtypes in forest sample plots established in Mamirauá Sustainable Development Reserve (MSDR), Central Amazon floodplain, Brazil. An RL ratio equal to 1 mean equal investment. Data points represent the mean RL ratio per forest plot. Dark green = High Várzea; light green = Low Várzea; orange = Chavascal.

5.3.3 NPP estimates from fine litterfall

Taking into account the mean annual fine litterfall production of 8.62±1.01 Mg ha^{-1}, we estimated mean NPP (above and belowground) of várzea forests in our study area as 25.64±1.77 Mg ha^{-1} (±95% confidence interval) or 12.04±0.83 Mg C ha^{-1}. Our estimates of total NPP for each forest type are given on Table 5.4.

Table 5.4: Estimates of total forest net primary productivity in terms of biomass (NPP in Mg ha^{-1} ± 95% confidence interval) and carbon fraction (NPP_{carbon} in Mg C ha^{-1} ± 95% confidence interval) by forest subtype in the várzea forests of Mamirauá Sustainable Development Reserve (Central Amazon, Brazil).

Vegetation type	NPP	NPP_{carbon}
High Várzea	28.09±9.34	13.19±4.38
Low Várzea	23.78±7.64	11.16±3.59
Chavascal	22.10±8.28	10.38±3.89

Since NPP is estimated from litterfall data, the same patterns of differences in NPP among forest types, its relation to flood duration, and the effect of flood duration controlling for forest subtype also apply to our NPP estimates (Table 5.5 and Figure 5.14).

Table 5.5: Paired differences in mean net primary productivity (NPP) between forest subtypes (in Mg ha^{-1}± confidence interval at 95% significance) in the Mamirauá Sustainable Development Reserve (Central Amazon, Brazil). Difference between means were tested with one-way ANOVA and post-hoc Tukey's honestly significant difference (HSD) test.

Forest subtypes	Difference	p_{adj}
Low Várzea - High Várzea	-4.31±8.10	0.37
Chavascal - High Várzea	-5.99±8.10	0.17
Chavascal - Low Várzea	-1.68±8.10	0.85

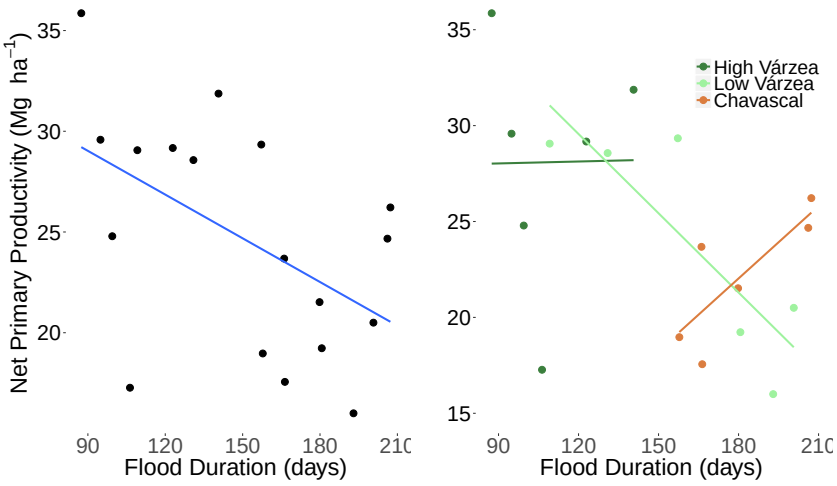

(a) Pooled forest plots. Linear fit; standartized slope $= -0.51, r^2 = 0.26, p = 0.03$

(b) Controlling for forest subtype. ANCOVA; $r^2 = 0.51, p = 0.09$

Figure 5.14: Relationship between net primary productivity and flood duration in forest sample plots established in Mamirauá Sustainable Development Reserve (MSDR), Central Amazon floodplain, Brazil. Data points are estimated net primary productivity per forest plot (N=18).

5.4 Discussion

Mean annual fine litter production we reported in this study is very similar to those already published for other forests in the Amazon, and in the upper limit of other várzea forests (Table 5.6). The comparison of litterfall and NPP between different forest subtypes under distinct flood regimes did not reached firm statistical results on which we can rely for solid conclusions due to our small sample size. Therefore, the specifics of litterfall and NPP of forest subtypes under distinct flood durations must be taken cautiously. Anywise, we still believe it is possible to infer some interesting ecological patterns which add important insights of how forest communities respond to varying flood regimes influencing their ecological processes.

Does fine litterfall production and dynamics differ among forest subtypes and flood regimes?

Our study supports the overarching hypothesis that the annual flood pulse represents a major factor modulating litterfall dynamics in Amazonian floodplain forests (Camargo et al. 2015; Klinge 1978; Klinge and Rodrigues 1968; Nebel et al. 2001; Worbes 1997), and we show that fine litterfall dynamics do differ between forest subtypes.

Litterfall in high várzea forests peaked four months after low várzea and chavascal and does not show any direct linear relationship with the flood pulse in our dataset. But when bi-weekly litterfall was lagged in 60 days a strong linear relationship emerges. The rationale behind is that high várzea forests

Table 5.6: Comparison of fine litterfall production in different Amazonian floodplain forests and non-floodable Terra Firme forests in distinct regions. Fine litter production values (Litter) are in Mg ha^{-1} year^{-1}.

Forest Type	Site	Litter	Source
Várzea	Eastern Amazon (tidal)	13.80	Cattanio et al. 2004
	Eastern Amazon (tidal)	8.50	Silva and Lobo 1982
	Central Amazon (low várzea)	7.80	Worbes 1997
	Central Amazon (low várzea)	13.70	Worbes 1997
	Central Amazon (low várzea)	6.39	Schöngart et al. 2010
	Central Amazon (high várzea)	6.84	Schöngart et al. 2010
	Central Amazon	9.95	Hawes and Peres 2016
	Central Amazon (high várzea)	**9.81**	**This study**
	Central Amazon (low várzea)	**8.30**	**This study**
	Central Amazon (chavascal)	**7.75**	**This study**
	Western Amazon (high várzea)	7.02	Nebel et al. 2001
	Western Amazon (low várzea)	7.14	Nebel et al. 2001
	Western Amazon (chavascal)	6.93	Nebel et al. 2001
Igapó	Eastern Amazon	6.80	Moreira 2006
	Eastern Amazon	10.35	Camargo et al. 2015
	Eastern Amazon	5.73	Camargo et al. 2015
	Eastern Amazon	4.99	Camargo et al. 2015
	Eastern Amazon	9.86	Camargo et al. 2015
	Central Amazon	6.70	Adis et al. 1979
Terra Firme	Eastern Amazon (primary forest)	8.80	Klinge 1978
	Eastern Amazon (primary forest	8.04	Dantas and Phillipson 1989
	Eastern Amazon (secondary forest)	5.04	Dantas and Phillipson 1989
	Central Amazon (primary forest)	10.29	Hawes and Peres 2016
	Central Amazon (primary forest)	7.50	Klinge and Rodrigues 1968
	Central Amazon (primary forest)	7.31	Rowland et al. 2018
	Southern Amazon (primary forest)	11.80	Selva et al. 2007

occur on higher topographical levels and very often behind low várzeas and farther from river channels (Ferreira-Ferreira et al. 2015). Thus, probably flood waters take longer to reach most high várzea stands. Schöngart et al. 2010 and Nebel et al. 2001 also detected different litterfall timings in different várzea forest subtypes. Schöngart et al. 2010 analyzed fine litterfall in high and low várzea in the same study area as ours between 2002 and 2003, however, unlike Camargo et al. 2015, Hawes and Peres 2016, Nebel et al. 2001, and our study, they did not found any correlation between litterfall and water levels. This is probably due to the location of the water level gauging station used by the authors, situated in the Japurá river and hence farther from the study area, what is supported by the 60-120 days of time lag between litterfall and water levels visible in their graphics (Schöngart et al. 2010).

Regarding mean annual production of fine litterfall among forest subtypes under distinct flood regimes, our ANCOVA analysis indicate that at least for low várzea and chavascal forests these differences seems to exist. Our analy-

sis suggests that low várzeas has lower litter production in stands situated on places subject to longer floods, while chavascal forests has the opposite litterfall behavior. Regarding litter production of low várzeas, one possible explanation for this pattern could be due to the relationship between flood and deciduousness. Under longstanding flooding, deciduousness is advantageous to decrease water loss by reduced transpiring area and thus balance the trend of tree water deficit (Borchert 1991). Forest stands subject to prolonged flooding tend to have slightly more deciduous species than those with less days of flood per year (Parolin and Wittmann 2010). Also, unlike evergreen species that shed and replace their leaves continuously, deciduous trees shed leaves mainly during the 3-4 months of high water levels (Parolin 2000; Schöngart et al. 2002). This results in lower annual litter production in low várzeas subject to longer flood durations and thus composed of more deciduous trees, which is supported by the more erratic leaf fall of visible in the Figure 5.8a. However, for the majority of várzea forests species, we still have no species-level information about leaf production strategies (deciduous, brevi-deciduous or evergreen) (Haugaasen and Peres 2005; Parolin 2002), so further studies are necessary to understand the functional responses and adaptations of leaf production and phenology of várzea tree species to different inundation regimes.

In chavascal forests, the higher mean annual litter productions under longer flood durations is probably linked to the severest anoxic conditions found in these forests, when compared to the other forest subtypes, which could induce more complete deciduousness under longer flood durations. Chavascal forests grow in terrain depressions and backswamps behind levees occupied by high várzeas and in depressions formed by old, sediment-fulfilled lakes (Ayres 1993; Ferreira-Ferreira et al. 2015), where soil clay content could reach 88% (Wittmann et al. 2004). According to our field observations, these forests commonly establish in topographical levels that are below the mean river level, which leads to waterlogging even before over-bank flow due to local precipitation and/or groundwater uplift. In addition, higher organic matter in the soil (Wittmann et al. 2004) increases microbial oxygen demand. The tree communities of chavascal forests are well adapted to waterlogging, having developed several strategies to cope with seasonal anoxia, like stilt and aerial roots (Wittmann and Parolin 2005). And we suggest that chavascal forest stands subject to longer flood durations, and thus to longer water deprivation in tree crows, could led to higher leaf abscission and hence higher litterfall production compared to those chavascal forests under shorter flood periods.

As far as we know, ours is only the second study in the literature to assess litterfall in chavascal forests, together with Nebel et al. 2001, and add to the seven published studies we could find that address ecological aspects of chavascal forest communities (Junk and Piedade 1997; Lamotte 1990; Nebel et al. 2001; Prance 1979; Wittmann et al. 2002, 2004; Wittmann and Parolin 2005) Therefore, more research effort must be carried to detail several aspects of these forest communities.

Our high várzea forest plots presented the largest variability among forest subtypes, covering almost the entire range of litter production of our dataset. This prevented us from making strong inferences about the relation between mean annual fine litter production and flood duration, with one specific extreme observation strongly influencing the analyses.

Do distinct forest types and flood regimes reveal different community-level signals of varying plant investment strategies into reproductive organs versus photosynthetic organs?

The investment into reproduction relative to the investment in photosynthesis, summarized by the mean RL ratio per forest plot, show that longer flood durations in general translate into lower resource allocation for reproductive organs, regardless the forest subtype.

The decreasing slopes in ANCOVA analysis along the flood gradient, from high várzeas to chavascal forests (Figure 5.13b), suggests that investment into reproductive organs in high várzeas is more sensitive to increasing flood durations, so that trees invest less into reproductive organs in favor of higher photosynthetic rates to provide energy stocks to cope with the anoxia of the flood season. Chavascal forests show the lowest sensitivity to flood duration and low várzeas intermediate sensitivity. Although it needs further data for confirmation, it seem reasonable to claim such hypothesis based on the current knowledge on várzea forests ecological development.

It has been long assumed that trees actually occupying floodable environments have originated from the surrounding non-floodable terra firme forests (Kubitzki 1989), which is supported by paleobotanical and paleoclimatic data (Haffer and Prance 2001). Short hypoxic or anoxic conditions are also present in non-flooded forests after soil saturation by heavy rains and the subsequent increase in microbial oxygen demand under in high temperatures (Junk and Piedade 2010).

Lopez and Kursar 1999 and Lopez and Kursar 2003 suggest that this conditions likely favor the development of a predisposition for waterlogging tolerance observed in Amazonian floodplain forests that allowed the establishment of some species in higher topographical levels within the floodplains. The degree of adaptation to anoxic conditions depends on the intrinsic potential of each species to develop metabolic, morphological, anatomical and phenological adjustments as well as the time extent taken to colonize floodplain environments (Ferreira et al. 2010; Kubitzki 1989; Parolin 2001).

As result, better adapted species were able to establish into lower portions of the flooding gradient and eventually speciate, as suggested by the higher degree of endemism of low várzea forests (Wittmann et al. 2012). Therefore, several tree species that actually occupy high várzea forests probably developed less pronounced adaptations to anoxic conditions than those of low várzea forests (Ferreira et al. 2010; Wittmann et al. 2002). And probably the same reasoning applies to chavascal forests, where species that developed a more efficient set of adaptations to anoxia were able to establish in this extremely harsh environments that could experiment more than nine months of oxygen deprivation in the root system. Wittmann and Parolin 2005 report the development of stilt roots up to six meters above the soil on stems, sometimes presenting the formation of buds and young shoots. The authors also report a high capacity for vegetative reproduction in chavascal species, which is fairly evident during our field work. Thus, while in high várzea forests the increasing flooding stress can result in most trees prioritizing photosynthesis, in chavascal this effect is less pronounceable.

Can we use litterfall dynamics to predict how the primary productivity of várzea forest could respond to hydrological variability and changes?

In a recent study in upper Solimões river in Peru (Ucayali river) from 1985 to 2015, Ronchail et al. 2018 found that since late 1990s the low water period consistently lasted longer, ending one month later than usual. The authors also report that the rising water period tended to be more abrupt, during two months whereas before 90s it used to last three months. Concomitantly an increase in the frequency of extreme river discharges has been observed in the Amazon basin in recent decades (Espinoza Villar et al. 2009; Gloor et al. 2015). An increase in the severity of flood pulse, mainly in the wet season, is also expected, with water discharges increasing between 7.5 and 12% for the 100 year return time floods to the end of the century Zulkafli et al. 2016. These results summarily means a strengthening seasonality, which agrees with the already observed intensification of the hydrological cycle in the Amazon basin recently demonstrated by Gloor et al. 2013 and Gloor et al. 2015. Nevertheless, general hydrological conditions are predicted to be drier than the current period in the Amazon basin for the end of the century (IPCC 2013).

Our results show that mean annual litter production in low várzea forests can be very sensitive to flood duration. Assuming that mean annual litterfall is a consistent proxy for total NPP, we can expect a large interannual variability of low várzea forests NPP under the scenario of a strengthened seasonality of the flood pulse. Drier than usual years or progressively extend dry seasons can increase the growing season length and result in higher NPP, both in low várzeas and high várzeas, while years with extreme flood events can probably cause a decrease in NPP of low várzeas. Although our data does not suggest patterns in NPP for high várzeas regarding flood duration, tree species in high várzea are less efficient under flooded conditions (Parolin et al. 2010), and we can expect lower NPP rates in years of extreme flooding.

In chavascal forests, our data suggests that longer flood durations increase mean annual litterfall, and thus NPP - assuming the proportion litterfall/NPP remains more or less constant. Wittmann and Parolin 2005 suggested that beyond the function of mechanical support, the primary function of stilt roots is aeration and also reported that species subject to longer flood periods tended to present more aboveground roots than those growing under shorter flooding. It is possible that better adapted chavascal species allocate more resources to the rhizosphere under longer flood periods, thus leading to higher total NPP. However, the almost complete lack of information regarding chavascal communities prevent us to draw further conclusions related to observed and predicted changes in hydrological conditions.

Chapter 6

SYNTHESIS AND CONCLUSION

Considering that forests comprise 85.5% (397,800 ha) of the total area of the Mamirauá Sustainable Development Reserve mapped by us (468,000 ha; Chapter 2), and taking into account the mean AGC found by us of 114.01± 11.63 Mg C ha^{-1} , which is consistent with the 107.17 Mg C ha^{-1} reported by Schöngart et al. 2010 for the same region, we then estimate a mean total carbon stock of 45.35±4.63 Tg C for the studied area. We estimated mean carbon stocks per forest subtype as 25.32±2.14, 11.20±2.02, and 5.94±0.88 Tg C for low várzeas, high várzeas and chavascal forests, respectively. As AGC values in our dataset are primarily differentiated by forest subtype, we can use our forest type mapping (Figure 2.5) to determine the approximate distribution of forest AGC across the mapped area.

We show that while low várzea forests have relatively higher aboveground carbon stocks, it was comparatively less productive than high várzeas per unit of area. This result in lower carbon residence times in high várzeas. Assuming our forest stands are in a quasi-equilibrium state, we can calculate the aboveground C residence time as the ratio of AGC to aboveground NPP (ANPP) (Malhi et al. 2004). For the sake of comparison of C residence times among forest subtypes, we can assume that 50% of total NPP is allocated to ANPP (Aragão et al. 2009). This results in mean aboveground C residence times of 13, 10, and 7 years for low várzea, high várzea and chavascal, respectively. Schöngart et al. 2010 also characterize várzea forests as highly dynamic ecosystems, with C residence times in the long-term carbon pool of aboveground coarse wood live biomass (AGWB) of only 26 years, compared to a mean 56-80 years in terra firme forests (Malhi et al. 2004). Since we are also considering short-lived components (canopy), our C residence times are much lower.

Up-scaling our NPP estimates per unit area for the year 2017, we can estimate an annual carbon assimilation of c.a 4.00 Tg C $year^{-1}$, distributed in 1.97±0.63, 1.15±0.82, 0.87±0.33 Tg C $year^{-1}$for low várzea, high várzea and chavascal forests, respectively. Although we report higher NPP rates per unit area in high várzea forests instead of low várzeas, high várzea forests cover only 18.7% of the total mapped area, while low várzea forests cover 37.7% of the area, thus resulting in a higher amount of carbon assimilation per year in low várzeas.

Our flood modeling approach proved promising, although further development is needed to reduce uncertainties. We can use our flood duration predictions to provide a first degree approximation of how heterogeneous NPP

distribution can be when taking into account the role of flood duration as well as forest subtypes. Figure 6.1 shows forest NPP as a linear function of flood duration (see Figure 5.14a), while Figure 6.2 shows the spatial distribution of NPP when predicted by flood duration, controlling for forest subtype (ANCOVA; Figure 5.14b). The flood duration model predictions were biased toward values of maximum flood duration, and since flood duration was inversely related to flood duration, our predicted NPP was biased towards low values. When controlling for forest subtype, the spatial prediction of NPP was mostly distributed within intermediate values, between 17 and 30 Mg C.

Even with large uncertainties, these maps highlight the remarkable heterogeneity expected from NPP in várzea forests, and stresses the importance of considering the role of flood duration and forest subtypes in estimates of carbon dynamics in the Amazon floodplains. The influence of flood duration on carbon stocks and fluxes is still one of the largest sources of uncertainty in these studies. Moreover, the effectiveness of bilateral and multilateral policies for reduction of greenhouse gas emissions, such as REDD+ (Reducing emissions from deforestation and forest degradation) require more accurate estimations of carbon stocks and assimilation capacity (Salimon et al. 2011). These sources of error can be minimized by improving and extending *in situ* monitoring of different forest formations under different hydrological regimes with remote sensing and modeling approaches such as conducted in this study, enabling to capture both vegetation structure and flooding under the forest canopy. With the expected new generation of synthetic aperture radar platforms, such as NISAR and BIOMASS, and advancements in SAR processing and machine learning methods, such approaches will be applicable at a basin-level scale.

Predicting how the carbon balance of Amazonian várzeas and Amazonian wetlands in general will respond to climatic and hydrological changes requires a more detailed and mechanistic understanding of carbon cycling and its relationship to ecohydrological factors, including the spatially explicit mapping of relevant wetland characteristics. This study advances our understanding by fulfilling these requirements.

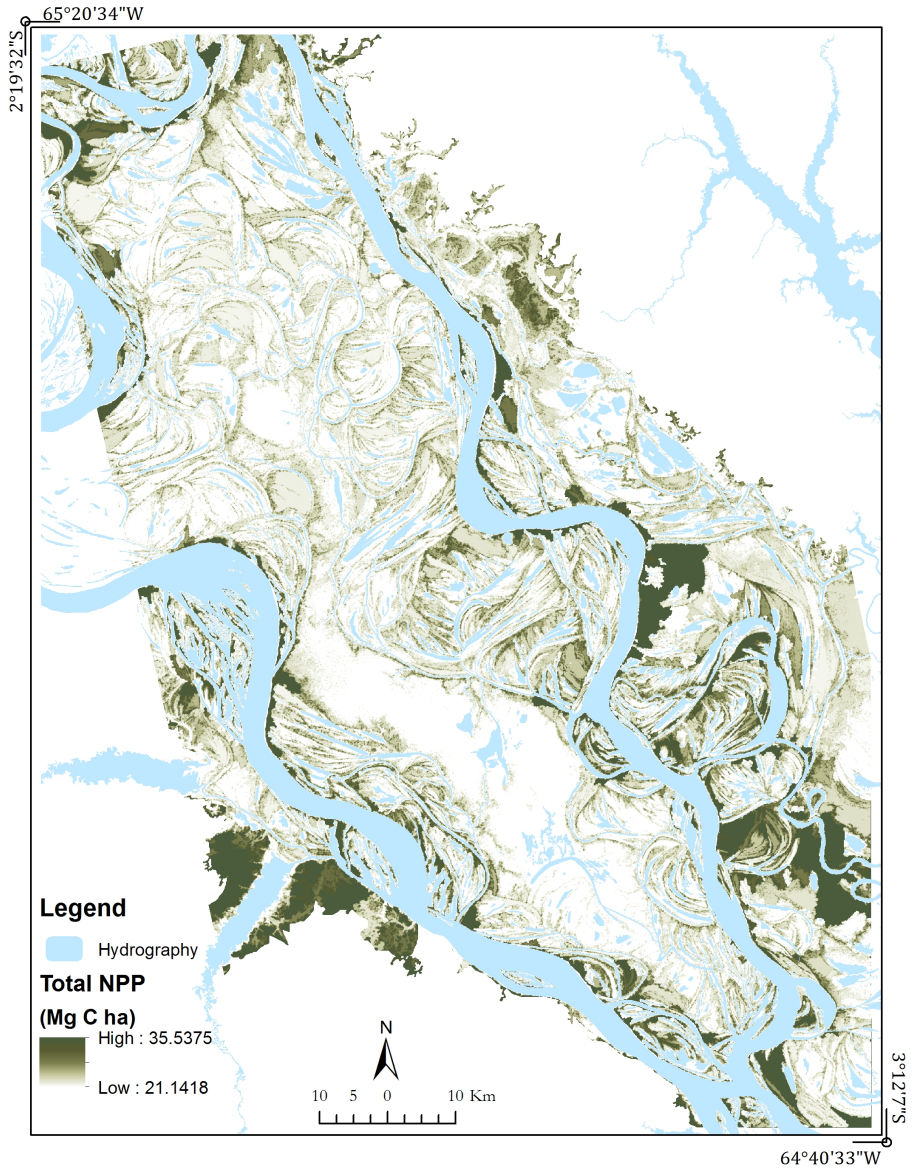

Figure 6.1: Spatial distribution of net primary productivity (NPP) in the várzeas forests of Mamirauá Sustainable Development Reserve (Central Amazon, Brazil). The NPP was predicted by a linear model using flood duration as predictor variable (see Figure 5.14a). The spatial distribution of flood durations were predicted using the logistic model for the year 2017, as in the Figure 3.4.

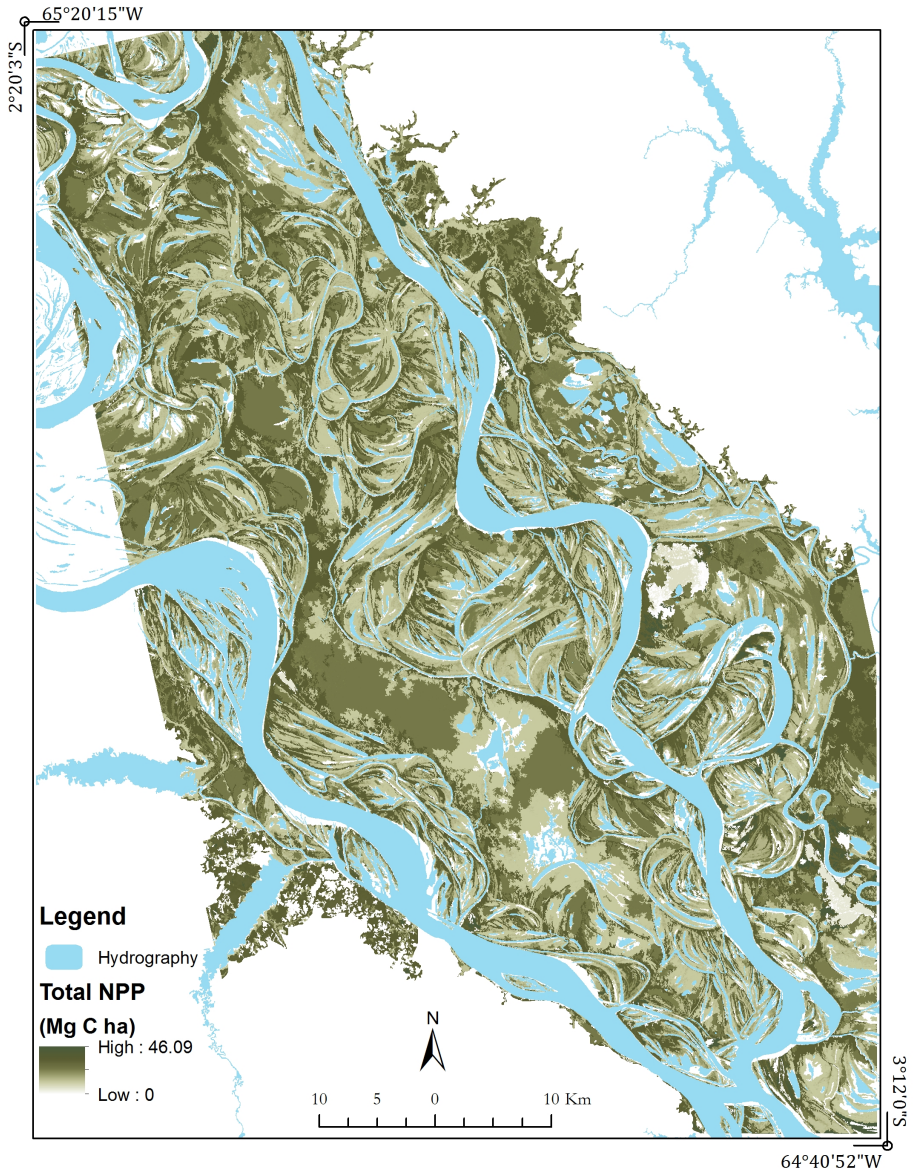

Figure 6.2: Spatial distribution of net primary productivity (NPP) as a function of flood duration controlling for forest subtype in the várzeas forests of Mamirauá Sustainable Development Reserve (Central Amazon, Brazil). The spatial distribution of flood durations were predicted using the logistic model for the year 2017, as in the Figure 3.4.

Bibliography

Aalde, Harald, Gonzalez, Patrick, Gytarsky, Michael, Krug, Thelma, Kurz, Werner A., Ogle, Stephen, Raison, John, Schoene, Dieter, Ravindranath, N H, Elhassan, Nagmeldin G, Heath, Linda S, Higuchi, Niro, Kainja, Samuel, Matsumoto, Mitsuo, Sánchez, María José Sanz, and Somogyi, Zoltan (2006). *IPCC guidelines for national greenhouse gas inventories, chapter 4: forest land*. Tech. rep. IPCC (cit. on pp. 44, 59).

Abril, Gwenaël, Martinez, Jean-Michel, Artigas, L Felipe, Moreira-Turcq, Patricia, Benedetti, Marc F, Vidal, Luciana, Meziane, Tarik, Kim, Jung-Hyun, Bernardes, Marcelo C, Savoye, Nicolas, Deborde, Jonathan, Souza, Edivaldo Lima, Albéric, Patrick, Landim de Souza, Marcelo F, and Roland, Fabio (2014). "Amazon River carbon dioxide outgassing fuelled by wetlands." In: *Nature* 505.7483, pp. 395–8 (cit. on p. 57).

Adis, J, Furch, K, and Irmler, U (1979). "Litter production of a Central-Amazonian black water inundation forest". In: *Tropical Ecology* 20.2, pp. 236–245 (cit. on p. 76).

Affonso, Adriana Gomes, Arraut, Eduardo de Moraes, Renó, Vivian Fróes, Leão, Joaquim Antônio Dionísio, Hess, Laura, Queiroz, Helder, and Novo, Evlyn Márcia Leão de Moraes (2011). "Estudo da dinâmica de inundação na várzea Amazônica através de termo-sensores de campo." In: (cit. on pp. 15, 18, 19).

Alsdorf, D (2004). "A New View of Amazon Floodplain Inundation Hydraulics". In: *AGU Fall Meeting Abstracts*, p. 1179 (cit. on p. 28).

Alsdorf, Doug, Bates, Paul, Melack, John M, Wilson, Matt, and Dunne, Thomas (2007a). "Spatial and temporal complexity of the Amazon flood measured from space". In: *Geophysical Research Letters* 34.8, p. L08402. DOI: 10.1029/2007GL029447 (cit. on p. 7).

Alsdorf, Douglas E., Rodríguez, Ernesto, and Lettenmaier, Dennis P (2007b). "Measuring surface water from space". In: *Reviews of Geophysics* 45.2, RG2002. DOI: 10.1029/2006RG000197 (cit. on pp. 28, 38).

Anderson, Elizabeth P, Jenkins, Clinton N, Heilpern, Sebastian, Maldonado-Ocampo, Javier A., Carvajal-Vallejos, Fernando M., Encalada, Andrea C, Rivadeneira, Juan Francisco, Hidalgo, Max, Cañas, Carlos M., Ortega, Hernan, Salcedo, Norma, Maldonado, Mabel, and Tedesco, Pablo A. (2018). "Fragmentation of Andes-to-Amazon connectivity by hydropower dams". In: *Science Advances* 4.1, eaao1642. DOI: 10.1126/sciadv.aao1642 (cit. on p. 28).

Anderson, Liana Oighenstein (2012). "Biome-Scale Forest Properties in Amazonia Based on Field and Satellite Observations". In: *Remote Sensing* 4.5, pp. 1245–1271. DOI: 10.3390/rs4051245 (cit. on p. 1).

Aragão, L. E. O. C., Malhi, Y., Metcalfe, D. B., Silva-Espejo, J. E., Jiménez, E., Navarrete, D., Almeida, S., Costa, a. C. L., Salinas, N., Phillips, O. L., Anderson, L. O ., Baker, T. R., Goncalvez, P. H., Huamán-Ovalle, J., Mamani-Solórzano, M., Meir, P., Monteagudo, a., Peñuela, M. C., Prieto, a., Quesada, C. a., Rozas-Dávila, a., Rudas, a., Silva Junior, J. a., and Vásquez, R. (2009). "Above- and below-ground net primary productivity across ten Amazonian forests on contrasting soils". In: *Biogeosciences Discussions* 6.1, pp. 2441–2488. DOI: 10.5194/bgd-6-2441-2009 (cit. on pp. 55, 56, 80).

Aragão, Luiz E. O. C., Poulter, Benjamin, Barlow, Jos B., Anderson, Liana O., Malhi, Yadvinder, Saatchi, Sassan, Phillips, Oliver L., and Gloor, Emanuel (2014). "Environmental change and the carbon balance of Amazonian forests". In: *Biological Reviews* 89.4, n/a–n/a. DOI: 10.1111/brv.12088 (cit. on p. 1).

Arnesen, Allan S., Silva, Thiago Sanna Freire, Hess, Laura L., Novo, Evlyn M.L.M., Rudorff, Conrado M., Chapman, Bruce D., and McDonald, Kyle C. (2013). "Monitoring flood extent in the lower Amazon River floodplain using ALOS/PALSAR ScanSAR images". In: *Remote Sensing of Environment* 130, pp. 51–61. DOI: 10.1016/j.rse.2012.10.035 (cit. on pp. 7, 11, 12, 28, 37).

Ashcroft, Michael B, Chisholm, Laurie A, and French, Kristine O (2009). "Climate change at the landscape scale: predicting fine-grained spatial heterogeneity in warming and potential refugia for vegetation". In: *Global Change Biology* 15.3, pp. 656–667 (cit. on p. 23).

Assis, Rafael L, Wittmann, Florian, Piedade, Maria T. F., and Haugaasen, Torbjørn (2015). "Effects of hydroperiod and substrate properties on tree alpha diversity and composition in Amazonian floodplain forests". In: *Plant Ecology* 216.1, pp. 41–54. DOI: 10.1007/s11258-014-0415-y (cit. on p. 3).

Ayres, José Márcio (1993). "As matas de várzea de Mamirauá". In: *Estudos de Mamirauá*. Ed. by Sociedade Civil Mamirauá. Brasília: MCT/CNPq, pp. 1–123 (cit. on pp. 6, 12, 23, 77).

Baccini, A., Goetz, S. J., Walker, W. S., Laporte, N. T., Sun, M., Sulla-Menashe, D., Hackler, J., Beck, P. S. A., Dubayah, R., Friedl, M. A., Samanta, S., and Houghton, R. A. (2012). "Estimated carbon dioxide emissions from tropical deforestation improved by carbon-density maps". In: *Nature Climate Change* 2, pp. 182–185. DOI: 10.1038/nclimate1354 (cit. on p. 41).

Baker, Timothy R, Phillips, Oliver L, Malhi, Yadvinder, Almeida, Samuel, Arroyo, Luzmila, Di Fiore, Anthony, Erwin, Terry, Higuchi, Niro, Killeen, Timothy J, Laurance, Susan G, Laurance, William F, Lewis, Simon L, Monteagudo, Abel, Neill, David A, Vargas, Percy Núñez, Pitman, Nigel C a, Silva, J Natalino M, and Martínez, Rodolfo Vásquez (2004). "Increasing biomass in Amazonian forest plots." In: *Philosophical transactions of the Royal Society of London. Series B, Biological sciences* 359.February, pp. 353–365. DOI: 10.1098/rstb.2003.1422 (cit. on p. 44).

Bar-On, Yinon M, Phillips, Rob, and Milo, Ron (2018). "The biomass distribution on Earth". In: *Proceedings of the National Academy of Sciences*, p. 201711842. DOI: 10.1073/pnas.1711842115 (cit. on p. 41).

Beja, Pedro, Santos, Carlos David, Santana, Joana, Pereira, Maria João, Marques, J Tiago, Queiroz, Hélder Lima, and Palmeirim, Jorge M (2010). "Seasonal patterns of spatial variation in understory bird assemblages across a mosaic of flooded and unflooded Amazonian forests". In: *Biodiversity and conservation* 19.1, p. 129 (cit. on p. 23).

Berger, Wolfgang H and Parker, Frances L (1970). "Diversity of planktonic foraminifera in deep-sea sediments". In: *Science* 168.3937, pp. 1345–1347 (cit. on p. 43).

Blaschke, T. (2010). "Object based image analysis for remote sensing". In: *ISPRS Journal of Photogrammetry and Remote Sensing* 65.1, pp. 2–16. DOI: 10.1016/j.isprsjprs.2009.06.004 (cit. on p. 12).

Bonnet, M. P., Barroux, G., Martinez, Jean-Michel, Seyler, F., Moreira-Turcq, P., Cochonneau, G., Melack, John M, Boaventura, G., Maurice-Bourgoin, L., León, J. G., Roux, E., Calmant, S., Kosuth, P., Guyot, J. L., and Seyler, P. (2008). "Floodplain hydrology in an Amazon floodplain lake (Lago Grande de Curuaí)". In: *Journal of Hydrology* 349.1-2, pp. 18–30. DOI: 10.1016/j.jhydrol.2007.10.055 (cit. on pp. 5, 27).

Borchert, R (1991). "Growth periodicity and dormancy". In: *Physiology of trees*. Ed. by A S Raghavendra, pp. 221–245 (cit. on p. 77).

Botero-Arias, Robinson, Marmontel, Miriam, and Queiroz, Helder Lima de (2009). "Projeto de manejo experimental de jacarés no Estado do Amazonas: Abate de jacarés no Setor Jarauá-Reserva de Desenvolvimento Sustentável Mamirauá, dezembro de 2008". In: *Scientific Magazine UAKARI* 5.2, pp. 49–57 (cit. on p. 24).

Bousquet, Philippe, Ciais, Philippe, Miller, J B, Dlugokencky, Edward J., Hauglustaine, D A, Prigent, C, Van der Werf, G R, Peylin, P, Brunke, E-G, Carouge, C, Langenfelds, R L, Lathière, J, Papa, F, Ramonet, M, Schmidt, M, Steele, L P, Tyler, S C, and White, J (2006). "Contribution of anthropogenic and natural sources to atmospheric methane variability." In: *Nature* 443.7110, pp. 439–43. DOI: 10.1038/nature05132 (cit. on p. 39).

Bray, J Roger and Gorham, Eville (1964). "Litter Production in Forests of the World". In: *Advances in Ecological Research*. Ed. by J B Cragg. Vol. 2. Advances in Ecological Research. Academic Press, pp. 101–157. DOI: https://doi.org/10.1016/S0065-2504(08)60331-1 (cit. on p. 56).

Breiman, Leo (2001). "Random Forests". In: *Machine Learning* 45.1, pp. 5–32. DOI: 10.1023/A:1010933404324 (cit. on p. 12).

Caeiro, Frederico and Mateus, Ayana (2014). *randtests: Testing randomness in R*. R package version 1.0 (cit. on p. 58).

Camargo, M., Giarrizzo, T., and Jesus, AJS. (2015). "Effect of seasonal flooding cycle on litterfall production in alluvial rainforest on the middle Xingu River (Amazon basin, Brazil)". In: *Brazilian Journal of Biology* 75.3 suppl 1, pp. 250–256. DOI: 10.1590/1519-6984.00514BM (cit. on pp. 75, 76).

Campbell, David G, Stone, Judy L, and Rosas, Arito (1992). "A comparison of the phytosociology and dynamics of three floodplain (Várzea) forests of known ages, Rio Juruá, western Brazilian Amazon". In: *Botanical Journal of the Linnean Society* 108.3, pp. 213–237. DOI: 10.1111/j.1095-8339.1992.tb00240.x (cit. on p. 56).

Cannell, M.G.R. (1984). "Woody biomass of forest stands". In: *Forest Ecology and Management* 8.3-4, pp. 299–312. DOI: 10.1016/0378-1127(84)90062-8 (cit. on p. 44).

Carabajal, Claudia C and Harding, David J (2006). "SRTM C-Band and ICEsat Laser Altimetry Elevation Comparisons as a Function of Tree Cover and Relief". In: *Photogrammetric Engineering & Remote Sensing* 72.3, pp. 287–298. DOI: 10.14358/PERS.72.3.287 (cit. on p. 38).

Carvalhais, Nuno, Forkel, Matthias, Khomik, Myroslava, Bellarby, Jessica, Jung, Martin, Migliavacca, Mirco, Mu, Mingquan, Saatchi, Sassan, Santoro, Maurizio, Thurner, Martin, Weber, Ulrich, Ahrens, Bernhard, Beer, Christian, Cescatti, Alessandro, Randerson, James T., and Reichstein, Markus (2014). "Global covariation of carbon turnover times with climate in terrestrial ecosystems". In: *Nature* 514.7521, pp. 213–217. DOI: 10.1038/nature13731 (cit. on p. 41).

Castello, Leandro, McGrath, David G., Hess, Laura L, Coe, Michael T, Lefebvre, Paul A, Petry, Paulo, Macedo, Marcia N, Renó, Vivian F., and Arantes, Caroline C (2013). "The vulnerability of Amazon freshwater ecosystems". In: *Conservation Letters* 6.4, pp. 217–229. DOI: 10.1111/conl.12008 (cit. on p. 27).

Cattanio, José H, Anderson, Anthony B, Rombold, John S, and Nepstad, Daniel C (2004). "Phenology, litterfall, growth, and root biomass in a tidal floodplain forest in the Amazon estuary". In: *Revista Brasileira de Botânica* 27.4, pp. 703–712. DOI: 10.1590/S0100-84042004000400010 (cit. on p. 76).

Chao, Kuo-Jung, Phillips, Oliver L., Gloor, Emanuel, Monteagudo, Abel, Torres-Lezama, Armando, and Martínez, Rodolfo Vásquez (2008). "Growth and wood density predict tree mortality in Amazon forests". In: *Journal of Ecology* 96.2, pp. 281–292. DOI: 10.1111/j.1365-2745.2007.01343.x. arXiv: arXiv:1011.1669v3 (cit. on p. 53).

Chapman, Bruce, McDonald, Kyle, Shimada, Masanobu, Rosenqvist, Åke, Schroeder, Ronny, and Hess, Laura (2015). "Mapping Regional Inundation with Spaceborne L-Band SAR". In: *Remote Sensing* 7.5, pp. 5440–5470. DOI: 10.3390/rs70505440 (cit. on pp. 28, 37).

Chave, J., Andalo, C., Brown, S., Cairns, M. a., Chambers, J. Q., Eamus, D., Fölster, H., Fromard, F., Higuchi, N., Kira, T., Lescure, J. P., Nelson, B. W., Ogawa, H., Puig, H., Riéra, B., and Yamakura, T. (2005). "Tree allometry and improved estimation of carbon stocks and balance in tropical forests". In: *Oecologia* 145.1, pp. 87–99. DOI: 10.1007/s00442-005-0100-x (cit. on p. 44).

Chave, J., Navarrete, D., Almeida, S., Álvarez, E., Aragão, L. E. O. C., Bonal, D., Châtelet, P., Silva-Espejo, J. E., Goret, J.-Y., Hildebrand, P. von, Jiménez, E., Patiño, S., Peñuela, M. C., Phillips, O. L., Stevenson, P., and Malhi, Y. (2010). "Regional and seasonal patterns of litterfall in tropical South America". In: *Biogeosciences* 7.1, pp. 43–55. DOI: 10.5194/bg-7-43-2010 (cit. on p. 58).

Chave, Jerome, Coomes, David, Jansen, Steven, Lewis, Simon L., Swenson, Nathan G., and Zanne, Amy E. (2009). "Towards a worldwide wood economics spectrum." In: *Ecology letters* 12.4, pp. 351–66. DOI: 10.1111/j.1461-0248.2009.01285.x (cit. on pp. 44, 53).

Chen, Xinli and Chen, Han Y. H. (2018). "Global effects of plant litter alterations on soil CO 2 to the atmosphere". In: *Global Change Biology* 24.8, pp. 3462–3471. DOI: 10.1111/gcb.14147 (cit. on p. 56).

Coe, Michael T., Costa, Marcos H., and Soares-Filho, Britaldo S. (2009). "The influence of historical and potential future deforestation on the stream flow of the Amazon River - Land surface processes and atmospheric feedbacks". In: *Journal of Hydrology* 369.1-2, pp. 165–174. DOI: 10.1016/j.jhydrol.2009.02.043 (cit. on p. 27).

Coe, Michael T, Marthews, Toby R, Costa, Marcos Heil, Galbraith, David R, Greenglass, Nora L, Imbuzeiro, Hewlley M A, Levine, Naomi M, Malhi, Yadvinder, Moorcroft, Paul R, Muza, Michel Nobre, Powell, Thomas L, Saleska, Scott R, Solorzano, Luis A, and Wang, Jingfeng (2013). "Deforestation and climate feedbacks threaten the ecological integrity of south-southeastern Amazonia". In: *Philosophical Transactions of the Royal Society B: Biological Sciences* 368.1619, pp. 20120155–20120155. DOI: 10.1098/rstb.2012.0155 (cit. on p. 27).

Congalton, Russell G. (1991). "A review of assessing the accuracy of classifications of remotely sensed data". In: *Remote Sensing of Environment* 37.October 1990, pp. 35–46. DOI: 10.1016/0034-4257(91)90048-B (cit. on p. 13).

Cook, Brian, Zeng, Ning, and Yoon, Jin Ho (2012). "Will Amazonia dry out? Magnitude and causes of change from IPCC climate model projections". In: *Earth Interactions* 16.3. DOI: 10.1175/2011EI398.1 (cit. on p. 27).

Costa, MPF, Silva, Thiago SF, and Evans, Teresa L (2013). "Wetland classification". In: *Remote Sensing of Natural Resources. CRC Press, Boca Raton-FL*, pp. 461–478 (cit. on p. 7).

Cox, Peter (2001). *Description of the "TRIFFID" Dynamic Global Vegetation Model - Hadley Centre technical note 24*. Tech. rep. Berkshire: Hadley Centre, p. 16 (cit. on p. 4).

Cox, Peter M, Harris, Phil P, Huntingford, Chris, Betts, Richard a, Collins, Matthew, Jones, Chris D, Jupp, Tim E, Marengo, José a, and Nobre, Carlos a (2008). "Increasing risk of Amazonian drought due to decreasing aerosol pollution." In: *Nature* 453.May, pp. 212–215. DOI: 10.1038/nature06960 (cit. on p. 27).

Da Silveira, Ronis, Ramalho, Emiliano E, Thorbjarnarson, John B, and Magnusson, William E (2010). "Depredation by jaguars on caimans and importance of reptiles in the diet of jaguar". In: *Journal of Herpetology* 44.3, pp. 418–424 (cit. on p. 24).

Dantas, Mario and Phillipson, John (1989). "Litterfall and litter nutrient content in primary and secondary amazonian terra firme rain forest". In: *Journal of Tropical Ecology* 5.1, pp. 27–36. DOI: 10.1017/S0266467400003199 (cit. on p. 76).

Definiens (2009). *Definiens developer 8: User Guide*. Ed. by The Imaging Intelligence Company. Munich (cit. on p. 12).

Ducke, A. and Black, G. A. (1954). "Notas sôbre a fitogeografia da Amazônia Brasileira". In: *Boletim Técnico do Instituto Agronômico do Norte* 29, pp. 1–62 (cit. on p. 6).

Engle, Diana L., Melack, John M., Doyle, Robert D., and Fisher, Thomas R. (2007). "High rates of net primary production and turnover of floating grasses on the Amazon floodplain: implications for aquatic respiration and regional CO2 flux". In: *Global Change Biology* 14.2, pp. 369–381. DOI: 10.1111/j.1365-2486.2007.01481.x (cit. on p. 39).

Espinoza Villar, Jhan Carlo, Guyot, Jean Loup, Ronchail, Josyane, Cochonneau, Gérard, Filizola, Naziano, Fraizy, Pascal, Labat, David, Oliveira, Eurides de, Ordoñez, Juan Julio, and Vauchel, Philippe (2009). "Contrasting regional discharge evolutions in the Amazon basin (1974-2004)". In: *Journal of Hydrology* 375.3-4, pp. 297–311. DOI: 10.1016/j.jhydrol.2009.03.004 (cit. on p. 79).

Ferreira-Ferreira, Jefferson, Silva, Thiago Sanna Freire, Streher, Annia Susin, Affonso, Adriana Gomes, de Almeida Furtado, Luiz Felipe, Forsberg, Bruce Rider, Valsecchi, João, Queiroz, Helder Lima, and de Moraes Novo, Evlyn Márcia Leão (2015). "Combining ALOS/PALSAR derived vegetation structure and inundation patterns to characterize major vegetation types in the Mamirauá Sustainable Development Reserve, Central Amazon floodplain, Brazil". In: *Wetlands Ecology and Management* 23.1, pp. 41–59. DOI: 10.1007/s11273-014-9359-1 (cit. on pp. 1, 4, 28, 30, 31, 34, 37, 38, 76, 77).

Ferreira, Cristiane S., Figueira, Antonio V. O., Gribel, Rogério, Wittmann, Florian, and Piedade, Maria T. F. (2010). "Genetic Variability, Divergence and Speciation in Trees of Periodically Flooded Forests of the Amazon: A Case Study of Himatanthus sucuuba (Spruce) Woodson". In: *Central Amazonian floodplain forests: ecophysiology, biodiversity and sustainable management*. Ed. by Wolfgang J. Junk, Maria T. F. Piedade, Florian Wittmann, Jochen Schöngart, and Pia Parolin. Dordrecht: Springer Netherlands. Chap. 15, pp. 301–312. DOI: 10.1007/978-90-481-8725-6_15 (cit. on p. 78).

Ferreira, Rafael Damiati, Leão, joaquim Antônio Dionísio, Silva, Thiago Sanna Freire, Rennó, Camilo Daleles, Novo, Evlyn M.L.M., and Barbosa, Cláudio Clemente F (2013). "Atualização e correção do delineamento de áreas alagáveis da bacia Amazônica". In: *Anais XVI Simpósio Brasileiro de Sensoriamento Remoto*. Foz do Iguaçu: INPE, pp. 5864–5871 (cit. on pp. 8, 12).

Firth, David (1993). "Bias Reduction of Maximum Likelihood Estimates". In: *Biometrika* 80.1, p. 27. DOI: 10.2307/2336755 (cit. on p. 33).

Fisher, Ronald A, Corbet, A Steven, and Williams, Carrington B (1943). "The relation between the number of species and the number of individuals in a random sample of an animal population". In: *The Journal of Animal Ecology*, pp. 42–58 (cit. on p. 43).

Flores, Olivier and Coomes, David a. (2011). "Estimating the wood density of species for carbon stock assessments". In: *Methods in Ecology and Evolution* 2.2, pp. 214–220. DOI: 10.1111/j.2041-210X.2010.00068.x (cit. on p. 44).

Forsberg, BR, Castro, JGD, Cargnin-Ferreira, E, and Rosenqvist, A (2001). "The structure and function of the Negro River ecosystem: insights from the Jaú Project". In: *Conservation and Management of Ornamental Fish Resources of the Rio Negro Basin, Amazonia, Brazil–Project Piaba. EDUA, Manaus*, pp. 125–144 (cit. on p. 22).

Forsberg, Bruce R., Melack, John M., Dunne, Thomas, Barthem, Ronaldo B., Goulding, Michael, Paiva, Rodrigo C. D., Sorribas, Mino V., Silva, Urbano L., and Weisser, Sabine (2017). "The potential impact of new Andean dams on Amazon fluvial ecosystems". In: *PLOS ONE* 12.8. Ed. by Guy J-P. Schumann, e0182254. DOI: 10.1371/journal.pone.0182254 (cit. on p. 28).

Fragal, Everton Hafemann, Silva, Thiago Sanna Freire, and Novo, Evlyn Márcia Leão de Moraes (2016). "Reconstructing historical forest cover change in the Lower Amazon floodplains using the LandTrendr algorithm". In: *Acta Amazonica* 46.1, pp. 13–24. DOI: 10.1590/1809-4392201500835. arXiv: 0052010 (cit. on p. 56).

Freitas, Flavio L. M., Englund, Oskar, Sparovek, Gerd, Berndes, Göran, Guidotti, Vinicius, Pinto, Luís F. G., and Mörtberg, Ulla (2018). "Who owns the

Brazilian carbon?" In: *Global Change Biology* 24.5, pp. 2129–2142. DOI: 10.1111/gcb.14011. arXiv: 0608246v3 [arXiv:physics] (cit. on p. 41).

Galbraith, David, Levy, Peter E, Sitch, Stephen, Huntingford, Chris, Cox, Peter, Williams, Mathew, and Meir, Patrick (2010). "Multiple mechanisms of Amazonian forest biomass losses in three dynamic global vegetation models under climate change." In: *The New phytologist* 187.3, pp. 647–665. DOI: 10.1111/j.1469-8137.2010.03350.x (cit. on p. 4).

Gibbs, Holly K, Brown, Sandra, Niles, John O, and Foley, Jonathan A (2007). "Monitoring and estimating tropical forest carbon stocks: making REDD a reality". In: *Environmental Research Letters* 2, p. 045023. DOI: 10.1088/1748-9326/2/4/045023 (cit. on p. 41).

Girardin, C. A.J., Malhi, Yadvinder, Aragão, L. E.O.C., Mamani, M., Huaraca Huasco, W., Durand, L., Feeley, K. J., Rapp, J., Silva-Espejo, J. E., Silman, M., Salinas, N., and Whittaker, R. J. (2010). "Net primary productivity allocation and cycling of carbon along a tropical forest elevational transect in the Peruvian Andes". In: *Global Change Biology* 16.12, pp. 3176–3192. DOI: 10.1111/j.1365-2486.2010.02235.x (cit. on p. 56).

Gloor, M, Barichivich, J, Ziv, G, Brienen, R, Schöngart, J, Peylin, P, Ladvocat Cintra, B. Barcante, Feldpausch, T., Phillips, O., and Baker, J. (2015). "Recent Amazon climate as background for possible ongoing and future changes of Amazon humid forests". In: *Global Biogeochemical Cycles* 29.9, pp. 1384–1399. DOI: 10.1002/2014GB005080 (cit. on pp. 27, 79).

Gloor, M, Brienen, R. J W, Galbraith, D., Feldpausch, T. R., Schöngart, J., Guyot, J. L., Espinoza, J. C., Lloyd, J., and Phillips, O. L. (2013). "Intensification of the Amazon hydrological cycle over the last two decades". In: *Geophysical Research Letters* 40.9, pp. 1729–1733. DOI: 10.1002/grl.50377 (cit. on pp. 27, 79).

Goulding, Michael, Smith, Nigel J H, and Mahar, Dennis (1995). *Floods of Fortune: Ecology and Economy Along the Amazon*. New York, NY: Columbia University Press, p. 184 (cit. on p. 3).

Guimberteau, Matthieu, Ciais, Philippe, Ducharne, Agnès, Boisier, Juan Pablo, Dutra Aguiar, Ana Paula, Biemans, Hester, De Deurwaerder, Hannes, Galbraith, David, Kruijt, Bart, Langerwisch, Fanny, Poveda, German, Rammig, Anja, Rodriguez, Daniel Andres, Tejada, Graciela, Thonicke, Kirsten, Von Randow, Celso, Von Randow, Rita C. S., Zhang, Ke, and Verbeeck, Hans (2017). "Impacts of future deforestation and climate change on the hydrology of the Amazon Basin: a multi-model analysis with a new set of land-cover change scenarios". In: *Hydrology and Earth System Sciences* 21.3, pp. 1455–1475. DOI: 10.5194/hess-21-1455-2017 (cit. on p. 27).

Hacke, Uwe G., Sperry, John S., Pockman, William T., Davis, Stephen D., and McCulloh, Katherine A. (2001). "Trends in wood density and structure are linked to prevention of xylem implosion by negative pressure". In: *Oecologia* 126.4, pp. 457–461. DOI: 10.1007/s004420100628 (cit. on p. 53).

Haffer, J and Prance, G T (2001). "Climatic forcing of evolution in Amazonia during the Cenozoic: On the refuge theory of biotic differentiation". In: *Amazoniana* 16, pp. 579–607 (cit. on p. 78).

Haugaasen, Torbjorn and Peres, Carlos A. (2005). "Tree Phenology in Adjacent Amazonian Flooded and Unflooded Forests". In: *Biotropica* 37.4, pp. 620–630. DOI: 10.1111/j.1744-7429.2005.00079.x (cit. on pp. 58, 77).

Hawes, Joseph E. and Peres, Carlos A. (2016). "Patterns of plant phenology in Amazonian seasonally flooded and unflooded forests". In: *Biotropica* 0.0, pp. 1–11. DOI: 10.1111/btp.12315 (cit. on pp. 26, 42, 57, 76).

Hawes, Joseph E., Peres, Carlos a., Riley, Louise B., and Hess, Laura L. (2012). "Landscape-scale variation in structure and biomass of Amazonian seasonally flooded and unflooded forests". In: *Forest Ecology and Management* 281, pp. 163–176. DOI: 10.1016/j.foreco.2012.06.023 (cit. on pp. 7, 28, 38, 53, 54).

Heinze, Georg, Ploner, Meinhard, Dunkler, Daniela, and Southworth, Harry (2013). *logistf: Firth's bias reduced logistic regression* (cit. on p. 33).

Heinze, Georg and Schemper, Michael (2002). "A solution to the problem of separation in logistic regression". In: *Statistics in Medicine* 21.16, pp. 2409–2419. DOI: 10.1002/sim.1047 (cit. on p. 33).

Henderson, Floyd M. and Lewis, Anthony J. (1998). *Principles and applications of imaging radar. Manual of remote sensing. Volume 2*. 3rd. New York, NY: Wiley, p. 896 (cit. on p. 37).

— (2008). "Radar detection of wetland ecosystems: a review". In: *International Journal of Remote Sensing* 29.20, pp. 5809–5835. DOI: 10.1080/01431160801958405 (cit. on p. 7).

Hess, Laura L., Melack, John M, Affonso, Adriana G., Barbosa, Claudio, Gastil-Buhl, Mary, and Novo, Evlyn M. L. M. (2015). "Wetlands of the Lowland Amazon Basin: Extent, Vegetative Cover, and Dual-season Inundated Area as Mapped with JERS-1 Synthetic Aperture Radar". In: *Wetlands* 35.4, pp. 745–756. DOI: 10.1007/s13157-015-0666-y (cit. on p. 27).

Hess, Laura L., Melack, John M, Novo, Evlyn M.L.M., Barbosa, Cláudio Clemente F, and Gastil, Mary (2003). "Dual-season mapping of wetland inundation and vegetation for the central Amazon basin". In: *Remote Sensing of Environment* 87.4, pp. 404–428. DOI: 10.1016/j.rse.2003.04.001 (cit. on pp. 8, 12).

Hess, Laura L, Affonso, Adriana Gomes, Arraut, EM, Novo, EMLM, Gielow, Ralf, Renó, V, Barbarisi, Bernard, and Marioni, Boris (2011). "Evaluation of low-cost tree-mounted temperature loggers for validation of satellite-based flood mapping on the Amazon floodplain". In: *Anais XV Simpósio Brasileiro de Sensoriamento Remoto*, pp. 5278–5283 (cit. on pp. 15, 19).

Hess, Laura L, Melack, John M, Filoso, Solange, and Wang, Yong (1995). "Delineation of Inundated Area and Vegetation Along the Amazon Floodplain with the SIR-C Synthetic Aperture Radar". In: *IEEE Transactions on Geoscience and Remote Sensing* 33.4 (cit. on pp. 7, 14, 37, 38).

Hoorn, Carina and Wesselingh, Frank P. (2011). *Amazonia: Landscape and Species Evolution: A look into the past*, p. 464. DOI: 10.1002/9781444306408 (cit. on p. 1).

Houghton, Richard A. (2009). "Terrestrial carbon and biogeochemical cycles". In: *The Princeton Guide to Ecology2*. Ed. by Simon A. Levin. 2nd. Princeton, NJ/USA: Princeton University Press. Chap. III.11, pp. 340–346 (cit. on p. 55).

Hueck, Kurt (1966). *Die Wälder Südamerikas: Ökologie, Zusammensetzung und wirtschaftliche Bedeutung*. Stuttgart: G. Fischer, p. 422 (cit. on p. 6).

IDSM (2013). *Banco de dados fluviométrico da Reserva de DEsenvolvimento Sustentável Mamirauá* (cit. on pp. 10, 11, 15, 30, 60–62, 64–68).

IPCC (2013). *Climate Change 2013: The Physical Science Basis. Contribution of Working Group I to the Fifth Assessment Report of the Intergovernmental Panel on Climate Change*. Ed. by Thomas F Stocker, Dahe Qin, G. -K. Plattner, M. Tignor, S. K. Allen, J. Boschung, A. Nauels, Y. Xia, V. Bex, and P. M. Midgley. Cambridge, United Kingdom and New York, NY, USA: Cambridge University Press, p. 1535 (cit. on pp. 54, 79).

Irion, G, Junk, Wolfgang J., and Mello, J A (1997). "The large central Amazonian river floodplains near Manaus: geological, climatological, hydrological an geomorphological aspects." In: *The Central Amazon floodplain: ecology of a pulsating system*. Ed. by Wolfgang J Junk. Berlin, Heidelberg: Springer-Verlag, pp. 23–46 (cit. on p. 6).

James, Gareth, Witten, Daniela, Hastie, Trevor, and Tibshirani, Robert (2013). *An Introduction to Statistical Learning*. Vol. 103. Springer Texts in Statistics. New York, NY: Springer New York. DOI: 10.1007/978-1-4614-7138-7 (cit. on p. 45).

Japan Space Systems (2012). *PALSAR User's Guide* (cit. on p. 10).

Jardine, Timothy D., Bond, Nicholas R., Burford, Michele A., Kennard, Mark J., Ward, Douglas P., Bayliss, Peter, Davies, Peter M., Douglas, Michael M., Hamilton, Stephen K., Melack, John M, Naiman, Robert J., Pettit, Neil E., Pusey, Bradley J., Warfe, Danielle M., and Bunn, Stuart E. (2015). "Does flood rhythm drive ecosystem responses in tropical riverscapes?" In: *Ecology* 96.3, pp. 684–692. DOI: 10.1890/14-0991.1 (cit. on p. 26).

Joetzjer, E., Douville, H., Delire, C., and Ciais, P. (2013). "Present-day and future Amazonian precipitation in global climate models: CMIP5 versus CMIP3". In: *Climate Dynamics* 41, pp. 2921–2936. DOI: 10.1007/s00382-012-1644-1 (cit. on pp. 4, 27).

Junk, Wolfgang J (1989). "Flood tolerance and tree distribution in central Amazonian floodplains." In: *Tropical forests: botanical dynamics, speciation and diversity*. Ed. by L B Holm-Nielsen, I C Nielsen, and H Balslev. London: Academic Press, pp. 47–64 (cit. on pp. 6, 26, 27, 39, 41, 42, 55).

— (1993). "Wetlands of tropical South America". In: *Wetlands of the world: Inventory, ecology and management Volume I*. Ed. by Dennis F. Whigham, Dagmar Dykyjová, and Slavomil Hejný. Dordrecht: Springer Netherlands, pp. 679–739. DOI: 10.1007/978-94-015-8212-4_14 (cit. on p. 27).

— (1997a). "General Aspects of Floodplain Ecology with Special Reference to Amazonian Floodplains". In: *The Central Amazon Floodplain: Ecology of a Pulsing System*. Ed. by Wolfgang J Junk. Springer Berlin Heidelberg, pp. 3–20. DOI: 10.1007/978-3-662-03416-3_1 (cit. on pp. 26, 39, 41).

— (1997b). *The Central Amazon Floodplain: Ecology of a Pulsing System*. New York, NY: Springer Berlin Heidelberg (cit. on pp. 5, 6, 55).

Junk, Wolfgang J. (1997c). "Structure and Function of the Large Central Amazonian River Floodplains: Synthesis and Discussion". In: pp. 455–472. DOI: 10.1007/978-3-662-03416-3_23 (cit. on p. 39).

Junk, Wolfgang J. and Piedade, Maria Teresa F. (1997). "Plant Life in the Floodplain with Special Reference to Herbaceous Plants". In: *The Central Amazon Floodplain: Ecology of a Pulsing System*. Ed. by Wolfgang J. Junk, pp. 147–185. DOI: 10.1007/978-3-662-03416-3_8 (cit. on p. 77).

Junk, Wolfgang J. and Piedade, Maria Teresa Fernandez (2010). "An Introduction to South American Wetland Forests: Distribution, Definitions and General Characterization". In: *Amazonian floodplain forests: ecophysiology biodi-*

versity and sustainable management. Ed. by Wolfgang J. Junk, Maria T. F. Piedade, Florian Wittmann, Jochen Schöngart, and Pia Parolin. Vol. 210, pp. 4–24. DOI: 10.1007/978-90-481-8725-6 (cit. on pp. 3, 78).

Junk, Wolfgang J, Bayley, Peter B., and Sparks, Richard E. (1989). "The Flood Pulse Concept in River-Floodplain Systems". In: *Canadian Special Publications of Fisheries and Aquatic Sciences* 106, pp. 110–127 (cit. on pp. 3, 5, 24, 26, 41, 55).

Junk, Wolfgang J, Piedade, Maria Teresa Fernandez, Schöngart, Jochen, Cohn-Haft, Mario, Adeney, J. Marion, and Wittmann, Florian (2011). "A classification of major naturally-occurring amazonian lowland wetlands". In: *Wetlands* 31.4, pp. 623–640. DOI: 10.1007/s13157-011-0190-7 (cit. on pp. 1, 2, 5, 23, 27, 41).

Junk, Wolfgang J, Piedade, Maria Teresa Fernandez, Schöngart, Jochen, and Wittmann, Florian (2012). "A classification of major natural habitats of Amazonian white-water river floodplains (várzeas)". In: *Wetlands Ecology and Management* 20.6, pp. 461–475. DOI: 10.1007/s11273-012-9268-0 (cit. on pp. 1, 5, 6, 12, 41).

Kasischke, Eric S, Melack, John M, and Craig Dobson, M (1997). "The use of imaging radars for ecological applications-A review". In: *Remote Sensing of Environment* 59.2, pp. 141–156. DOI: 10.1016/S0034-4257(96)00148-4 (cit. on p. 7).

Kleinbaum, David G. and Klein, Mitchel (2010). *Logistic Regression*. Statistics for Biology and Health. New York, NY: Springer New York. DOI: 10.1007/978-1-4419-1742-3 (cit. on p. 33).

Klinge, H (1978). "Litter production in tropical ecosystems". In: *Malayan Nature Journal* (cit. on pp. 75, 76).

Klinge, H and Rodrigues, W A (1968). "Litter production in an area of Amazonian terra firme forest. Part I. Litter-fall, organic carbon and total nitrogen contents of litter". In: *Amazoniana* 1.4, pp. 287–302 (cit. on pp. 75, 76).

Kubitzki, K. (1989). "The ecogeographical differentiation of Amazonian inundation forests". In: *Plant Systematics and Evolution* 162.1-4, pp. 285–304. DOI: 10.1007/BF00936922 (cit. on pp. 2, 78).

Lake, Sam, Bond, Nick, and Reich, Paul (2006). "Floods Down Rivers: From Damaging to Replenishing Forces". In: *Advances in Ecological Research*. Vol. 39. 06, pp. 41–62. DOI: 10.1016/S0065-2504(06)39003-4 (cit. on p. 26).

Lamotte, Sandrine (1990). "Fluvial dynamics and succession in the lower Ucayali River basin, Peruvian Amazonia". In: *Forest Ecology and Management* 33-34.C, pp. 141–156. DOI: 10.1016/0378-1127(90)90189-I (cit. on p. 77).

Lees, A. C., Peres, C. A., Fearnside, Philip M., Schneider, M., and Zuanon, J.A.S. (2016). "Hydropower and the future of Amazonian biodiversity". In: *Journal of Applied Ecology* 25.3, pp. 451–466. DOI: 10.1007/s10531-016-1072-3 (cit. on p. 28).

Lesack, Lance F. W. and Melack, John M (1995). "Flooding Hydrology and Mixture Dynamics of Lake Water Derived from Multiple Sources in an Amazon Floodplain Lake". In: *Water Resources Research* 31.2, p. 329. DOI: 10.1029/94WR02271 (cit. on pp. 5, 27).

Lewis, William M., Hamilton, Stephen K., Lasi, Margaret a., Rodríguez, Marco, and Saunders, James F. (2000). "Ecological Determinism on the Orinoco

Floodplain". In: *BioScience* 50.8, p. 681. DOI: 10.1641/0006-3568(2000)050[0681:EDOTOF]2.0.CO;2 (cit. on pp. 26, 39).

Liaw, Andy and Wiener, Matthew (2002). "Classification and Regression by randomForest". In: *R News* 2.December, pp. 18–22 (cit. on p. 12).

Lima, Danielle dos Santos, Marmontel, Miriam, and Bernard, Enrico (2012). "Site and refuge use by giant river otters (Pteronura brasiliensis) in the Western Brazilian Amazonia". In: *Journal of Natural History* 46.11-12, pp. 729–739 (cit. on p. 24).

Lindenmayer, David, Hobbs, Richard J, Montague-Drake, Rebecca, Alexandra, Jason, Bennett, Andrew, Burgman, Mark, Cale, Peter, Calhoun, Aram, Cramer, Viki, Cullen, Peter, et al. (2008). "A checklist for ecological management of landscapes for conservation". In: *Ecology letters* 11.1, pp. 78–91 (cit. on p. 22).

Lopez, Omar R. and Kursar, Thomas A. (1999). "Flood tolerance of four tropical tree species". In: *Tree Physiology* 19.14, pp. 925–932. DOI: 10.1093/treephys/19.14.925 (cit. on p. 78).

— (2003). "Does flood tolerance explain tree species distribution in tropical seasonally flooded habitats?" In: *Oecologia* 136.2, pp. 193–204. DOI: 10.1007/s00442-003-1259-7 (cit. on p. 78).

Lucas, Christine M., Schöngart, Jochen, Sheikh, Pervaze, Wittmann, Florian, Piedade, Maria T.F., and McGrath, David G. (2014). "Effects of land-use and hydroperiod on aboveground biomass and productivity of secondary Amazonian floodplain forests". In: *Forest Ecology and Management* 319, pp. 116–127. DOI: 10.1016/j.foreco.2014.02.008 (cit. on pp. 53, 54).

Luize, Bruno G, Silva, Thiago Sanna Freire, Wittmann, Florian, Assis, Rafael L, and Venticinque, Eduardo M (2015). "Effects of the Flooding Gradient on Tree Community Diversity in Várzea Forests of the Purus River, Central Amazon, Brazil". In: *Biotropica* 0.0, n/a–n/a. DOI: 10.1111/btp.12203 (cit. on pp. 3, 26, 39, 42, 53, 54).

Luize, Bruno Garcia, Magalhães, José Leonardo Lima, Queiroz, Helder, Lopes, Maria Aparecida, Venticinque, Eduardo Martins, Leão de Moraes Novo, Evlyn Márcia, and Silva, Thiago Sanna Freire (2018). "The tree species pool of Amazonian wetland forests: Which species can assemble in periodically waterlogged habitats?" In: *PLOS ONE* 13.5. Ed. by Andrés Viña, e0198130. DOI: 10.1371/journal.pone.0198130 (cit. on p. 1).

Luz-Agostinho, KDG., Agostinho, AA., Gomes, LC., Júlio-Jr., HF., and Fugi, R (2009). "Effects of flooding regime on the feeding activity and body condition of piscivorous fish in the Upper Paraná River floodplain". In: *Brazilian Journal of Biology* 69.2, pp. 481–490. DOI: 10.1590/S1519-69842009000300004 (cit. on p. 26).

Malhi, Y., Doughty, C., and Galbraith, D. (2011). "The allocation of ecosystem net primary productivity in tropical forests". In: *Philosophical Transactions of the Royal Society B: Biological Sciences* 366.1582, pp. 3225–3245. DOI: 10.1098/rstb.2011.0062 (cit. on pp. 56, 59).

Malhi, Yadvinder, Baker, Timothy R., Phillips, Oliver L., Almeida, Samuel, Alvarez, Esteban, Arroyo, Luzmilla, Chave, Jerome, Czimczik, Claudia I., Di Fiore, Anthony, Higuchi, Niro, Killeen, Timothy J., Laurance, Susan G., Laurance, William F., Lewis, Simon L., Montoya, Lina María Mercado, Monteagudo, Abel, Neill, David a., Vargas, Percy Núnez, Patino, Sandra, Pitman, Nigel C a, Quesada, Carlos Alberto, Salomao, Rafael, Silva, José Natalino

Macedo, Lezama, Armando Torres, Martínez, Rodolfo Vásquez, Terborgh, John, Vinceti, Barbara, and Lloyd, Jon (2004). "The above-ground coarse wood productivity of 104 Neotropical forest plots". In: *Global Change Biology* 10.5, pp. 563–591. DOI: 10.1111/j.1529-8817.2003.00778.x (cit. on p. 80).

Malhi, Yadvinder, Roberts, J Timmons, Betts, Richard a, Killeen, Timothy J, Li, Wenhong, and Nobre, Carlos a (2008). "Climate Change, Deforestation, and the Fate of the Amazon". In: *Science* 319.January, pp. 169–172. DOI: 10.1126/science.1146961 (cit. on p. 23).

Malhi, Yadvinder, Wood, Daniel, Baker, Timothy R., Wright, James, Phillips, Oliver L., Cochrane, Thomas, Meir, Patrick, Chave, Jerome, Almeida, Samuel, Arroyo, Luzmilla, Higuchi, Niro, Killeen, Timothy J., Laurance, Susan G., Laurance, William F., Lewis, Simon L., Monteagudo, Abel, Neill, David a., Vargas, Percy Nunez, Pitman, Nigel C. a., Quesada, Carlos Alberto, Salomao, Rafael, Silva, Jose Natalino M., Lezama, Armando Torres, Terborgh, John, Martinez, Rodolfo Vasquez, and Vinceti, Barbara (2006). "The regional variation of aboveground live biomass in old-growth Amazonian forests". In: *Global Change Biology* 12.7, pp. 1107–1138. DOI: 10.1111/j.1365-2486.2006.01120.x (cit. on p. 41).

Marengo, Jose a., Chou, Sin Chan, Kay, Gillian, Alves, Lincoln M., Pesquero, J. F., Soares, Wagner R., Santos, Daniel C., Lyra, a. a., Sueiro, Gustavo, Betts, Richard, Chagas, Diego J., Gomes, Jorge L., Bustamante, Josiane F., and Tavares, Priscila (2012). "Development of regional future climate change scenarios in South America using the Eta CPTEC/HadCM3 climate change projections: Climatology and regional analyses for the Amazon, São Francisco and the Paraná River basins". In: *Climate Dynamics* 38, pp. 1829–1848. DOI: 10.1007/s00382-011-1155-5 (cit. on pp. 4, 27).

Marthews, Toby R, Riutta, T, Oliveras Menor, I, Urrutia, R, Moore, S, Metcalfe, Daniel B., Malhi, Yadvinder S., Phillips, Oliver L, Huaraca Huasco, W., Ruiz Jaén, M, Girardin, Cecile, Butt, Nathalie, Cain, R, and colleagues from RAINFOR and GEM Networks (2014). *Measuring Tropical Forest Carbon Allocation and Cycling: A RAINFOR-GEM Field Manual for Intensive Census Plots (v3.0)*. Tech. rep., p. 116 (cit. on p. 57).

Martinez, Jean-Michel and Letoan, T (2007). "Mapping of flood dynamics and spatial distribution of vegetation in the Amazon floodplain using multitemporal SAR data". In: *Remote Sensing of Environment* 108.3, pp. 209–223. DOI: 10.1016/j.rse.2006.11.012 (cit. on pp. 7, 22, 28, 37, 38).

Melack, John M., Hess, Laura L., Gastil, Mary, Forsberg, Bruce R., Hamilton, Stephen K., Lima, Ivan B.T., Novo, Evlyn M.L.M., Barbara, Santa, Barbara, Santa, Corners, Hickory, and Espaciais, De Pesquisas (2004). "Regionalization of methane emissions in the Amazon Basin with microwave remote sensing". In: *Global Change Biology* 10.5, pp. 530–544. DOI: 10.1111/j.1365-2486.2004.00763.x (cit. on p. 39).

Melack, John M and Coe, Michael T. (2013). "Climate Change and the Floodplain Lakes of the Amazon Basin". In: *Climatic Change and Global Warming of Inland Waters*. Ed. by Charles R Goldman, Michio Kumagai, and Richard D Robarts. Chichester, UK: John Wiley & Sons, Ltd. Chap. 17, pp. 295–310. DOI: 10.1002/9781118470596.ch17 (cit. on p. 23).

Melack, John M and Forsberg, Bruce Rider (2001). "Biogeochemistry of Amazon floodplain lakes and associated wetlands". In: *The Biogeochemistry of the*

Amazon Basin. Ed. by Michael E. McClain, Reynaldo Victoria, and Jeffrey E. Richey. Oxford, UK: Oxford University Press. Chap. 14, pp. 235–274 (cit. on pp. 1, 26, 41).

Melack, John M and Hess, Laura L (2010). "Remote sensing of the distribution and extent of wetlands in the Amazon basin". In: *Amazonian floodplain forests: ecophysiology, biodiversity and sustainable management*. Ed. by Wolfgang J Junk, Maria Teresa Fernandez Piedade, Florian Wittmann, Jochen Schongart, and Pia Parolin. Berlin: Springer, pp. 43–59 (cit. on pp. 3, 5, 27, 41).

Melack, John M, Novo, Evlyn Márcia Leão de Moraes, Forsberg, Bruce Rider, Piedade, Maria Teresa Fernandez, and Maurice, Laurence (2009a). "Floodplain ecosystem processes". In: *Amazonia and Global Change*. Ed. by Michael Keller, Mercedes Bustamante, John Gash, and Pedro Silva Dias. American Geophysical Union. Chap. D4, p. 576 (cit. on p. 5).

Melack, John M, Victoria, Reynaldo Luiz, and Tomasella, Javier (2009b). "Surface Waters in Amazonia: Key Findings and Perspectives". In: *Amazonia and Global Change*. Ed. by Michael Keller, Mercedes Bustamante, John Gash, and Pedro Silva Dias. Washington, D. C.: American Geophysical Union, pp. 485–488 (cit. on p. 56).

Mertes, Leal A K (1994). "Rates of flood-plain sedimentation on the central Amazon River". In: *Geology* 22.2, p. 171. DOI: 10.1130/0091-7613(1994)022<0171:ROFPSO>2.3.CO;2 (cit. on p. 56).

Mertes, Leal A K, Daniel, Darin L, Melack, John M, Nelson, Bruce, Martinelli, A, and Forsberg, Bruce R (1995). "Spatial patterns of hydrology, geomorphology, and vegetation on the floodplain of the Amazon River in Brazil from a remote sensing perspective". In: *Geomorphology* 13, pp. 215–232 (cit. on pp. 7, 56).

Mertes, Leal A K and Dunne, Thomas (2007). "Effects of Tectonism, Climate Change, and Sea-level Change on the Form and Behaviour of the Modern Amazon River and its Floodplain". In: *Large Rivers: Geomorphology and Management*. Ed. by Avijit Gupta. Chichester, UK: John Wiley & Sons, pp. 115–144. DOI: 10.1002/9780470723722.ch8 (cit. on p. 1).

Mitsch, W. J. and Gosselink, J. G. (2000). "The value of wetlands: Importance of scale and landscape setting". In: *Ecological Economics* 35.1, pp. 25–33. DOI: 10.1016/S0921-8009(00)00165-8 (cit. on p. 1).

Mitsch, William J. and Gosselink, J. G. (2015). *Wetlands*. 5th. Hoboken, NJ: John Wiley & Sons (cit. on pp. 3, 26).

Mitsch, William J., Nahlik, Amanda, Wolski, Piotr, Bernal, Blanca, Zhang, Li, and Ramberg, Lars (2010). "Tropical wetlands: seasonal hydrologic pulsing, carbon sequestration, and methane emissions". In: *Wetlands Ecology and Management* 18.5, pp. 573–586. DOI: 10.1007/s11273-009-9164-4 (cit. on pp. 26, 27, 41).

Moreira, K S (2006). "Avaliação da sazonalidade sobre a dinâmica de liteira em uma floresta de transição no Parque Estadual do Cantão, entorno da Ilha do Bananal, estado do Tocantins". In: *Universidade Federal do Tocantins* (cit. on p. 76).

Nahlik, Amanda M. and Mitsch, WIlliam J. (2011). "Methane emissions from tropical freshwater wetlands located in different climatic zones of Costa Rica". In: *Global Change Biology* 17.3, pp. 1321–1334. DOI: 10.1111/j.1365-2486.2010.02190.x (cit. on p. 39).

Nebel, Gustav, Dragsted, Jens, and Vega, Angel Salazar (2001). "Litter fall, biomass and net primary production in flood plain forests in the Peruvian Amazon". In: *Forest Ecology and Management* 150.1-2, pp. 93–102. DOI: 10.1016/S0378-1127(00)00683-6 (cit. on pp. 42, 53, 55, 75–77).

Nobre, A.D., Cuartas, L.a., Hodnett, M., Rennó, C.D., Rodrigues, G., Silveira, A., Waterloo, M., and Saleska, S. (2011). "Height Above the Nearest Drainage - a hydrologically relevant new terrain model". In: *Journal of Hydrology* 404.1-2, pp. 13–29. DOI: 10.1016/j.jhydrol.2011.03.051 (cit. on p. 31).

Ozesmi, Stacy L and Bauer, Marvin E (2002). "Satellite remote sensing of wetlands". In: *Wetlands ecology and management* 10.5, pp. 381–402 (cit. on p. 7).

Paim, Fernanda Pozzan, Valsecchi, João, Harada, Maria Lúcia, Queiroz, Helder Lima de, et al. (2013). "Diversity, geographic distribution and conservation of squirrel monkeys, Saimiri (Primates, Cebidae), in the floodplain forests of Central Amazon". In: *International Journal of Primatology* 34.5, pp. 1055–1076 (cit. on pp. 23, 24).

Pangala, Sunitha R., Enrich-Prast, Alex, Basso, Luana S., Peixoto, Roberta Bittencourt, Bastviken, David, Hornibrook, Edward R.C., Gatti, Luciana V., Marotta, Humberto, Calazans, Luana Silva Braucks, Sakuragui, Cassia Mônica, Bastos, Wanderley Rodrigues, Malm, Olaf, Gloor, Manuel, Miller, John Bharat, and Gauci, Vincent (2017). "Large emissions from floodplain trees close the Amazon methane budget". In: *Nature* 552.7684, pp. 230–234. DOI: 10.1038/nature24639 (cit. on p. 1).

Parolin, Pia (2000). "Phenology and CO2 assimilation of trees in Central Amazonian floodplains". In: *Journal of Tropical Ecology* 16.03, pp. 465–473 (cit. on pp. 3, 39, 42, 77).

— (2001). "Morphological and physiological adjustments to waterlogging and drought in seedlings of Amazonian floodplain trees". In: *Oecologia* 128.3, pp. 326–335. DOI: 10.1007/s004420100660 (cit. on p. 78).

— (2002). "Submergence tolerance vs. escape from submergence: two strategies of seedling establishment in Amazonian floodplains". In: *Environmental and Experimental Botany* 48.2, pp. 177–186. DOI: 10.1016/S0098-8472(02)00036-9 (cit. on p. 77).

Parolin, Pia, Waldhoff, Danielle, and Piedade, Maria Teresa Fernandez (2010). "Gas Exchange and Photosynthesis". In: *Amazonian floodplain forests: ecophysiology, biodiversity and sustainable management*. Ed. by Wolfgang J Junk, Maria Teresa Fernandez Piedade, Florian Wittmann, Jochen Schöngart, and Pia Parolin. Dordrecht: Springer Netherlands. Chap. 10, pp. 203–222. DOI: 10.1007/978-90-481-8725-6 (cit. on pp. 3, 26, 42, 79).

Parolin, Pia and Wittmann, Florian (2010). "Tree Phenology in Amazonian Floodplain Forests". In: *Amazonian floodplain forests: ecophysiology, biodiversity and sustainable management2*. Ed. by Wolfgang J. Junk, Maria Teresa Fernandez Piedade, Florian Wittmann, Jochen Schöngart, and Pia Parolin. Dordrecht: Springer Netherlands. Chap. 5, pp. 105–126. DOI: 10.1007/978-90-481-8725-6 (cit. on pp. 3, 6, 39, 42, 77).

Peixoto, Juliana Maerschner Aguiar, Nelson, Bruce Walker, and Wittmann, Florian (2009). "Spatial and temporal dynamics of river channel migration and vegetation in central Amazonian white-water floodplains by remote-sensing techniques". In: *Remote Sensing of Environment* 113.10, pp. 2258–2266. DOI: 10.1016/j.rse.2009.06.015 (cit. on pp. 6, 56).

Pereira, Maria João Ramos, Marques, João Tiago, Santana, Joana, Santos, Carlos David, Valsecchi, João, De Queiroz, Helder Lima, Beja, Pedro, and Palmeirim, Jorge M (2009). "Structuring of Amazonian bat assemblages: the roles of flooding patterns and floodwater nutrient load". In: *Journal of Animal Ecology* 78.6, pp. 1163–1171 (cit. on p. 23).

Pires, J. M. and Koury, H.M. (1959). "Estudo de um trecho de mata de várzea próximo a Belém". In: *Boletim Técnico do Instituto Agronômico do Norte* 36, pp. 3–44 (cit. on pp. 6, 56).

Pontius, Robert Gilmore and Millones, Marco (2011). "Death to Kappa: birth of quantity disagreement and allocation disagreement for accuracy assessment". In: *International Journal of Remote Sensing* 32.15, pp. 4407–4429. DOI: 10.1080/01431161.2011.552923 (cit. on pp. 13, 14).

Prance, Ghillean T (1979). "Notes on the vegetation of Amazonia III. The terminology of Amazonian forest types subject to inundation". In: *Brittonia* 31.1, pp. 26–38 (cit. on pp. 2, 5, 6, 56, 77).

Prentice, I, Bondeau, Alberte, Cramer, Wolfgang, Harrison, Sandy, Hickler, Thomas, Lucht, Wolfgang, Sitch, Stephen, Smith, Ben, and Sykes, Martin (2007). "Dynamic Global Vegetation Modeling: Quantifying Terrestrial Ecosystem Responses to Large-Scale Environmental Change". In: *Terrestrial Ecosystems in a Changing World*, pp. 175–192. DOI: doi:10.1007/978-3-540-32730-1_15 (cit. on p. 4).

Queiroz, Helder Lima and Peralta, Nelissa (2006). "Reserva de Desenvolvimento Sustentável : Manejo Integrado dos Recursos Naturais e Gestão Participativa". In: *Dimensões Humanas da Biodiversidade*. Ed. by Irene Garay and Bertha K Becker. Petrópolis, RJ: Vozes, pp. 447–476 (cit. on pp. 7, 9).

Quesada, C. A., Lloyd, J., Schwarz, M., Patiño, S., Baker, T. R., Czimczik, C., Fyllas, N. M., Martinelli, L., Nardoto, G. B., Schmerler, J., Santos, A. J B, Hodnett, M. G., Herrera, R., Luizão, F. J., Arneth, A., Lloyd, G., Dezzeo, N., Hilke, I., Kuhlmann, I., Raessler, M., Brand, W. A., Geilmann, H., Filho, J. O Moraes, Carvalho, F. P., Filho, R. N Araujo, Chaves, J. E., Cruz, O. F., Pimentel, T. P., and Paiva, R. (2010). "Variations in chemical and physical properties of Amazon forest soils in relation to their genesis". In: *Biogeosciences* 7.5, pp. 1515–1541. DOI: 10.5194/bg-7-1515-2010 (cit. on p. 55).

R Core Team (2018). *R: A Language and Environment for Statistical Computing*. R Foundation for Statistical Computing. Vienna, Austria (cit. on pp. 43, 59).

Ramalho, Emiliano E., Macedo, J., Vieira, T. M., Valsecchi, João, Calvimontes, J., Marmontel, Miriam, and Queiroz, Helder Lima de (2009). "Ciclo hidrológico nos ambientes de várzea da reserva de desenvolvimento sustentável mamirauá - médio rio solimões, período de 1990 a 2008". In: *Uakari* (cit. on pp. 5, 9–11, 15, 27, 30, 41, 55, 60–62, 64–68).

Rejou-Mechain, Maxime, Tanguy, Ariane, Piponiot, Camille, Chave, Jerome, and Herault, Bruno (2017). *BIOMASS: Estimating Aboveground Biomass and Its Uncertainty in Tropical Forests*. R package version 1.1 (cit. on p. 43).

Rennó, Camilo Daleles, Nobre, Antonio Donato, Cuartas, Luz Adriana, Soares, João Vianei, Hodnett, Martin G., Tomasella, Javier, and Waterloo, Maarten J. (2008). "HAND, a new terrain descriptor using SRTM-DEM: Mapping terra-firme rainforest environments in Amazonia". In: *Remote Sensing of*

Environment 112.9, pp. 3469–3481. DOI: 10.1016/j.rse.2008.03.018 (cit. on p. 31).

Rennó, Camilo Daleles, Novo, Evlyn M.L.M., and Banon, Lise Christine (2013). "Correção geométrica da máscara de áreas alagáveis da bacia amazônica". In: *Anais XVI Simpósio Brasileiro de Sensoriamento Remoto*. Foz do Iguaçu: INPE, pp. 5507–5514 (cit. on pp. 8, 12).

Renó, Vivian F, Novo, Evlyn MLM, Suemitsu, Chieno, Rennó, Camilo D, and Silva, Thiago SF (2011). "Assessment of deforestation in the Lower Amazon floodplain using historical Landsat MSS/TM imagery". In: *Remote Sensing of Environment* 115.12, pp. 3446–3456 (cit. on p. 7).

Richey, Jeffrey E, Melack, John M, Aufdenkampe, Anthony K., Ballester, Maria Victoria Ramos, and Hess, Laura L. (2002). "Outgassing from Amazonian rivers and wetlands as a large tropical source of atmospheric CO2." In: *Nature* 416.6881, pp. 617–20. DOI: 10.1038/416617a (cit. on pp. 26, 56, 57).

Rodrigues, William A (1961). *Estudo preliminar de mata de várzea alta de uma ilha do baixo Rio Negro, de solo argiloso e úmido*. INPA Manaus (cit. on p. 6).

Rodriguez, E, Morris, C. Cs, and Belz, J. Je (2006). "A global assessment of the SRTM performance". In: *Photogrammetric Engineering and Remote Sensing* 72.3, pp. 249–260. DOI: 10.14358/PERS.72.3.249 (cit. on p. 38).

Ronchail, Josyane, Espinoza, Jhan Carlo, Drapeau, Guillaume, Sabot, Manon, Cochonneau, Gérard, and Schor, Tatiana (2018). "The flood recession period in Western Amazonia and its variability during the 1985–2015 period". In: *Journal of Hydrology: Regional Studies* 15.November 2017, pp. 16–30. DOI: 10.1016/j.ejrh.2017.11.008 (cit. on pp. 54, 79).

Rosenqvist, Åke, Forsberg, Bruce R., Pimentel, T., Rauste, Y. A., and Richey, J. E. (2002). "The use of spaceborne radar data to model inundation patterns and trace gas emissions in the central Amazon floodplain". In: *International Journal of Remote Sensing* 23.7, pp. 1303–1328. DOI: 10.1080/01431160110092911 (cit. on pp. 7, 22, 28, 38).

Rosenqvist, Åke, Shimada, M., Suzuki, S., Ohgushi, F., Tadono, T., Watanabe, M., Tsuzuku, K., Watanabe, T., Kamijo, S., and Aoki, E. (2014). "Operational performance of the ALOS global systematic acquisition strategy and observation plans for ALOS-2 PALSAR-2". In: *Remote Sensing of Environment* 155, pp. 3–12. DOI: 10.1016/j.rse.2014.04.011 (cit. on p. 10).

Rosenqvist, Åke, Shimada, Masanobu, Ito, Norimasa, and Watanabe, Manabu (2007). "ALOS PALSAR: A Pathfinder Mission for Global-Scale Monitoring of the Environment". In: *IEEE Transactions on Geoscience and Remote Sensing* 45.11, pp. 3307–3316. DOI: 10.1109/TGRS.2007.901027 (cit. on p. 10).

Rosenqvist, Åke, Shimada, Masanobu, Lucas, Richard, Chapman, Bruce D., Paillou, P., Hess, Laura L., and Lowry, J. (2010). "The Kyoto & Carbon Initiative - A Brief Summary". In: *IEEE Journal of Selected Topics in Applied Earth Observations and Remote Sensing* 3.4, pp. 551–553 (cit. on p. 10).

Rowland, L, Costa, A C L da, Oliveira, A A R, Almeida, S S, Ferreira, L V, Malhi, Yadvinder, Metcalfe, D B, Mencuccini, M, Grace, J, and Meir, P (2018). "Shock and stabilisation following long-term drought in tropical forest from 15 years of litterfall dynamics". In: *Journal of Ecology* May 2017, pp. 1–10. DOI: 10.1111/1365-2745.12931 (cit. on p. 76).

Rudorff, Conrado M., Melack, John M, and Bates, Paul D. (2014a). "Flooding dynamics on the lower Amazon floodplain: 1. Hydraulic controls on water elevation, inundation extent, and river-floodplain discharge". In: *Water Resources Research* 50.1, pp. 619–634. DOI: 10.1002/2013WR014091 (cit. on pp. 28, 38).

— (2014b). "Flooding dynamics on the lower Amazon floodplain: 2. Seasonal and interannual hydrological variability". In: *Water Resources Research* 50.1, pp. 635–649. DOI: 10.1002/2013WR014714 (cit. on p. 28).

Saatchi, S. S., Houghton, R. A., Dos Santos Alvalá, R. C., Soares, J. V., and Yu, Y. (2007). "Distribution of aboveground live biomass in the Amazon basin". In: *Global Change Biology* 13.4, pp. 816–837. DOI: 10.1111/j.1365-2486.2007.01323.x (cit. on p. 1).

Saatchi, Sassan S, Harris, Nancy L, Brown, Sandra, Lefsky, Michael, Mitchard, Edward T a, Salas, William, Zutta, Brian R, Buermann, Wolfgang, Lewis, Simon L, Hagen, Stephen, Petrova, Silvia, White, Lee, Silman, Miles, and Morel, Alexandra (2011). "Benchmark map of forest carbon stocks in tropical regions across three continents." In: *Proceedings of the National Academy of Sciences of the United States of America* 108.24, pp. 9899–904. DOI: 10.1073/pnas.1019576108 (cit. on p. 41).

Salimon, Cleber I., Putz, Francis E., Menezes-Filho, L., Anderson, Anthony, Silveira, Marcos, Brown, I. Foster, and Oliveira, L. C. (2011). "Estimating state-wide biomass carbon stocks for a REDD plan in Acre, Brazil". In: *Forest Ecology and Management* 262.3, pp. 555–560. DOI: 10.1016/j.foreco.2011.04.025 (cit. on p. 81).

Salo, Jukka, Kalliola, Risto, Häkkinen, Ilmari, Mäkinen, Yrjö, Niemelä, Pekka, Puhakka, Maarit, and Coley, Phyllis D. (1986). "River dynamics and the diversity of Amazon lowland forest". In: *Nature* 322.6076, pp. 254–258. DOI: 10.1038/322254a0 (cit. on p. 56).

Sayer, Emma J. (2006). "Using experimental manipulation to assess the roles of leaf litter in the functioning of forest ecosystems". In: *Biological Reviews* 81.01, p. 1. DOI: 10.1017/S1464793105006846 (cit. on p. 56).

Schöngart, Jochen and Junk, Wolfgang J. (2007). "Forecasting the flood-pulse in Central Amazonia by ENSO-indices". In: *Journal of Hydrology* 335.1-2, pp. 124–132. DOI: 10.1016/j.jhydrol.2006.11.005 (cit. on p. 24).

Schöngart, Jochen, Junk, Wolfgang J, Piedade, Maria Teresa Fernandez, Ayres, José Marcio, Hüttermann, Aloys, and Worbes, Martin (2004). "Teleconnection between tree growth in the Amazonian floodplains and the El Niño-Southern Oscillation effect". In: *Global Change Biology* 10.5, pp. 683–692. DOI: 10.1111/j.1529-8817.2003.00754.x. arXiv: j.1529-8817.2003.00754.x [10.1111] (cit. on p. 10).

Schöngart, Jochen, Piedade, M. T F, Wittmann, Florian, Junk, Wolfgang J, and Worbes, Martin (2005). "Wood growth patterns of Macrolobium acaciifolium (Benth.) Benth. (Fabaceae) in Amazonian black-water and white-water floodplain forests". In: *Oecologia* 145.3, pp. 454–461. DOI: 10.1007/s00442-005-0147-8 (cit. on p. 3).

Schöngart, Jochen, Piedade, Maria Teresa F., Ludwigshausen, Sabine, Horna, Viviana, and Worbes, Martin (2002). "Phenology and stem-growth periodicity of tree species in Amazonian floodplain forests". In: *Journal of Tropical Ecology* 18.04, pp. 581–597. DOI: 10.1017/S0266467402002389 (cit. on p. 77).

Schöngart, Jochen and Queiroz, Helder Lima De (2010). "Traditional Timber Harvesting in the Central Amazonian Floodplains". In: *Central Amazonian floodplain forests: ecophysiology, biodiversity and sustainable management*. Ed. by Wolfgang J. Junk, Maria Teresa Fernandez Piedade, Florian Wittmann, Jochen Schöngart, and Pia Parolin. Vol. 210. Berlin: Springer Netherlands, pp. 419–436. DOI: 10.1007/978-90-481-8725-6_20 (cit. on pp. 9, 24).

Schöngart, Jochen, Wittmann, Florian, and Worbes, Martin (2010). "Biomass and Net Primary Production of Central Amazonian Floodplain Forests". In: *Amazonian floodplain forests: ecophysiology, biodiversity and sustainable management*. Ed. by Wolfgang J. Junk, Maria Teresa Fernandez Piedade, Florian Wittmann, Jochen Schöngart, and Pia Parolin. Vol. 210. New York: Springer Verlag. Chap. 18, pp. 347–388. DOI: 10.1007/978-90-481-8725-6_18 (cit. on pp. 3, 42, 44, 53–56, 76, 80).

Secretariat, Ramsar (2013). "The list of wetlands of international importance". In: *The Secretariat of the Convention on Wetlands, Gland, Switzerland* (cit. on p. 8).

Selva, Evandro Carlos, Couto, Eduardo Guimarães, Johnson, Mark S., and Lehmann, Johannes (2007). "Litterfall production and fluvial export in headwater catchments of the southern Amazon". In: *Journal of Tropical Ecology* 23.03, pp. 329–335. DOI: 10.1017/S0266467406003956 (cit. on p. 76).

Shi, Zhenghao and Fung, Ko B (1994). "A comparison of digital speckle filters". In: *Proceedings of IGARSS '94 - 1994 - IEEE International Geoscience and Remote Sensing Symposium*. Vol. 4. 3, pp. 2129–2133. DOI: 10.1109/IGARSS.1994.399671 (cit. on p. 12).

Shimada, Masanobu, Isoguchi, Osamu, Tadono, Takeo, and Isono, Kazuo (2009). "PALSAR radiometric and geometric calibration". In: *IEEE Transactions on Geoscience and Remote Sensing* 47.12, pp. 3915–3932. DOI: 10.1109/TGRS.2009.2023909 (cit. on p. 11).

Silva, Fabrício B, Shimabukuro, Yosio E, Aragão, Luiz E O C, Anderson, Liana O, Pereira, Gabriel, Cardozo, Franciele, and Arai, Egídio (2013a). "Large-scale heterogeneity of Amazonian phenology revealed from 26-year long AVHRR/NDVI time-series". In: *Environmental Research Letters* 8.2, p. 024011. DOI: 10.1088/1748-9326/8/2/024011 (cit. on pp. 1, 7).

Silva, Manoela Ferreira Fernandes da and Lobo, Maria da Graça A (1982). "Nota sobre deposição de matéria orgânica em floresta de terra firme, varzea e igapó." In: (cit. on p. 76).

Silva, Thiago Sanna Freire, Costa, Maycira P F, Melack, John M, and Novo, Evlyn M L M (2008). "Remote sensing of aquatic vegetation: theory and applications." In: *Environmental monitoring and assessment* 140.1-3, pp. 131–45. DOI: 10.1007/s10661-007-9855-3 (cit. on pp. 14, 38).

Silva, Thiago Sanna Freire, Costa, Maycira P.F., and Melack, John M (2010). "Spatial and temporal variability of macrophyte cover and productivity in the eastern Amazon floodplain: A remote sensing approach". In: *Remote Sensing of Environment* 114.9, pp. 1998–2010. DOI: 10.1016/j.rse.2010.04.007 (cit. on pp. 1, 11, 22, 37, 39).

Silva, Thiago Sanna Freire, Melack, John M, and Novo, Evlyn M L M (2013b). "Responses of aquatic macrophyte cover and productivity to flooding variability on the Amazon floodplain." In: *Global Change Biology* 19.11, pp. 3379–3389. DOI: 10.1111/gcb.12308 (cit. on pp. 10, 26, 39, 42).

Silva, Thiago Sanna Freire, Melack, John M, Streher, Annia Susin, Ferreira-Ferreira, Jefferson, and Furtado, Luiz Felipe de Almeida (2015). "Capturing the Dynamics of Amazonian Wetlands Using Synthetic Aperture Radar: Lessons Learned and Future Directions". In: *Remote Sensing of Wetlands: Applications and Advances*. Ed. by Ralph W. Tiner, Megan W. Lang, and Victor V. Klemas. London: CRC Press. Chap. 21, pp. 455–472. DOI: 10.1201/b18210-25 (cit. on pp. 37, 38).

Silvapulle, Mervyn J (1981). "On the Existence of Maximum Likelihood Estimators for the Binomial Response Models". In: *Journal of the Royal Statistical Society. Series B (Methodological)* 43.3, pp. 310–313 (cit. on p. 33).

Sioli, Harald (1954). "Beiträge zur regionalen Limnologie des Amazonasgebietes". In: *Archiv für Hydrobiologie* 45, pp. 267–283 (cit. on pp. 1, 2, 5).

Sitch, S. et al. (2013). "Trends and drivers of regional sources and sinks of carbon dioxide over the past two decades". In: *Biogeosciences Discussions* 10.12, pp. 20113–20177. DOI: 10.5194/bgd-10-20113-2013 (cit. on p. 4).

Slik, J. W.Ferry et al. (2013). "Large trees drive forest aboveground biomass variation in moist lowland forests across the tropics". In: *Global Ecology and Biogeography* 22.12, pp. 1261–1271. DOI: 10.1111/geb.12092. arXiv: 2731 (cit. on p. 54).

Sørensen, Thorvald (1948). "A method of establishing groups of equal amplitude in plant sociology based on similarity of species and its application to analyses of the vegetation on Danish commons". In: *Biol. Skr.* 5, pp. 1–34 (cit. on p. 44).

Sorribas, Mino Viana, Paiva, Rodrigo C D, Melack, John M, Bravo, Juan Martin, Jones, Charles, Carvalho, Leila, Beighley, Edward, Forsberg, Bruce, and Costa, Marcos Heil (2016). "Projections of climate change effects on discharge and inundation in the Amazon basin". In: *Climatic Change* 136.3-4, pp. 555–570. DOI: 10.1007/s10584-016-1640-2 (cit. on p. 27).

Sousa Jr, Paulo Teixeira de, Piedade, Maria Teresa Fernandez, and Candotti, Ennio (2011). "Ecological oversight: Brazil's forest code puts wetlands at risk." In: *Nature* 478.7370, p. 458. DOI: 10.1038/478458b (cit. on p. 41).

Takeuchi, Masayuki (1962). "The structure of the Amazonian vegetation, 4˜ 6." In: *Journal of the Faculty of Science, University of Tokyo Section 3 Botany* 8.4 (cit. on p. 6).

Thomaz, Sidinei M., Bini, Luis Mauricio, and Bozelli, Reinaldo Luiz (2007). "Floods increase similarity among aquatic habitats in river-floodplain systems". In: *Hydrobiologia* 579.1, pp. 1–13. DOI: 10.1007/s10750-006-0285-y (cit. on p. 26).

Townsend, P A (2002). "Relationships between forest structure and the detection of flood inundation in forested wetlands using C-band SAR". In: *International Journal of Remote Sensing* 23.3, pp. 443–460. DOI: 10.1080/01431160010014738 (cit. on p. 37).

Trigg, Mark a., Wilson, Matthew D., Bates, Paul D., Horritt, Matthew S., Alsdorf, Douglas E., Forsberg, Bruce R., and Vega, Maria C. (2009). "Amazon flood wave hydraulics". In: *Journal of Hydrology* 374.1-2, pp. 92–105. DOI: 10.1016/j.jhydrol.2009.06.004 (cit. on p. 28).

UNEP/CBD (2003). *Inland water ecosystems: review, further elaboration and refinement of the programme of work*. United Nations Environment Programme/Convention on Biological Diversity (cit. on p. 27).

Viana, João P, Castello, Leandro, Damasceno, José Maria B, Amaral, ESR, Estupiñan, GMB, Arantes, Carolina, Batista, GS, Garcez, DS, Barbosa, Saíde, and Blanc, D (2007). "Manejo Comunitário do Pirarucu Arapaima gigas na Reserva de Desenvolvimento Sustentável Mamirauá-Amazonas, Brasil". In: *Áreas aquáticas protegidas como instrumento de gestão pesqueira. Série Áreas Protegidas do Brasil* 4, pp. 239–261 (cit. on p. 24).

Villa, Jorge A and Mitsch, William J (2014). "Methane emissions from five wetland plant communities with different hydroperiods in the Big Cypress Swamp region of Florida Everglades". In: *Ecohydrology & Hydrobiology* 14.4, pp. 253–266. DOI: 10.1016/j.ecohyd.2014.07.005 (cit. on p. 39).

Vitousek, Peter M (1984). "Litterfall, Nutrient Cycling, and Nutrient Limitation in Tropical Forests". In: *Ecology* 65.1, pp. 285–298. DOI: 10.2307/1939481 (cit. on p. 55).

Wald, A. and Wolfowitz, J. (1940). "On a Test Whether Two Samples are from the Same Population". In: *The Annals of Mathematical Statistics* 11.2, pp. 147–162. DOI: 10.1214/aoms/1177731909 (cit. on p. 58).

Ward, J. V., Tockner, K., Arscott, D. B., and Claret, C. (2002). "Riverine landscape diversity". In: *Freshwater Biology* 47.4, pp. 517–539. DOI: 10.1046/j.1365-2427.2002.00893.x (cit. on p. 26).

Wesselingh, Frank P. and Hoorn, Carina (2011). "Geological Development of Amazon and Orinoco Basins". In: *Historical Biogeography of Neotropical Freshwater Fishes*. University of California Press, pp. 58–67. DOI: 10.1525/california/9780520268685.003.0003 (cit. on p. 39).

Wilson, Matthew, Bates, Paul, Alsdorf, Doug, Forsberg, Bruce, Horritt, Matthew, Melack, John M, Frappart, Frédéric, and Famiglietti, James (2007). "Modeling large-scale inundation of Amazonian seasonally flooded wetlands". In: *Geophysical Research Letters* 34.15, p. L15404. DOI: 10.1029/2007GL030156 (cit. on pp. 28, 38).

Wittmann, Florian, Anhuf, Dieter, and Funk, Wolfgang J. (2002). "Tree species distribution and community structure of central Amazonian várzea forests by remote-sensing techniques". In: *Journal of Tropical Ecology* 18.06, pp. 805–820. DOI: 10.1017/S0266467402002523 (cit. on pp. 6, 7, 9, 12, 23, 26, 39, 42, 53, 55, 56, 77, 78).

Wittmann, Florian, Householder, Ethan, Piedade, Maria T. F., Assis, Rafael L. de, Schöngart, Jochen, Parolin, Pia, and Junk, Wolfgang J (2012). "Habitat specifity, endemism and the neotropical distribution of Amazonian white-water floodplain trees". In: *Ecography* 36.6, pp. 690–707. DOI: 10.1111/j.1600-0587.2012.07723.x (cit. on pp. 1, 78).

Wittmann, Florian, Junk, Wolfgang J, and Piedade, Maria T.F (2004). "The várzea forests in Amazonia: flooding and the highly dynamic geomorphology interact with natural forest succession". In: *Forest Ecology and Management* 196.2-3, pp. 199–212. DOI: 10.1016/j.foreco.2004.02.060 (cit. on pp. 3, 6, 77).

Wittmann, Florian and Parolin, Pia (2005). "Aboveground roots in Amazonian floodplain trees". In: *Biotropica* 37.4, pp. 609–619. DOI: 10.1111/j.1744-7429.2005.00078.x (cit. on pp. 77–79).

Wittmann, Florian, Schöngart, Jochen, De Brito, J. M., Wittmann, A. O., Piedade, Maria Teresa Fernandez, Parolin, Pia, Junk, Wolfgang J, and Guillaumet, J. L. (2010a). *Manual of trees in Central Amazonian várzea flood-*

plains: taxonomy, ecology, and use. Manaus: INPA, p. 286 (cit. on pp. 9, 53).

Wittmann, Florian, Schöngart, Jochen, and Junk, Wolfgang J (2010b). "Phytogeography, species diversity, community structure and dynamics of central Amazonian floodplain forests". In: *Amazonian floodplain forests: ecophysiology, biodiversity and sustainable management*. Ed. by Wolfgang J. Junk, Maria Teresa Fernandez Piedade, Florian Wittmann, Jochen Schöngart, and Pia Parolin. New York: Springer Verlag. Chap. Chapter 4, pp. 61–102. DOI: 10.1007/978-90-481-8725-6 (cit. on pp. 2, 3, 6, 9, 22, 39, 53, 55, 56).

Wittmann, Florian, Schöngart, Jochen, Montero, Juan Carlos, Motzer, Thomas, Junk, Wolfgang J, Piedade, Maria T. F., Queiroz, Helder L., and Worbes, Martin (2006a). "Tree species composition and diversity gradients in white-water forests across the Amazon Basin". In: *Journal of Biogeography* 33.8, pp. 1334–1347. DOI: 10.1111/j.1365-2699.2006.01495.x (cit. on pp. 3, 23, 26, 39, 42, 54).

Wittmann, Florian, Schöngart, Jochen, Parolin, Pia, Worbes, Martin, Piedade, Maria T F, Junk, Wolfgang J., and Schöngart, Jochen (2006b). "Wood specific gravity of trees in Amazonian white-water forests in relation to flooding". In: *IAWA Journal* 27.3, pp. 255–268. DOI: 10.1163/22941932-90000153 (cit. on p. 53).

Worbes, Martin (1997). "The Forest Ecosystem of the Floodplains". In: *The Central Amazon Floodplain: Ecology of a Pulsing System*. Ed. by Wolfgang J Junk. Berlin, Heidelberg: Springer Berlin Heidelberg. Chap. 11, pp. 223–265. DOI: 10.1007/978-3-662-03416-3 (cit. on pp. 3, 53, 75, 76).

Worbes, Martin, Klinge, Hans, Revilla, Juan D., and Martius, Christopher (1992). "On the dynamics, floristic subdivision and geographical distribution of várzea forests in Central Amazonia". In: *Journal of Vegetation Science* 3.4, pp. 553–564. DOI: 10.2307/3235812 (cit. on p. 53).

Wu, J., Albert, L. P., Lopes, A. P., Restrepo-Coupe, N., Hayek, M., Wiedemann, K. T., Guan, K., Stark, S. C., Christoffersen, B., Prohaska, N., Tavares, J. V., Marostica, S., Kobayashi, H., Ferreira, M. L., Campos, K. S., Silva, R. da, Brando, P. M., Dye, D. G., Huxman, T. E., Huete, A. R., Nelson, B. W., and Saleska, S. R. (2016). "Leaf development and demography explain photosynthetic seasonality in Amazon evergreen forests". In: *Science* 351.6276, pp. 972–976. DOI: 10.1126/science.aad5068 (cit. on p. 56).

Zanne, A. E., Lopez-Gonzalez, G., Coomes, D.A. A, Ilic, J., Jansen, S., Lewis, Simon L S.L., Miller, R.B. B, Swenson, N.G. G, Wiemann, M.C. C, and Chave, Jerome (2009). *Global wood density database*. Tech. rep., p. 33. DOI: 10.5061/dryad.234 (cit. on p. 44).

Zevenbergen, Lyle W and Thorne, Colin R (1987). "Quantitative analysis of land surface topography". In: *Earth Surface Processes and Landforms* 12.1, pp. 47–56. DOI: 10.1002/esp.3290120107 (cit. on p. 31).

Zhang, Ke, Castanho, Andrea D De Almeida, Galbraith, David R., Moghim, Sanaz, Levine, Naomi, Bras, Rafael L., Coe, Michael, Costa, Marcos H., Malhi, Yadvinder, Longo, Marcos, Knox, Ryan G., McKnight, Shawna, Wang, Jingfeng, and Moorcroft, Paul R. (2015). "The Fate of Amazonian Ecosystems over the Coming Century Arising from Changes in Climate, Atmospheric CO 2 and Land-use". In: *Global Change Biology* 617, n/a–n/a. DOI: 10.1111/gcb.12903 (cit. on p. 4).

Zhao, M. and Running, S. W. (2011). "Drought-Induced Reduction in Global Terrestrial Net Primary Production from 2000 Through 2009". In: *Science* 333.6046, pp. 1093–1093. DOI: 10.1126/science.1199169 (cit. on p. 55).

Zulkafli, Zed, Buytaert, Wouter, Manz, Bastian, Rosas, Claudia Véliz, Willems, Patrick, Lavado-Casimiro, Waldo, Guyot, Jean-Loup, and Santini, William (2016). "Projected increases in the annual flood pulse of the Western Amazon". In: *Environmental Research Letters* 11.1, p. 014013. DOI: 10.1088/1748-9326/11/1/014013 (cit. on pp. 54, 79).